Development of Nickel- and Palladium-Mediated Decarbonylative Coupling of Carboxylic Acid Derivatives: From Organometallic Reactivity to Catalysis

by

Conor Brigham

A dissertation submitted in partial fulfillment
of the requirements for the degree of
Doctor of Philosophy
(Chemistry)
in the University of Michigan
2022

Doctoral Committee:

Professor Melanie S. Sanford, Chair
Assistant Professor Peter Scott
Associate Professor Nathanial Szymczak
Associate Professor Paul Zimmerman

Conor Brigham

cbrig@umich.edu

ORCID iD: 0000-0003-0532-6651

Dedication

To my parents, Erin and Gerard, my brother, Maclaren, and my grandparents, Mary & Edward McLaughlin, and Isabell & Robert Brigham.

Acknowledgements

Professor James “Jim” Devery III was my first advisor at Loyola University Chicago. I reached out to Jim when he first arrived at LUC at the beginning of my junior year, and he welcomed me into his new lab. The experience I had helping Jim start his new lab is what inspired me to pursue a graduate degree in chemistry. Not only did he give me valuable lessons regarding lab techniques and practices, but he taught me how to present one’s research at a high level, and he gave me the confidence to pursue a degree at the University of Michigan. Thank you so much Jim; I wouldn’t be here without you.

Professor Melanie Sanford was my graduate advisor at the University of Michigan. I am forever grateful for my time working in her lab and to experience working alongside such a brilliant and kind scientist. Her unbelievable patience, understanding and care she has for her students is contagious, and I will always stive to be more like Melanie. Thank you, Melanie, for giving me the privilege of working with you, and for demonstrating not only how to be an excellent researcher, but an exceptional person.

Thank you to my committee members, Professor Nate Szymczak, Professor Paul Zimmerman, and Professor Peter Scott, for all your support and guidance. A special thanks to Professor Szymczak for your mentorship during my rotation in your lab.

Dr. Christian Malapit was my mentor when I joined the Sanford lab. He provided me with an amazing platform to build my thesis on. His pioneering work on our group’s decarbonylative chemistry is what started the work in this thesis. His breadth of knowledge as a synthetic organic

chemist has always been a valuable resource for me. Christian has helped me throughout my time in graduate school, even after he had finished his post-doc in our group. From all the late nights going though my slides as a rotator and pre-candidate, to the zoom calls during the pandemic, and even through editing this dissertation, I cannot thank you enough, Christian, for all the help you have been.

My other mentors that I have worked with in the Sanford lab, including James Bour, who was the first to teach me how to carry out organometallic experiments with acid fluoride decarbonylations. Devin Ferguson was also instrumental for my development as a researcher and was a great resource to learn about organometallics. Tolani "Kuam" Salvador was another post-doc in our lab that, though he did not directly mentor me on any project, was an exceptional friend who made working in lab a joy, despite his flaws as a Miami Dolphins fan. In addition, thank you to all the other students and post docs that welcomed me into the Sanford lab when I first joined, including Dr. Patick Melvin, Dr. Courtney Roberts, Mark Mantell, Anushka Shrestha, Ellen Aguilera, Pronay Roy, thank you all for being such amazing people.

A special thanks to Naish Lalloo. Naish and I met as roommates on our recruitment weekend in the spring of 2017, and five years later we have been on two papers together with more to come. Thank you Naish for being such an amazing friend; it has been a blast working together over these years, I couldn't have done it without you.

To all the members of the Sanford lab that I have had the pleasure of working with, thank you all for being such great friends. I could not have asked for a better group of individuals to learn from and with over the last five years.

Table of Contents

List of Tables

List of Figures

Abstract

Transition metal catalyzed cross coupling reactions are among the most widely used transformations in organic chemistry. While there has been tremendous work regarding aryl halide cross coupling, there has been growing interest in using carboxylic acid derived electrophiles in catalysis. Carboxylic acids can be derivatized into highly tunable, modular electrophiles. A weak $C_{(acyl)}$-X bond (X = OR, Cl, F, SR, NR_2) allows for addition into nucleophilic low valent transition metals. Our interest is utilizing these carboxylic acid derivatives in a decarbonylative manner, that is where carbonyl deinsertion on the metal removes CO. This can then introduce aryl or alkyl organic groups in an analogous fashion to aryl halides. A persisting challenge decarbonylative cross coupling is balancing selectivity for acyl-retaining products. Ultimately, gaining better insights into reaction mechanisms may help with further development of these types of transformations.

Chapter 1 describes the current state of decarbonylative cross coupling chemistry. Here we will go through recent history of relevant palladium and nickel catalyzed decarbonylation methodologies of carboxylic acid derivatives. Key features of these reactions include the choice of metal, choice of phosphine ligand/ligand-type (i.e. mono- vs. bi-dentate ligands), temperature, coupling partner and necessary additives.

Chapter 2 begins with our work on decarbonylation of aryl carboxylic acid derivatives. Initial experiments demonstrate the feasibility of oxidative addition and decarbonylation for acid fluoride electrophiles. While C-F reductive elimination is not observed, we found that Ni-F intermediates could undergo base-free transmetallation with boronic acids. This leads to the

discovery of two cross-coupling methodologies, a Suzuki-Miyaura C-C coupling and aryl amination C-N coupling. ((Diphenyl)methyl)phosphine (PPh_2Me) demonstrated high selectivity of the decarbonylated product due to rapid carbonyl deinsertion under the Suzuki-Miyaura conditions. Blocking background amidation was main challenge for C-N coupling, which was solved by utilizing alternative aryl acid derivatives, aryl phenyl esters, with silyl-protected amines.

Chapter 3 describes out detailed studies of the decarbonylation of fluoroalkyl thioesters to their corresponding fluoroalkyl thioether. Development of a nickel catalyst was optimized with difluoromethyl thioesters, and the scope was broad for aryl and alkyl thiols. Importantly, we demonstrate that we can successfully decarbonylate several fluoroalkyl acid thioesters. This was our first demonstration of decarbonylative coupling of several fluoroalkyl substituents.

Chapter 4 follows our work on intramolecular fluoroalkylation as we pursue a general intermolecular coupling. With the information learned in Chapters 2 and 3, we applied our understandings of decarbonylative cross coupling to highly electrophilic fluoroalkyl acid derivatives. This chapter will describe several possible acid-derivatives, and discuss the pros and cons to each. Ultimately, this has so far led to two decarbonylative couplings ($R_F = CF_2H$ and CF_2Ph).

Chapter 1 - Introduction

1.1 Background

Transition metal catalysis has emerged as one of the most powerful approaches for the formation of carbon-carbon and carbon-heteroatom bonds. Owing to the well-established nature of these methodologies and their impact on the synthetic community, the pioneering work of Suzuki, Negishi and Heck involving palladium-catalyzed C–C coupling was honored with the Nobel Prize in Chemistry in 2010. Traditional transition metal-catalyzed cross couplings involve an aryl-(pseudo)halide electrophile that is coupled with an organometallic nucleophile, [M]-R' (Figure 1-1). These widely used transformations have been developed for numerous types of bond formations (C-C, C-N, C-O, C-S,).[1-3]

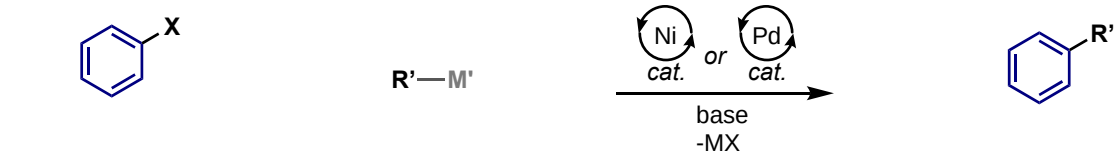

Figure 1-1. Traditional cross coupling reactions of aryl (pseudo)halides.

Carbonyl-containing compounds have more recently gained significant attention as electrophiles for transition metal cross-coupling reactions. [4-12] These functionalities (i.e. which include aldehydes, ketones, carboxylic acids, amides, acyl halides, esters, and anhydrides) are among the most common function groups in organic chemistry and are found in a variety of pharmaceuticals, agrochemicals, polymers, and other organic materials. Transition metals have

been known to undergo oxidative addition into C(acyl)-X bonds as early as the 1960's. The Tsuji-Wilkinson decarbonylation reaction is a well-studied early example of a Rh-mediated insertion into the C–H bond of an aldehyde. This is followed by CO de-insertion and reductive elimination, thus converting the aldehyde to an alkane (Figure 1-2). [13-14]

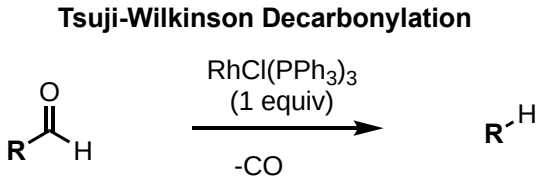

Figure 1-2. Stoichiometric decarbonylation of aldehydes.

Carbonyl-based electrophiles have increasingly been used in these types of transformations due to the weakened $C_{(acyl)}$-X bond, which can undergo oxidative addition into a low valent metal to from metal-acyl intermediate **I**. Carbonyl de-insertion (often reversible) then generates an organometallic intermediate **II** that can either undergo *intramolecular* reductive elimination forming a new R-X bond (Figure 1-3; pathway i) or react with an external nucleophile in an *intermolecular* fashion, analogous to traditional cross-coupling reactions of organohalides (Figure 1-3; pathway ii).

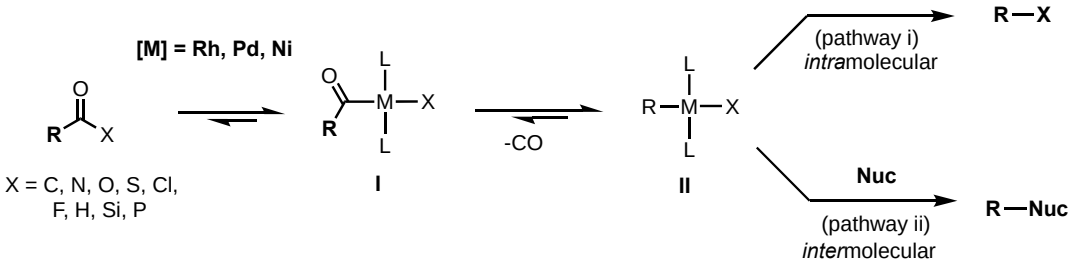

Figure 1-3. General reaction pathway for decarbonylative coupling.

Early examples of this type of transformation were largely conducted using stoichiometric quantities of a low valent metal (e.g., Rh(I) in Figure 1-2). The CO by-product would then remain ligated to the low valent metal following reductive elimination of the product. Catalytic turnover

in these systems was achieved by heating (often to >200 ºC) to liberate carbon monoxide from the metal. In 2003, Rovis reported an example of stoichiometric decarbonylative coupling using Ni(0) to cross couple cyclic *meso*-anhydrides with diaryl zinc reagents. Interestingly, an extra half of an equivalent of Ni(0) was needed to favor the desired decarbonylation. [15] Due to the reversibility of carbonyl de-insertion/insertion, liberation of carbon monoxide from the metal is necessary to drive the reaction towards decarbonylated products. Rovis and coworkers found that after CO migrates to the metal following oxidative addition, a second Ni(0) complex permanently removes CO, as this Ni(0) is far more electron rich than Ni(II) (Figure 1-4). Catalytic reactions can be achieved, though elevated temperatures are typically required to scrub CO from the catalyst.

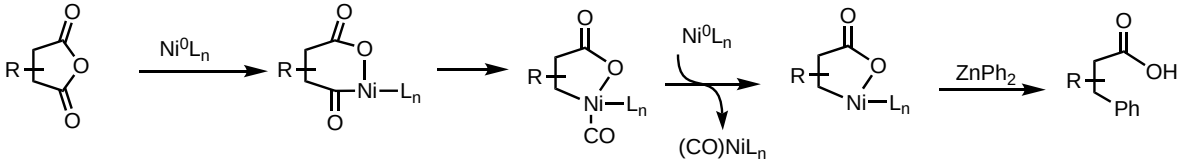

Figure 1-4. Removal of CO from the metal is crucial for favoring decarbonylation over carbonyl insertion.

1.2 Introduction of palladium- and nickel-catalyzed decarbonylations

Palladium- and nickel-catalysts are among the most common transition metals used in cross-coupling reactions. While palladium has received widespread attention as a coupling catalyst due to its prevalent ability to forge challenging bonds, there has been an increased focused on its group 10 congener nickel. Nickel is significantly more earth abundant and less expensive than palladium. In addition, it can participate in similar catalytic cycles as Pd (i.e., $M^{0/II}$ catalysis), but also in complementary single electron pathways. As a first-row transition metal, nickel generally undergoes more facile oxidative addition with both aryl halides and carboxylic acid derivatives

than palladium. Correspondingly, reductive elimination reactions are typically more facile at Pd^{II} as compared to the analogous Ni^{II} centers. As detailed below, both nickel and palladium catalysts have been used in decarbonylative transformations, and examples of both will be discussed and developed throughout his thesis.

1.3 Phenyl esters in decarbonylative catalysis

Recently, significant effort has been directed towards decarbonylative cross coupling of aryl carboxylic acid derivatives, specifically with phenyl esters.[7,12] Pioneering work by Yamamoto et al. was originally carried out in 1980, where they demonstrated stoichiometric oxidative addition of aryl carboxylates into Ni(0).[16] Recently, Itami and Yamaguchi together published significant findings for decarbonylative methodologies using aryl phenyl ester electrophiles with nickel catalysts and palladium catalysts (Figure 1-5). In 2012, they developed a decarbonylative C-H activation of azoles with a Ni^0/dcype (dcype = 1,2-Bis(dicyclohexylphosphino)ethane) catalyst (Figure 1-5, a).[17] They followed this work a few years later with a decarbonylative Suzuki-Miyaura coupling of aryl esters and aryl boronic acids with only minor changes to the catalytic system (ligand = P^nBu_3 instead of dcype; Figure 1-5, b).[18] One limitation to their nickel-catalyst was that it was incompatible with 2-azine carboxylates. To address this limitation, they turned to a palladium-based catalyst (Figure 1-5, c).[19] Around the same time, the Love group published similar work using azinecarboxylate phenyl esters in C-C coupling with a nickel catalyst (Figure 1-6).[20] An interesting finding from this work was the isolation of $Ni(CO)_2(PCy_3)_2$ from stoichiometric decarbonylations, indicating that Ni(0) sequesters CO in these transformations. Notably, all of these transformations employed super-stoichiometric quantities of a base (K_3PO_4, Na_2CO_3, or Cs_2CO_3), presumably to promote the transmetalation step of the catalytic cycle.

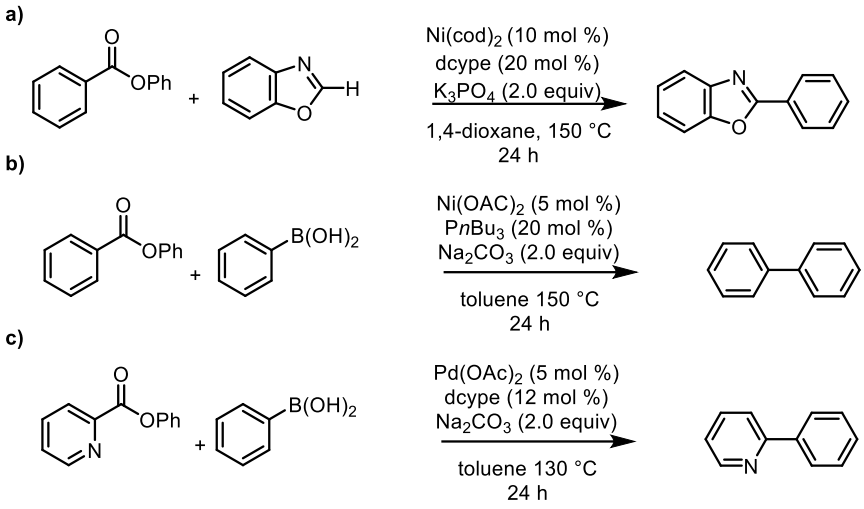

Figure 1-5. Early examples of Pd and Ni-catalyzed decarbonylative coupling of aryl esters.

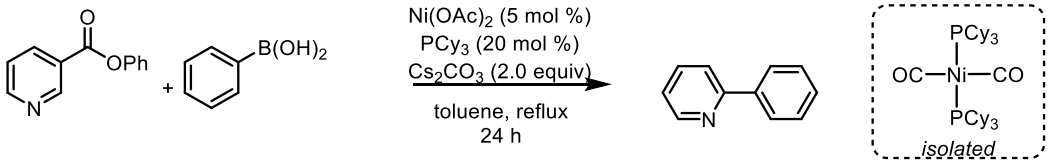

Figure 1-6. Ni-catalyzed decarbonylative Suzuki-Miyaura coupling of azinecarboxylates.

To date, the majority of decarbonylative coupling with aryl esters has been used in an *inter*molecular fashion and for C-C coupling (Figure 1-3, pathway ii). However, one example from Yamaguchi and Itami demonstrated the decarbonylative *intra*molecular coupling of 2-azinecarboxylate esters to form C-C bonds (Figure 1-3, pathway i). This reaction was carried out with both palladium-based and nickel-based catalysts. Relatively specialized phosphine ligands, dcypt and dcppt (dcypt = 3,4-bis(dicyclohexylphosphino)-thiophene; dcppt = 3,4-bis(dicyclopenylphosphino)-thiophene) (Figure 1-7), were required.[21] Again, super-stoichiometric base (K_3PO_4) was employed, although it is not clear why this is needed in this system, since there is not a transmetalation step in the catalytic cycle for intramolecular decarbonylative coupling.

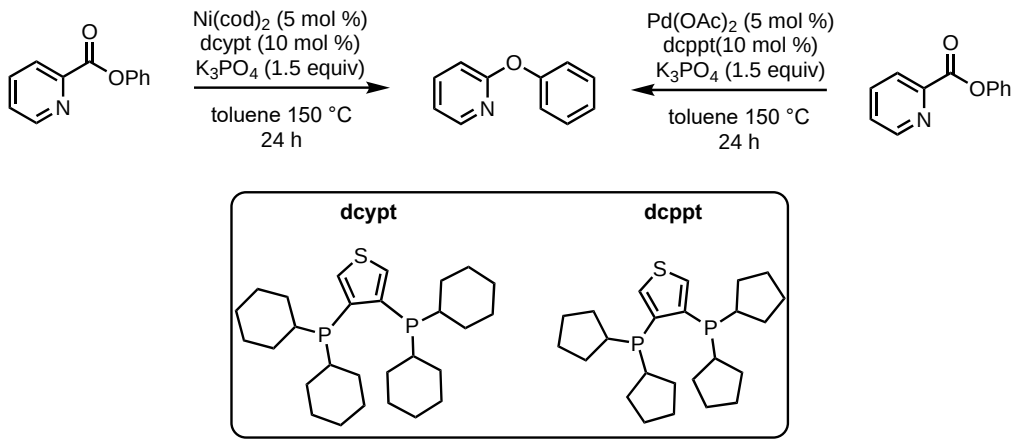

Figure 1-7. Ni- and Pd-catalyzed decarbonylative ether synthesis using 2-azinecarboxylates.

In 2016, Shi and coworkers demonstrated that C–B and C–Si bond formations could be achieved via decarbonylative coupling. They reported both a decarbonylative borylation (with $B_2(neo)_2$) and a decarbonylative silylation (with TMS-B(pin)) of aryl phenyl esters using nickel N-heterocyclic carbene and dcype-based catalysts, respectively (Figure 1-8).[22] Like previous reports, these systems required elevated temperatures and a base additive (Na_2CO_3). The latter presumably facilitates transmetalation of $B_2(neo)_2$ or TMS-B(pin).

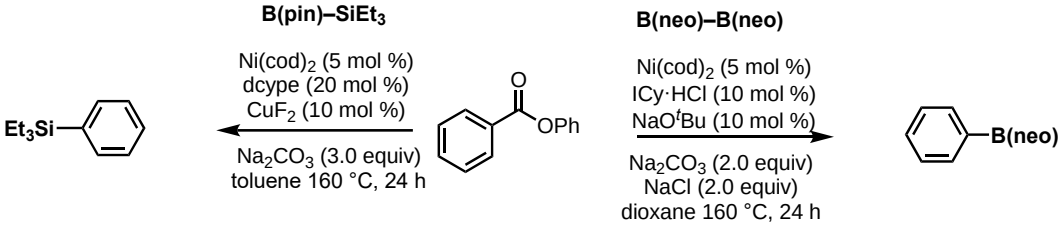

Figure 1-8. Ni- and Pd-catalyzed decarbonylative ether synthesis using 2-azinecarboxylates.

1.4 Aryl amide electrophiles in decarbonylative coupling

Another common acyl electrophile employed in transition metal catalyzed decarbonylative coupling reactions are twisted amides (Figure 1-9).[23] These contain a weaker weakend $C_{(acyl)}$-N

bond than “normal” amides and can thus readily undergo oxidative addition to a low valent metal. In 2016, Szostak reported the first use of C-N amide bond cleavage for a Ni-catalyzed decarbonylative Suzuki-Miyuara biaryl synthesis (Figure 1-9).[23] Glutarimide electrophiles were particularly effective in this system due to the out-of-plane twist of the amide with the aryl carbonyl, weakening that $C_{(acyl)}$-N bond for metal activation. PCy_3 was employed as a ligand for the Ni catalyst, and super stoichiometric base (4.5 equiv of Na_2CO_3) was added, presumably to promote transmetalation of the boronic acid.

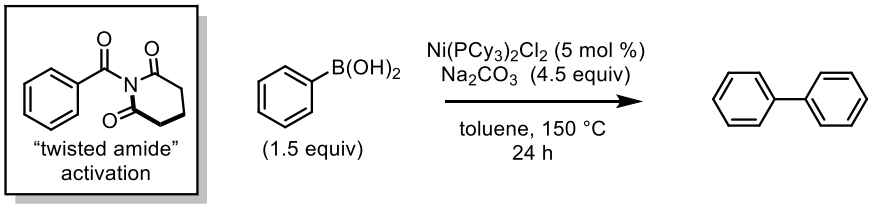

Figure 1-9. Ni-catalyzed decarbonylative biaryl synthesis using glutaramides as electrophiles.

1.5 Acid halides in decarbonylative coupling

Acid halide electrophiles have been well established as good electrophiles in transition metal catalyzed reactions, whether for carbonyl-retaining acylation coupling or decarbonylative coupling. Recently they have garnered more attention for decarbonylative transformations at both nickel or palladium. A general challenge with these highly reactive electrophiles is limiting competitive acylation reactions. These can occur via either direct, uncatalyzed addition of the nucleophile to the carbonyl, or though carbonyl-retaining transmetallation from acyl intermediate **I** (Figure 1-10).

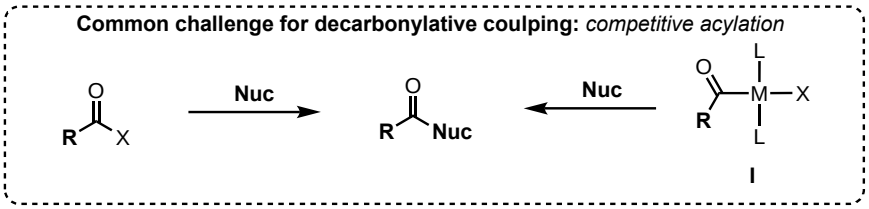

Figure 1-10. Competitive acylation of the nucleophile is the major challenge for decarbonylative cross coupling.

In 2018, Schoenebeck reported the first use of aryl acid fluorides for a decarbonylative trifluoromethylation (Figure 1-11).[24] This was achieved using a mild trifluoromethyl-based nucleophile ($TESCF_3$) in combination with Pd^0/Xantphos catalyst. High temperature was required to promote CO de-insertion in this system, and super-stoichiometric K_3PO_4 was employed.

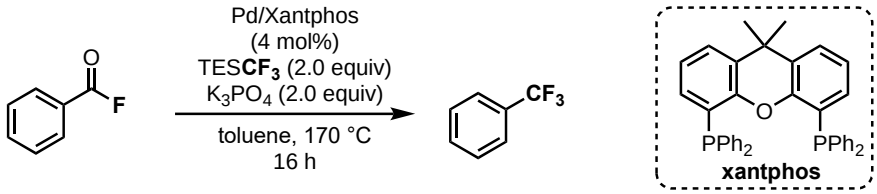

Figure 1-11. Pd-catalyzed decarbonylative cross coupling with aroyl fluorides.

At the time that we initiated our work in this area, all of the reported Ni- and Pd-catalyzed decarbonylative coupling reactions reported in the literature employed super-stoichiometric quantities of base as an additive. It is generally understood in cross coupling methods that base is needed to facilitate transmetalation between the nucleophile and the metal center. However, this added base can hinder the development of certain decarbonylative transformations by promoting completive degradation of the electrophiles. In addition, base can be problematic for certain classes of substrates. For instance, fluorinated boronic acid are prone to rapid protodeboronation at elevated pH.

A central hypothesis of this thesis was that base-free decarbonylative couplings could be achieved by fine-tuning the reactive of the X-leaving group on the carboxylic acid (Figure 1-12).

Oxidative addition introduces the X-group directly onto the catalyst and thus, in the absence of exogeneous base, the nucleophile must directly react with the M-X intermediate. To prevent carbonyl retention in the coupled product, fast and irreversible carbonyl de-insertion will have to take place prior to transmetalation.

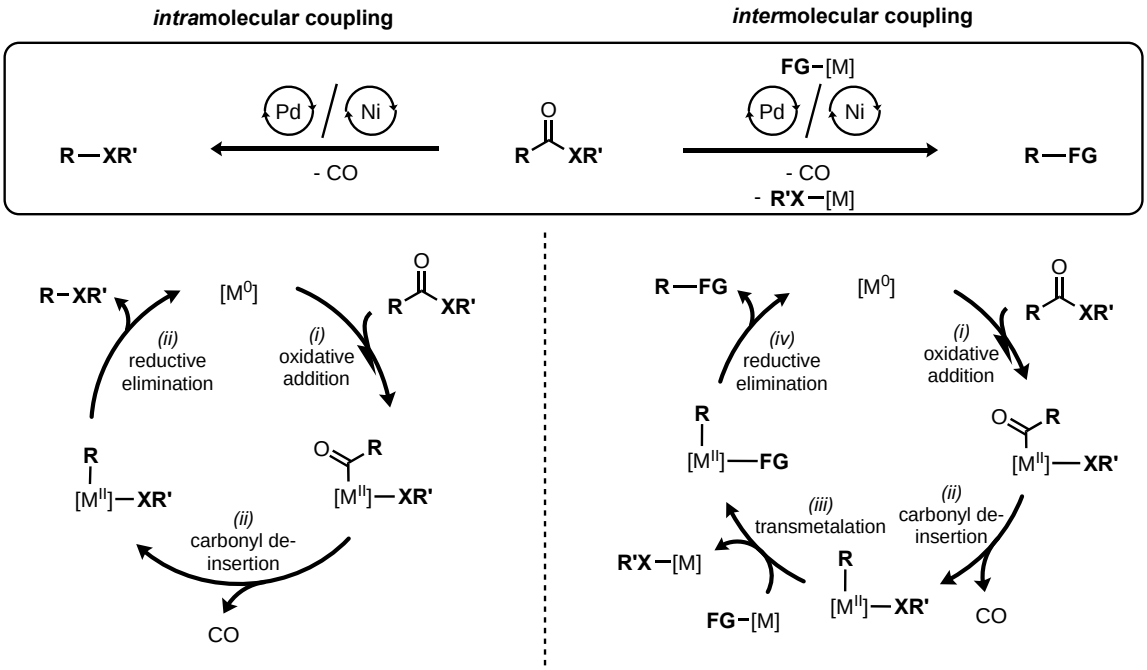

Figure 1-12. Catalytic cycles for intra- and intermolecular decarbonylations.

This thesis details our investigations developing base-free decarbonylative coupling reactions. Though stoichiometric organometallic investigations, we identify and isolate key metal-intermediates and study their reactivity for each step in the catalytic cycle. Once we establish the feasibility of these steps, we translate many of these systems to catalysis. Chapter 2 highlights our findings for base-free decarbonylative cross couplings of aryl carboxylic acid derivatives. Chapter 3 explores a base-free *intra*molecular decarbonylation of fluoroalkyl thioesters. This is the first demonstration that fluoroalkyl acid derivatives can be employed in decarbonylation coupling. Finally, in Chapter 4, we take the lessons learned from Chapters 2 and 3 and apply them to decarbonylative fluoroalkylations of [M]-aryl species (M = B, Si, Sn).

1.6 References

1) Biffis, A.; Centomo, P.; Del Zotto, A.; Zecca, M. *Chemical Reviews*, **2018** *118* (4), 2249-2295.
2) Ananikov, V. P., *ACS Catalysis*, **2015** *5* (3), 1964-1971.
3) Han, F.-S., ***Chem. Soc. Rev.***, **2013**,***42***, 5270-5298.
4) Gooßen, L. J,; Gooßen, K.; Rodríguez, N.; Blanchot, M.; Linder, C.; Zimmermann, B. *Pure Appl. Chem*., **2008**, *80*, 1725–1733.
5) Liu, C.; Szostak, M., *Org. Biomol. Chem*., **2018**, *16*, 7998-8010.
6) Guo, L.; Reuping, M.; *Chem. Eur. J*. **2018**, *24*, 7794 –7809.
7) Guo, L.; Reuping, M.; *Acc. Chem. Res*. **2018**, *51*, 1185 –1195.
8) Rodriguez.; Gooßen, L. J., *Chem. Soc. Rev*. **2011**, *40*, 5030 – 5048.
9) Dzik, W. I.; Lange, P. P.; Gooßen, L. J., *Chem. Sci*. **2012**, *3*, 2671 – 2678.
10) Dermenci, A.; Dong, G. B. *Sci. China Chem*. **2013**, *56*, 685 – 701.
11) Takise, R.; Muto, K.; Yamaguchi, J., *Chem. Soc. Rev*. **2017**, *46*, 5864 – 5888.
12) Lu, H.; Yu, T.-Y.; Xu, P.-F.; Wei, H., *Chem. Rev*. **2021**, *121*, 365–411.
13) Tsuji, J.; Ohno, K., *Tetrahedron Lett*. **1965**, *6*, 3969−3971.
14) Ohno, K.; Tsuji, J., *J. Am. Chem. Soc*. **1968**, *90*, 99−107.
15) O'Brien, E. M.; Bercot, E. A.; Rovis, T., *J. Am. Chem. Soc*. **2003**, 125, 10498–10499.
16) Yamamoto, T.; Ishizu, J.; Kohara, T.; Komiya, S.; Yamamoto, A., *J. Am. Chem. Soc*. **1980**, *102*, 3758−3764.
17) Amaike, K.; Muto, K.; Yamaguchi, J.; Itami, K., *J. Am. Chem. Soc*. **2012**, *134*, 13573−13576.
18) Muto, K.; Yamaguchi, J.; Musaev, D. G.; Itami, K., *Nat. Commun*. **2015**, *6*, 7508.
19) Muto, K.; Hatakeyama, T.; Itami, K.; Yamaguchi, J., *Org. Lett*. **2016**, *18*, 5106−5109.
20) LaBerge, N. A.; Love, J. A., *Eur. J. Org. Chem*. **2015**, 5546−5553.
21) Takise, R.; Isshiki, R.; Muto, K.; Itami, K.; Yamaguchi, J., *J. Am. Chem. Soc*. **2017**, *139*, 3340−3343.
22) Pu, X.; Hu, J.; Zhao, Y.; Shi, Z., *ACS Catal*. **2016**, *6*, 6692−6698.
23) Shi, S.; Meng, G.; Szostak, M. *Angew. Chem. Int. Ed*. **2016**, *55*, 6959.
24) Keaveney, S. T.; Schoenebeck, F., *Angew. Chem., Int. Ed*. **2018**, *57*, 4073−4077.

Chapter 2 - Nickel-Catalyzed Decarbonylative Cross-Coupling of Aryl Carboxylic Acids

*Portions of this work have been published in:

Malapit, C. A; Bour, J. R.; Brigham, C. E.; Sanford, M. S. Base-free Nickel-catalyzed Decarbonylative Suzuki-Miyaura Coupling of Acid Fluorides. *Nature.* **2018**, *10*, 8315–8320.

Malapit, C. A; Borrell, M; Milbauer, M. W.; Brigham, C. E.; Sanford, M. S. Nickel-catalyzed Decarbonylative Amination of Carboxylic Acid Esters. *J. Am. Chem. Soc.* **2020**, *142*, 5918–5923.

2.1 Background

Over the last century, transition metal catalysis has emerged as one of the most powerful tools in organic synthesis for forging new bond connections. Metal-catalyzed reactions serve as convenient approaches to functionalizing aromatic and vinylic moieties, are they are routinely used in the preparation of pharmaceutically relevant compounds.[1,2] Nickel-catalyzed cross-coupling has also gained significant interest, as nickel represents an earth-abundant potential alternative to palladium.[3,4] In addition, the propensity of nickel for readily undergoing oxidative addition allows for the use of electrophiles that are less reactive with palladium. In this regard, widely abundant carboxylic acid derivatives such as esters and amides have been targeted as electrophiles in Ni-catalyzed cross-coupling as alternatives to more traditional aryl halides.[5-13] Using carboxylic acid-derived electrophiles in place of aryl halides eliminates the generation of corrosive halide containing byproducts. Carboxylic acids are widely abundant, inexpensive commercial reagents and are common functional groups in natural products.

For these reasons, their utilization in transition metal catalyzed transformations has grown in recent years. One such transformation is decarbonylative methodologies, where CO is extruded following an oxidative addition into the C(acyl)–X bond. A major challenge for the development of these transformations is overcoming the high barrier for oxidative addition into these poor electrophiles. Pioneering work by Yamamoto in the 1980's demonstrated the feasibility of stoichiometric oxidative addition of C(acyl)–O at phosphine nickel(0) complexes. The resulting Ni^{II} acyl intermediates then underwent carbonyl de-insertion, leading to isolable $Ni(CO)_nL_n$ complexes. Since then, significant work was focused on nickel-catalyzed cross coupling reactions of aryl ester electrophiles. Itami et al. contributed significant findings of the first examples of decarbonylative biaryl synthesis with nickel catalysts beginning in 2014, as well as the Love group around the same time.

2.2 Attempts at C-F reductive elimination from Ni(II)

One type of bond forming reaction that has gained significant attention both in our group and the broader synthetic chemistry community is the construction of carbon-fluorine bonds. Fluorine is increasingly common in biologically active compounds in the pharmaceutical and agrochemical industries.[14-19] The high BDE of the C-F bond renders fluorinated molecules inert to oxidation reactions, thus blocking known metabolic pathways.[18-21] The introduction of fluorine also increases the lipophilicity of organic molecules, which can lower the dose required for therapeutic efficacy.[20,21] In addition, the isotope ^{18}F is one of the most common positron emitters used in PET.[21,22] Fluorine's growing importance to the synthetic community has culminated in over 30% of new drugs coming on the market containing at least one fluorine atom.[18,19]

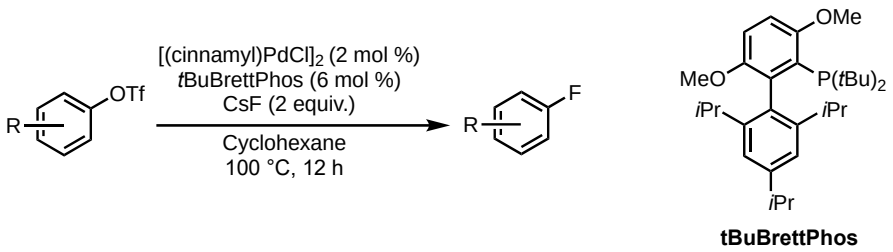

Figure 2-1. Palladium catalyzed aryl fluorination by Buchwald and coworkers.

While the demand for fluorine continues to grow, C–F bond-forming reactions remain challenging.[14-15,23] In particular, most common C(sp^2)–F coupling reactions require forcing reaction conditions (≥100 ºC) and are often restricted to simple (unfunctionalized) aromatic substrates.[15] While transition metal catalyzed cross coupling has been successfully employed for numerous C(sp^2)-C and C(sp^2)-heteroatom bond forming reactions, metal catalyzed C(sp^2)-F bond formation is less prevalent, particularly for the group 10 metals palladium and nickel.[24] To date, the most prominent example of group 10 metal-catalyzed C(sp^2)–F coupling is Buchwald's reaction of aryl halide- and pseudohalide electrophiles with CsF catalyzed by Pd(0) and ^{t}BuBrettphos (Figure 2-1).[25]

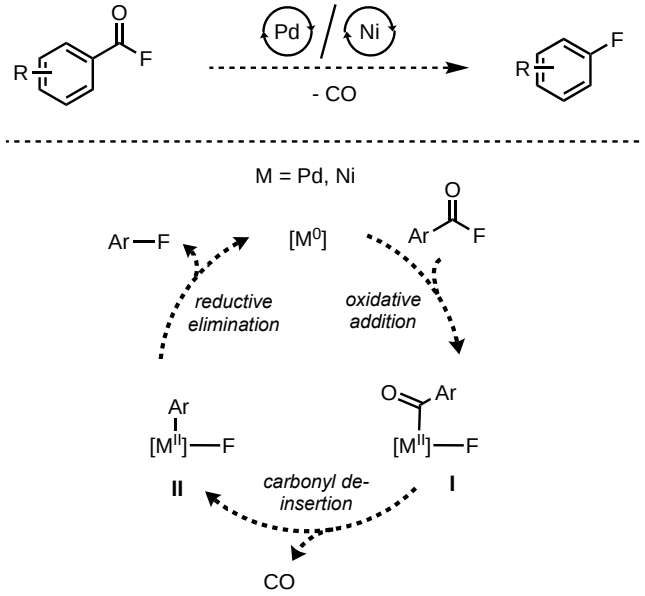

Figure 2-2. Proposed decarbonylative aryl fluorination from acid fluorides

We hypothesized that aryl carboxylic acid fluorides (aroyl fluorides) could serve as reagents for aryl fluorination via a Ni(0)- or Pd(0)-catalyzed intramolecular decarbonylation reaction (Figure 2-2). Oxidative addition of aroyl fluorides at Ni(0) and Pd(0) centers is known,[26] and this step would install the desired fluoride ligand onto the catalyst without the need for an external fluoride source to perform an exchange. Carbonyl de-insertion would liberate CO and generate a metal–aryl bond. Subsequent aryl–F bond-forming reductive elimination would then release the desired aryl-fluoride product. Our group previously had success developing a related intramolecular decarbonylation of aroyl chlorides to form aryl chlorides (Figure 2-3).[27] This was the first example of decarbonylative halogenation using a palladium catalyst.

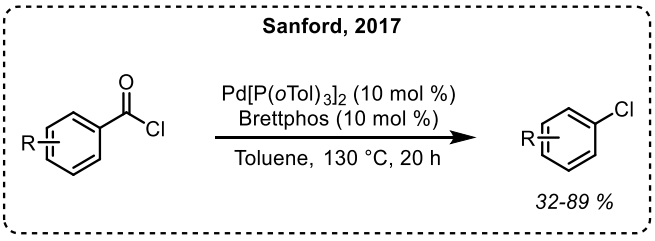

Figure 2-3 Palladium-catalyzed decarbonylative aryl chlorination (Sanford, 2017)

Our initial studies of decarbonylative fluorination began with stoichiometric experiments to probe the viability of each step in the proposed catalytic cycle. Previous conditions reported by Buchwald for the palladium-catalyzed fluorination of aryl halides (Figure 2-1) utilized bulky biaryl dialkyl phosphine ligands,[25] and similar ligand scaffolds were used for our chlorination conditions (Figure 2-3).[27] However, with aroyl fluorides, the desired aryl fluorination products were never observed using these phosphines in combination with various Pd(0) precursors. Stoichiometric and catalytic experiments suggested that oxidative addition and carbonyl deinsertion are challenging

steps with Pd-based catalysts. To address this challenge, my studies focused the group 10 congener, nickel. Oxidative addition of acyl fluorides at nickel(0) is well-precedented,[26,28] and carbonyl de-insertion is also far more facile at nickel(II) than at palladium(II).[8,29] In contrast, C(sp^2)–F bond-forming reductive elimination from Ni(II)(aryl)(F) complexes has not been reported, and we anticipated that this would likely be the most challenging step of the catalytic cycle .

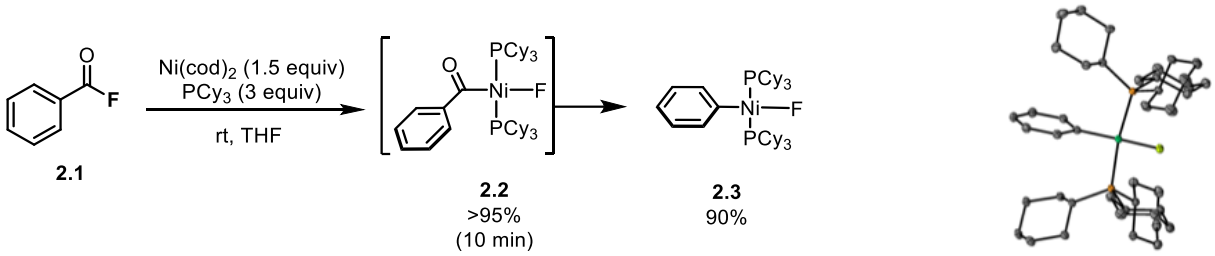

Figure 2-4. Stoichiometric reaction of benzoyl fluoride with Ni0/PCy3.

Initial reactivity and synthetic pathways were discovered and optimized in collaboration with Dr. Christian Malapit. These studies revealed that Ni^0 phosphine complexes (generated by combining $Ni(cod)_2$ and PR_3) react with aroyl fluorides to produce stable aryl-nickel fluoride complexes under mild conditions. For instance, as shown in Figure 2.4, the reaction of 1 equiv of $Ni(cod)_2$ and 3 equiv of PCy_3 with 1 equiv of benzoyl fluoride (**2.1**) led to quantitative conversion to the bisphosphine acyl-Ni^{II}-F oxidative addition product **2.2** within 10 min at room temperature. Carbonyl de-insertion to form the bisphosphine aryl-Ni^{II}-F product **2.3** then proceeded more slowly at room temperature, over the course of a 1-2 h. Complex **2.3** was isolated in 90% yield and could be handled outside of the glovebox. An x-ray crystal structure was obtained confirming that this is the σ-aryl complex. Notably, an analogous bisphosphine aryl-Ni^{II}-F was accessed in

75% yield via reaction of the commercial aryl-Ni^{II}-chloride complex **2.4** with CsF or tetramethylammonium fluoride (TMAF) for 3 h at room temperature in THF (Figure 2-5).

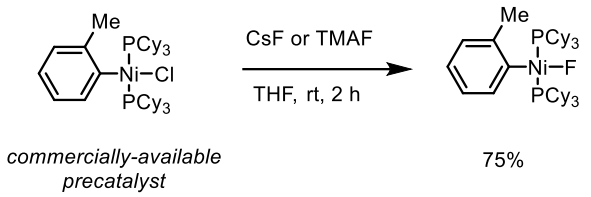

Figure 2-5. Synthesis of (o-tolyl)Ni(PCy3)2F via halogen exchange

Stoichiometric studies were carried out to compare the rates of oxidative addition and carbonyl de-insertion as a function of phosphine ligand (PCy_3 versus PPh_2Me). A solution of Ni/ligand (1.5 equiv/3 equiv) was added to the acid fluoride **2.6** (1 equiv) in a glovebox, and the reaction progress was monitored by ^{19}F NMR spectroscopy. As shown in Figure 2.6, for PCy_3, fast oxidative addition was observed, yielding over 60% yield of the acyl-Ni^{II}-F species **2.7** within 10 min at room temperature. The diagnostic Ni-F signal of **2.7** appears as triplet at -330.61 ppm (J = 45 Hz). After the first 20-30 min, this signal begins to decrease with concomitant formation of a new Ni-F signal as a triplet at -370 ppm (J = 45 Hz). This new signal corresponds to the aryl-Ni^{II}-F intermediate **2.5** (confirmed through the independent synthesis of this complex in Figure 2.5). The plot in Figure 2-6 shows that the disappearance of **2.7** proceeds at a similar rate to the appearance of **2.5**.

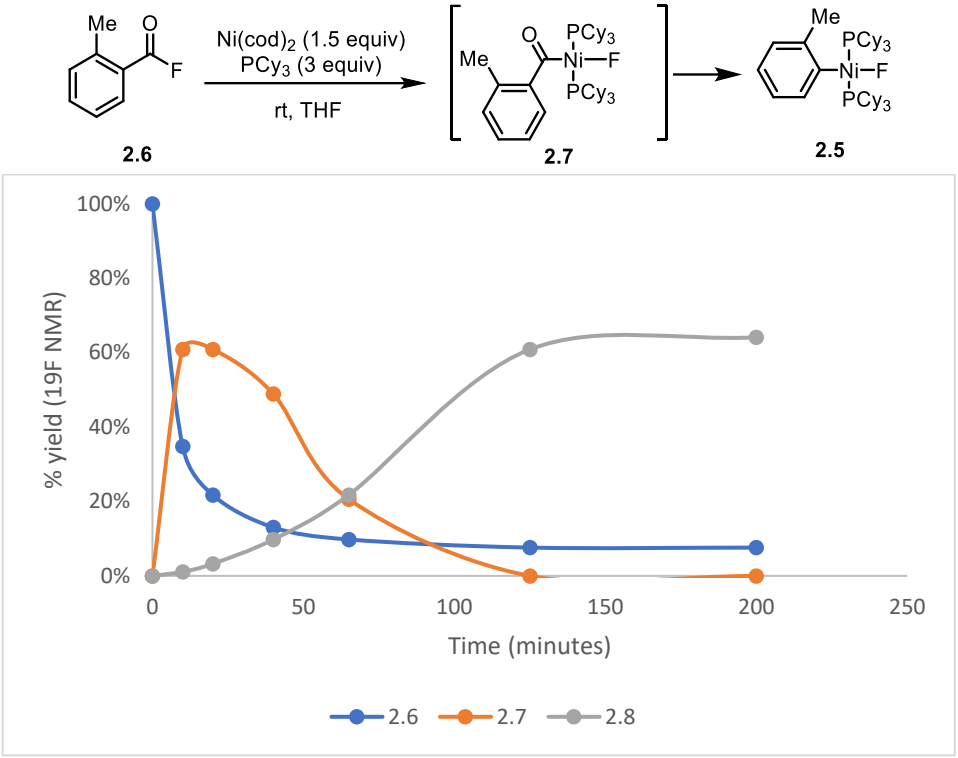

Figure 2-6. Stoichiometric reaction of 2.6 with Ni0/PCy3.

In marked contrast, when the same stoichiometric reaction was carried out with PPh_2Me, no acyl-Ni-F signal was observed by ^{19}F NMR spectroscopy (Figure 2-7). Instead, only one Ni-F triplet was detected by ^{19}F NMR spectroscopy throughout the reaction (a triplet at -350 ppm, J = 45 Hz). ^{31}P NMR revealed a doublet (-1.5 ppm, J = 45 Hz). The yield of this intermediate (assigned as **2.8**) was relatively low, reaching only ~20% after 40 min. This complex could not be isolated cleanly form the decarbonylation reaction, likely due to poor stability. To confirm its identity as the *trans*-bisphosphine aryl-Ni^{II}-F, we synthesized **2.8** independently from the aryl-Ni-Cl analogue using the procedure shown in Figure 2-8. First, we performed a phosphine ligand exchange on the readily available complex **2.9**, displacing triphenylphosphine with PPh_2Me to form **2.10**. Next, a salt metathesis with TMAF yielded the target aryl-Ni^{II}-F complex **2.8**. As predicted, the ^{19}F NMR

and ^{31}P NMR signals associated with this independently synthesized **2.8** were identical to those observed during the decarbonylation of **2.6**. (^{19}F NMR: -350 ppm (t, J = 45 Hz); ^{31}P NMR: -1.5 ppm, (d, J = 45 Hz)). Overall, in the stoichiometric reactions with PPh_2Me, the oxidative addition product acyl-Ni^{II}-F appears to be too short-lived to be observed by ^{19}F NMR spectroscopy, indicating that the rate of CO de-insertion is very fast relative to that of oxidative addition.

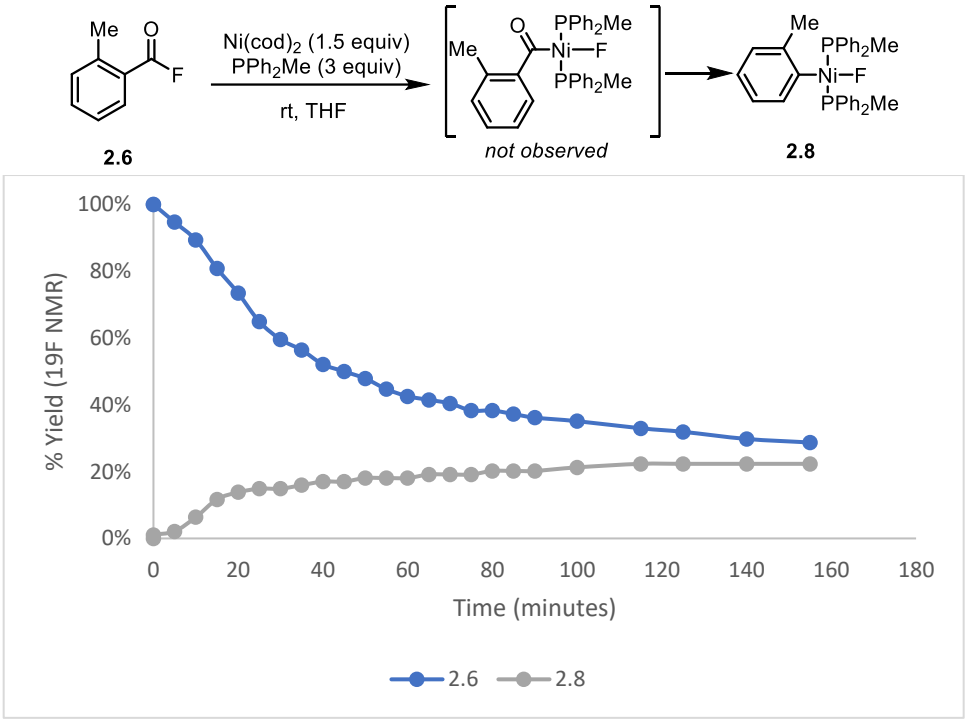

Figure 2-7. Stoichiometric reaction of **2.6** with Ni^0/PPh_2Me.

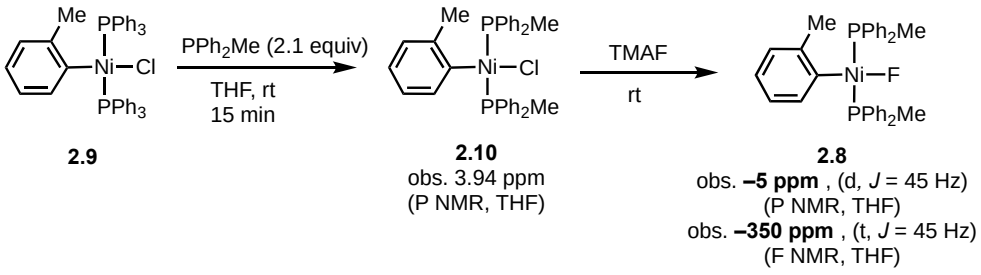

Figure 2-8. Synthesis of **2.11** authentic sample

We next sought to evaluate the reactivity of these Ni^{II}(aryl)(F) complexes towards C(sp^2)–F bond-forming reductive elimination (Figure 2-9). However, disappointingly, heating **2.3** up to 190 ºC in a wide variety of solvents did not lead to the formation of even traces of the reductive elimination product **2.11**. Under these conditions, the ^{19}F NMR signal for **2.3** disappeared, but no identifiable organic products were observed. We hypothesized that different ligands might be needed to promote C–F coupling. As such **2.3** was also heated in the presence of various Buchwald-type phosphines (e.g., BrettPhos, ^{t}BuBrettPhos, AlPhos, RuPhos, SPhos), with the hypothesis that they could undergo ligand exchange and subsequent C–F coupling. However, again, none of **2.11** was detected. Finally, we reasoned that a higher oxidation state of nickel might facilitate C-F reductive elimination.[30] As such, **2.3** was treated with F^+ oxidants such as NFSI and Selectfluor. However, again, the aryl fluoride product was not observed.

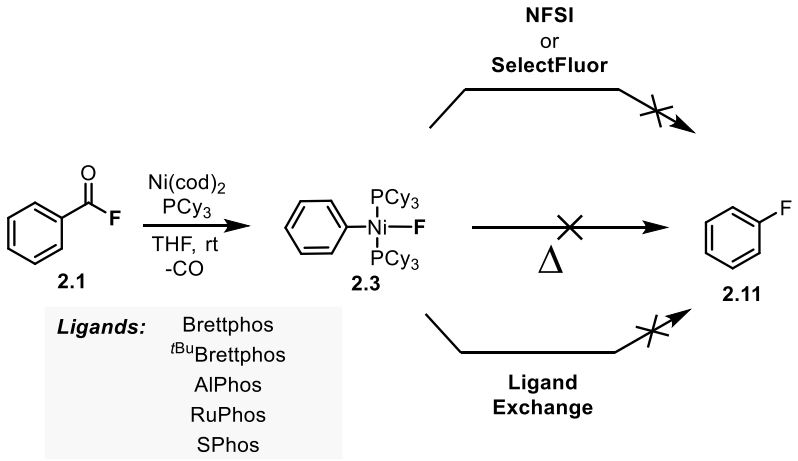

Figure 2-9. Attempts at C(sp2)–F reductive elimination from Aryl-Ni-F

Though C-F reductive elimination proved challenging in these systems, we hoped to find other useful transformations with these Ni^{II}(aryl)(F) complexes. With this goal in mind, stoichiometric reactions were carried out between Ni^{II}(aryl)(F) complex **2.3** and other nucleophilic coupling partners. A key finding from this study was that **2.3** reacts readily with aryl boronic acids under base-free conditions. As shown in Figure 2-10, the treatment of **2.3** with *para*-fluorophenylboronic acid **2.12** resulted in 90% yield of biaryl **2.13** within 1 hour at room temperature in THF (as determined by ^{19}F NMR stpectroscopic monitoring of the reaction). Notably, no exogeneous base was required for this sequence, which presumably proceeds via transmetalation at Ni(II) followed by rapid C–C bond-forming reductive elimination. Notably, most Suzuki-Miyaura-type couplings require a base to facilitate transmetallation with the aryl boron coupling partner. This discovery that Ni^{II}(aryl)(fluoride) complexes (1) can be formed readily from aroyl fluorides and (2) are "transmetallation active" with boronic acids led us to pursue Ni-catalyzed decarbonylative cross couplings between aroyl fluorides and aryl boranes. The overall goal of this work (which is detailed in the next section, 2.2) was to achieve a base-free Suzuki-Miyaura-type coupling.

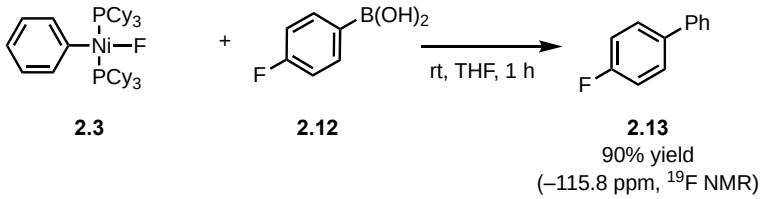

Figure 2-10. Base-free biaryl synthesis from Aryl-Ni-F.

2.3 Decarbonylative Suzuki-Miyaura Coupling of Acid Fluorides

The development of a base-free Suzuki-Miyaura coupling would enable the use of base-sensitive organoboron partners that are traditionally inaccessible in these reactions.[31-33] Examples include polyfluorinated arenes, pyridyl boronic acids, and alpha-heteroaryl boronic acids.[32,33] In the presence of base, these reagents decompose within seconds to the proto-deborylated products (Figure 2-11), rendering them inactive in catalysis.[32,33] Based on the stoichiometric experiments outlined in Figure 2-10, we aimed to develop a base-free decarbonylative Suzuki-Miyaura-type coupling between acid fluorides and boronic acids.

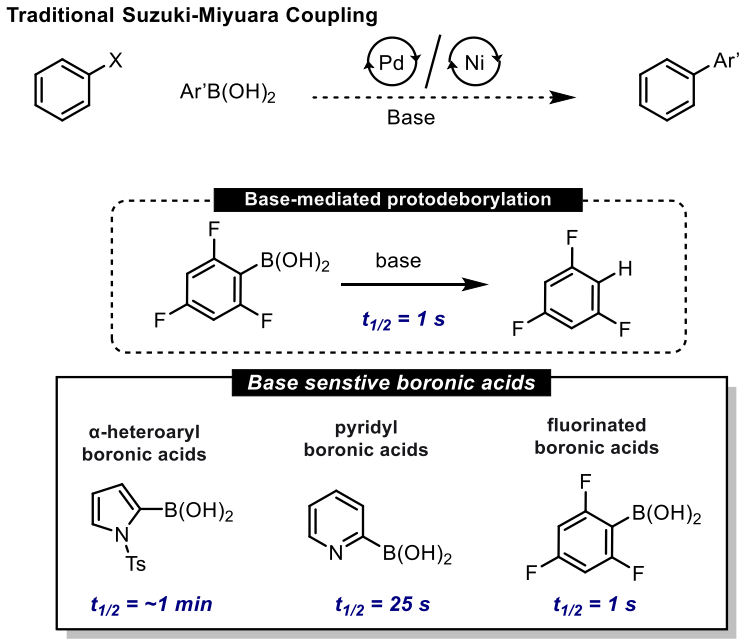

Figure 2-11. Base sensitivity of (hetero)arylboronic acids.[31-33]

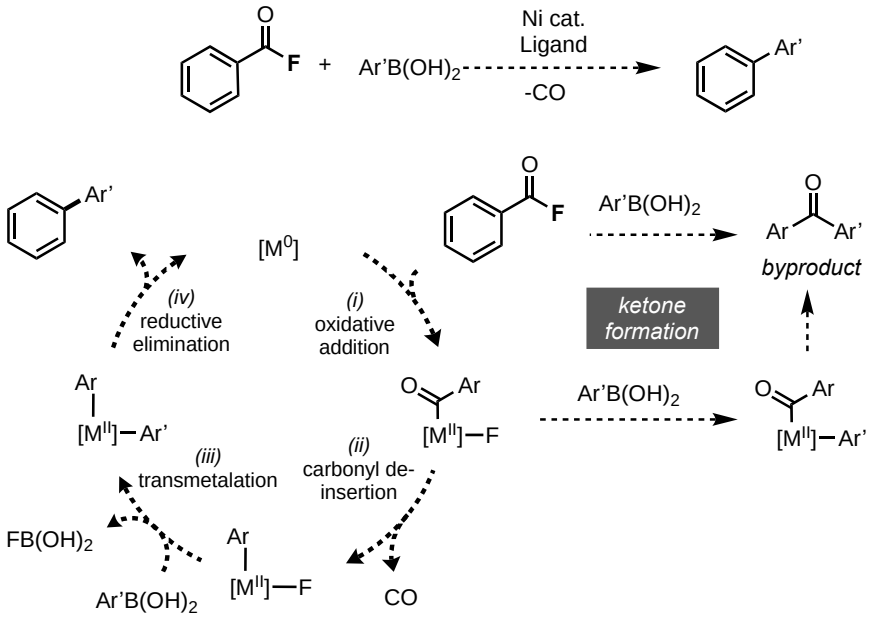

Figure 2-12. Proposed decarbonylative Suzuki-Miyuara coupling.

A catalytic cycle for this transformation is outlined in Figure 2-12. In the first step, acid fluoride oxidatively adds to the Ni(0) catalyst forming an acyl-Ni^{II}-F intermediate (step i). From here, carbonyl de-insertion yields an aryl-Ni^{II}-F (step ii). This species is the "transmetalation active" intermediate that engages with the aryl boron nucleophile (step iii). C-C reductive elimination (step iv) then yields the target biaryl product and regenerates the catalyst. At the outset of this project, a significant concern was that the acyl-Ni^{II}-F intermediate formed in step i could also engage with the aryl boron nucleophile, leading to undesired ketones byproducts. Such ketones could also form via an uncatalyzed background reaction between the acyl electrophile and boronic acid. However, the second route to ketones was ruled out through control reactions, which showed that acid fluorides are compatible with boronic acids. No significant amount ketone was formed upon heating these reagents in the absence of Ni(0). This indicates that any ketone formation under catalytic conditions would originate from premature transmetalation.

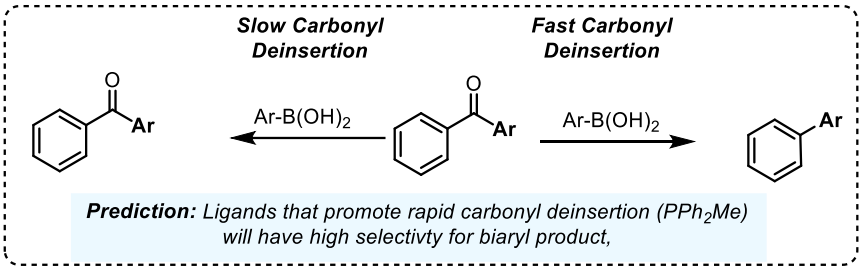

Figure 2-13. Nickel-fluoride intermediates demonstrate base-free transmetallation activity.

We reasoned that a key to limiting ketone formation would be to minimize the concentration of the acyl-Ni^{II}-F intermediate by achieving fast carbonyl de-insertion. As shown in Figure 2-13, we hypothesized that this could be achieved by varying the phosphine ligand. We noted that in the stoichiometric reaction with PCy_3 as a ligand (Figure 2-6), the acyl intermediate was detectable and persisted in solution for 100 min. In contrast, in the analogous experiment with PPh_2Me as the ligand (Figure 2-7), no acyl-Ni-F was detected because CO de-insertion was extremely fast. This led us to predict that PPh_2Me-based Ni-catalyst would provide higher selectivity in catalysis for formation of the biaryl product relative to the PCy_3 analogues.

Our initial attempts for catalysis began with reacting benzoyl fluoride **2.14** and aryl boronic acid **2.15** with 10 mol % $Ni(cod)_2$ and 20 mol % of various monodentate phosphine ligands. As predicted above, the selectivity for the ketone product **2.16** versus biaryl product **2.17** was highly dependent on the choice of phosphine ligand. Electron-rich (triethyl)phosphine (PEt_3), while low yielding, favored ketone **2.16** formation in a 30:70 ratio. PCy_3 demonstrated better conversion (>80% yield) and favored the decarbonylated product **2.17**, 85:15. However, significant quantities of ketone were still observed. As predicted based on the stoichiometric studies, PPh_2Me provided extremely high selectivity (99:1) for the biaryl product as well as good yield (Figure 2-14).

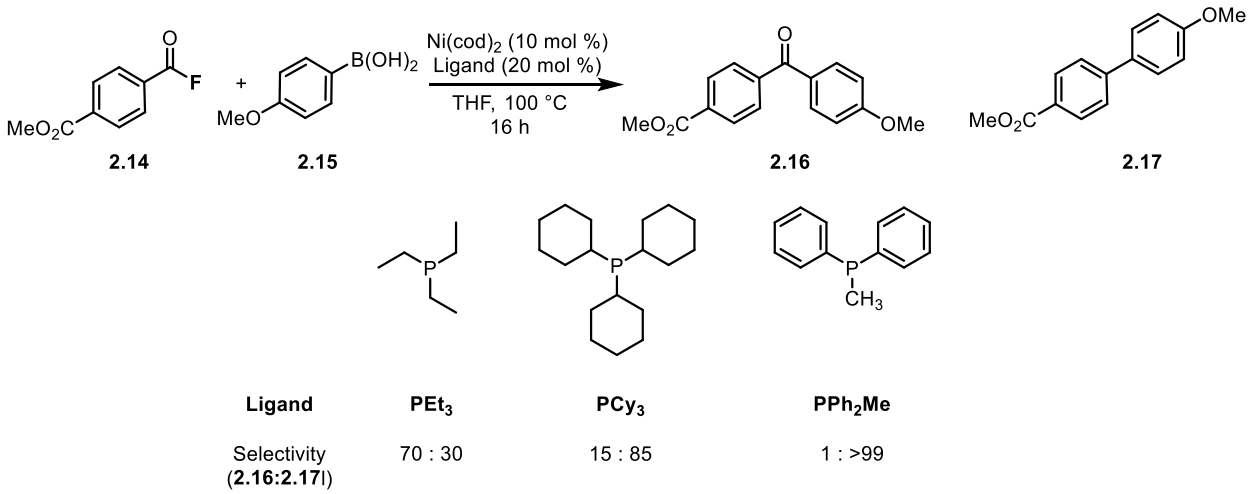

Figure 2-14. Selectivity of ketone to biaryl as a function of ligand.

The scope of this transformation for the electrophilic carboxylic acids and the nucleophilic boronic acids can be found in Figures 2-15 and 2-16, respectively. Dr. Christian Malapit carried out all isolation and characterization of biaryl products. A variety of electron rich and electron poor aryl carboxylic acids performed well in catalysis. Esters, nitriles, sulfonamides, amides, alkenes, imidazoles, oxazoles, and pinacolboronate esters are all compatible with the reaction conditions. Aryl chlorides and aryl phenyl esters, common electrophiles in cross-coupling catalysis, are tolerated, demonstrating the orthogonality of this method. Heteroaromatic carboxylic acids are also effective coupling partners. Finally, various carboxylic acid-containing bioactive molecules, including probenecid, bexarotene, tamibarotene, telmisartan, flavone, and febuxostat participated as coupling partners in this methodology.

Using probenecid as the electrophile, the scope of boronic acids was also explored. A key advantage of this methodology is that base-sensitive boronic acids can be used. Substrates known to undergo rapid protodeborylation, such as alpha-heteroaryl boronic acids and polyfluorinated arenes were also successfully coupled in good yields.

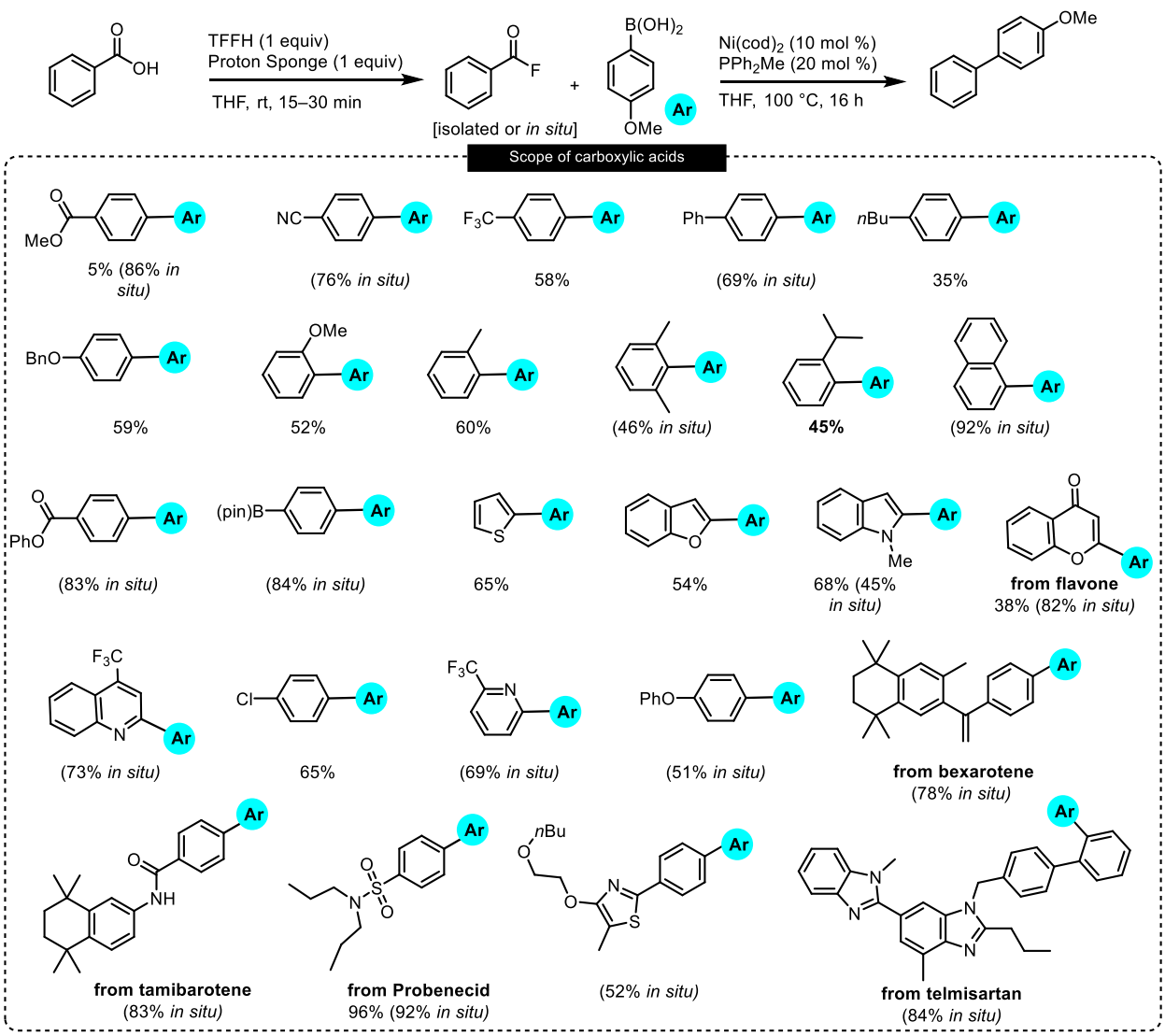

Figure 2-15. Scope of aryl carboxylic acids.

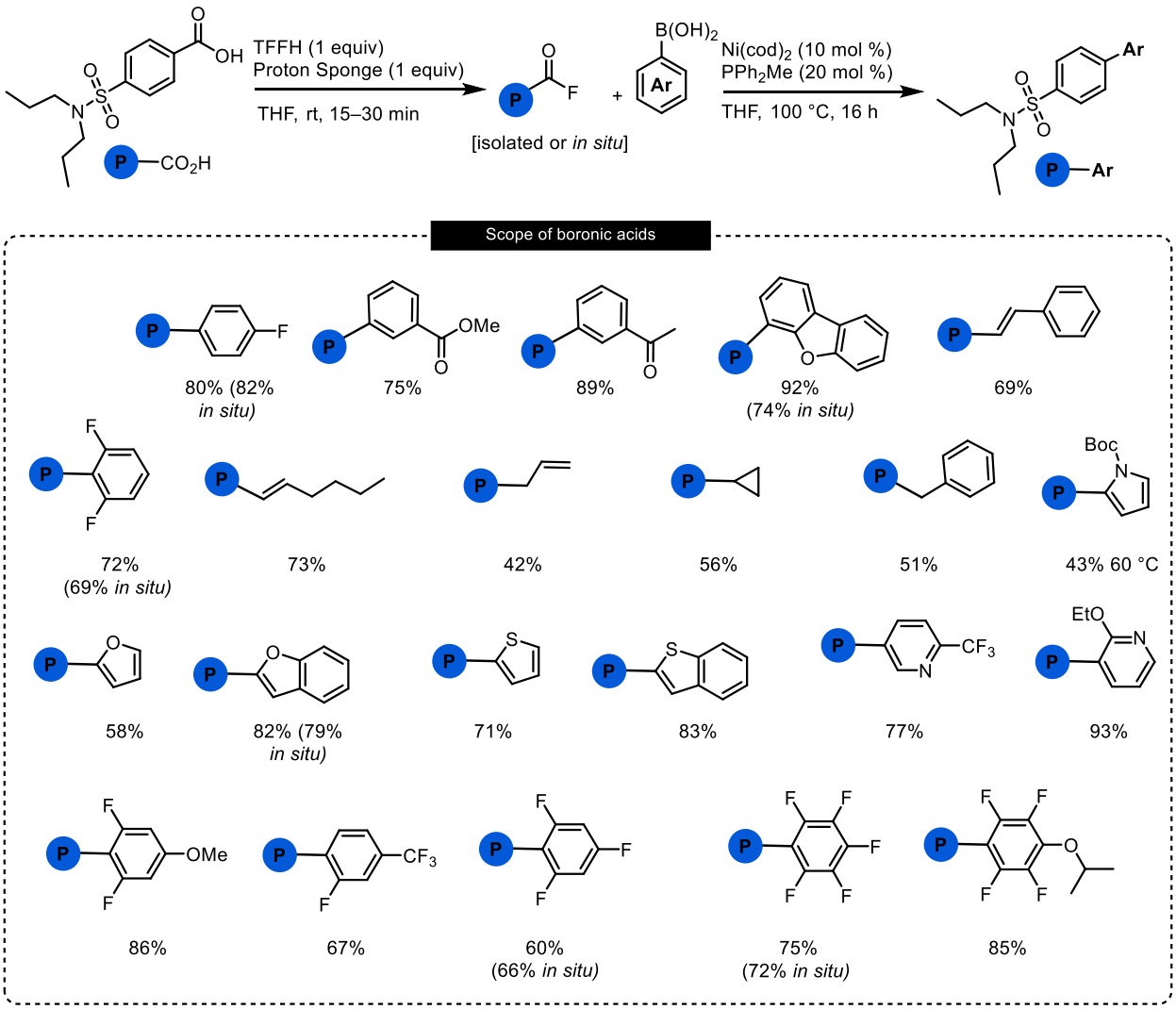

Figure 2-16. Scope of boronic acids.

2.4 Investigation for a Decarbonylative Synthesis of Aryl Amines

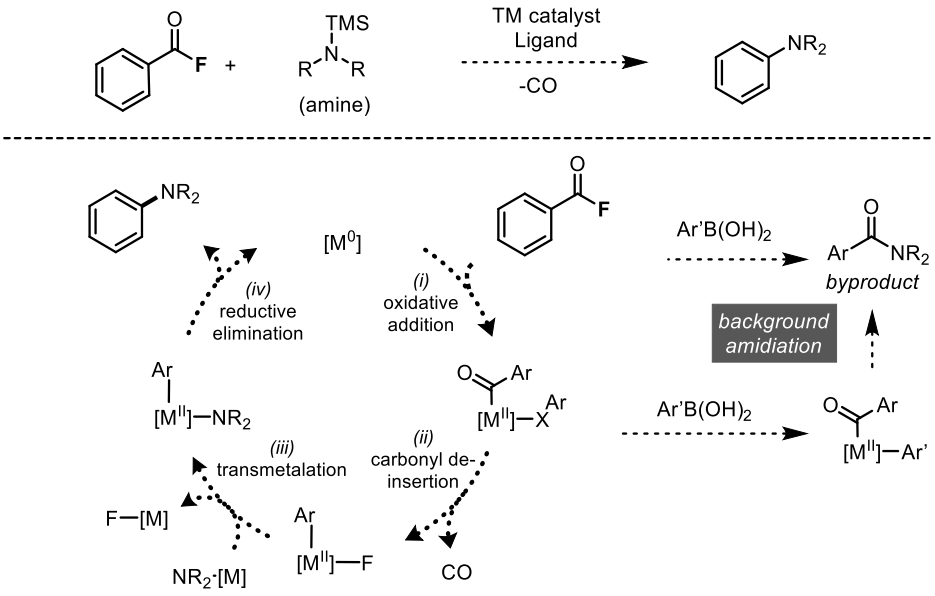

Figure 2-17. Proposed decarbonylative synthesis of aryl amines.

While there has been a large focus on decarbonylative C-C coupling, there is a need for greater development for decarbonylative C-N amination (Figure 2-17). The major challenge associated decarbonylative aminations is the competitive side reactivity with highly nucleophilic partners to form amide byproducts.[34,35] Buchwald and Hartwig set the standard for efficient C-N cross-coupling with their independently developed Pd-catalyzed amination protocols,[36] and these methods have since been expanded to nickel catalysts.[37-46] When we initiated this work, most decarbonylative cross-coupling methodologies of carboxylic acid derivatives had focused on C–C coupling and only a very few had been reported for synthesizing C(sp^2)–N bonds.[7] A major challenge for achieving decarbonylative C–N coupling is preventing direct amidation of the carboxylic acid derivative, whether uncatalyzed or catalyzed. We sought to investigate the feasibility of a decarbonylative amination of arenes via a nickel-catalyst system. Through initial stoichiometric investigations we aimed to (1) identify a combination of acid derivative and amine

nucleophile to prevent background amidation while preserving transmetallation activity, (2) test the viability of each step in the catalytic cycle, and (3) optimize the nickel/ligand platform for productive and efficient catalysis.

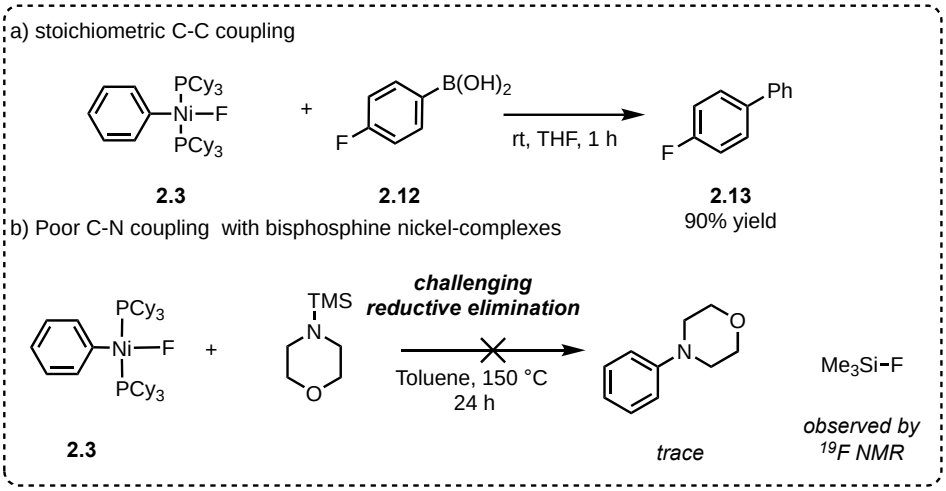

Figure 2-18. Stoichiometric transmetallation from Ph(PCy3)2Ni(F).

Initial experiments focused on the use of acid fluorides as electrophiles in conjunction with *N*-trimethylsilyl (TMS) amines as nucleophiles (Figure 2-18). Notably, the silyl protected amines (rather than the free amines) were employed to minimize background uncatalyzed amidation of the acid fluoride. As described in sections 2.1 and 2.2, benzoyl fluoride reacts with Ni(0)/PCy_3 to form aryl-Ni^{II}-F **2.3** via oxidative addition followed by carbonyl de-insertion. Complex **2.3** was then treated with TMS-morpholine to probe the viability of the transmetallation and reductive elimination steps to form the desired aminated product (Figure 2-18, b). After 24 h at 150 ºC, TMSF was detected ^{19}F NMR spectroscopy (as a singlet at -151 ppm). However, only a trace of the aryl amine was observed by GC/GCMS. We hypothesized that this was due to slow slow C(sp^2)–N bond-forming reductive elimination from the PCy_3-ligated Ni^{II} complex.

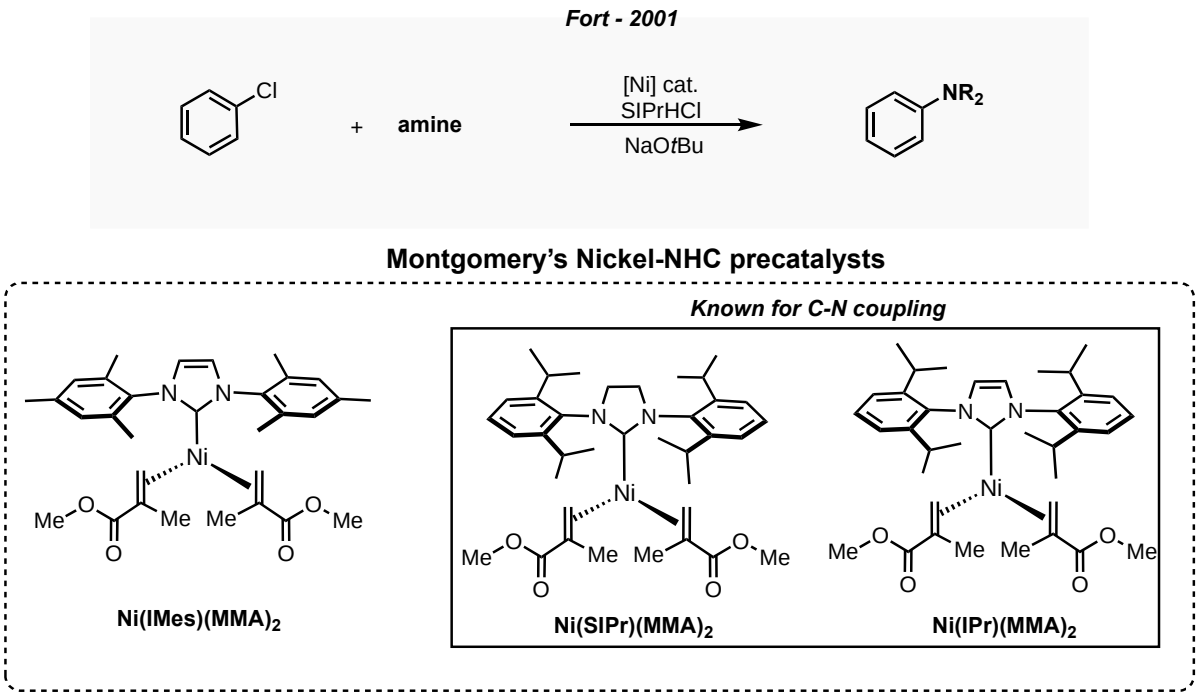

Figure 2-19. NHC ligands are known to facilitate C-N reductive elimination from Ni(II).

To address this challenge, we sought alternative ligands that were known to show high reactivity in Ni-catalyzed C-N bond-forming reactions. *N*-Heterocyclic carbenes (NHCs) were selected due to their known ability as ligands for Ni-catalyzed cross-coupling between aryl halides with amines [IMes = 1,3-bis(2,4,6-trimethylphenyl)-1,3-dihyddro-2*H*-imidazole-2-ylidene; SIPr = 1,3-bis(2,6-diisopropylphenyl)-4,5-dihydroimidazole-2-ylidene ; IPr = 1,3-bis(2,6-diisopropylphenyl)imidazole-2-ylidene; MMA = (methyl)methacrylate] (Figure 2-19).[47-49] Here, we began a collaboration with the Montgomery group, where we evaluated their Ni^0-NHC precatalysts for decarbonylative coupling.[49] We reasoned that their Ni(0)-precatalysts with the NHC ligands already ligated would allow for straightforward evaluation of stoichiometric reactions with aroyl fluorides.

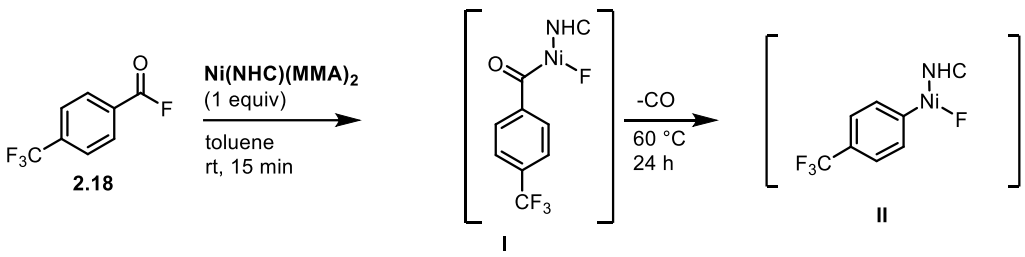

Entry	NHC	% yield I (ppm)	% Yield II (ppm)
1	IMes	55 (-375 ppm)	57 (-402 ppm)
2	SIPr	20 (-371 ppm)	47 (-398 ppm)
3	IPr	10 (-377 ppm)	40 (-404 ppm)

Figure 2-20. Stoichiometric decarbonylation of aroyl fluorides with Ni-NHC precatalysts.

The treatment of Ni-NHC complexes with aroyl fluoride **2.18** resulted in low- to moderate-conversion to an acyl Ni-F intermediate **I** detected by ^{19}F NMR spectroscopy (observed as a singlet at between -370 and -380 ppm). The solutions were then gently heated to 60 °C overnight. After heating, all Ni-F signals shifted to approximately -400 ppm, consistent with CO de-insertion to form Ni^{II}(aryl)(fluoride) **II** (Figure 2-20). However, these products were less stable than the analogous bi-sphosphine complexes, and all isolation attempts for proved fruitless.

Nonetheless, we could still test the viability of C-N reductive elimination in these systems via *in* situ generation of the complex followed by addition of the amine nucleophile. Bulky, electron-rich IPr ligand was chosen for our model system. Ni/IPr catalyst systems have been used in several C-N bond forming reactions.[47,49] For this reason, we believed that this metal/ligand combination could potentially allow us to access a challenging C-N reductive elimination, if our silylamines can transfer with the nickel-fluoride. When we carried out this *in situ* sequence with Ni(IPr)$(MMA)_2$, we observed the formation of **II** in 12% yield by ^{19}F NMR spectroscopy (lower yield of Ni-F was observed due to the reaction being heated at 60 °C for only 2 hours instead of overnight). The treatment of this solution with 2 equiv of TMS-morpholine led to quantitative

formation to the desired aryl amine product **2.19** (yield determined based on amount of **II** in solution; Figure 2-21). This sequence demonstrates the feasibility of each step in the proposed catalytic cycle.

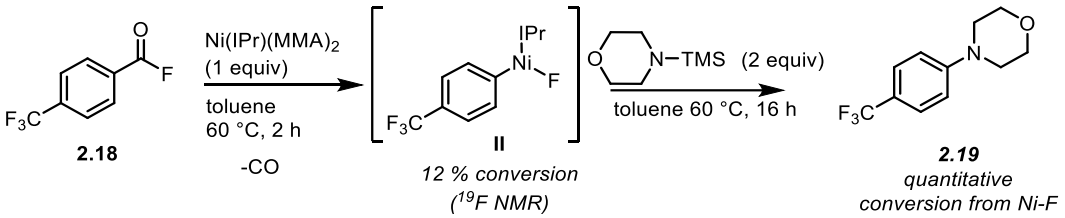

Figure 2-21. Stoichiometric decarbonylation/amination of acid fluoride via (aryl)Ni(IPr)F

The next aim of this project was to translate these stoichiometric studies into an efficient catalytic method. A major challenge for designing such a reaction was achieving selectivity for the desired aryl amine coupled product **2.19** relative to the formation of amide **2.20**. As shown in Figure 2-17, after oxidative addition, the acyl-Ni^{II}-F intermediate has two possible reaction pathways. First, it could undergo carbonyl de-insertion before reacting with the TMS-amine to yield amide. The second option would be to undergo transmetallation with the (silyl)amine before decarbonylation could occur. Subsequent C–N coupling at this stage would result in amide byproduct. Similar to section 2.2, our proposed solution was to use ligand design to increase the rate of carbonyl de-insertion while slowing the rate of transmetalation in these systems in order to minimize Ni-catalyzed amide formation. As detailed below, this required tuning of the NHC ligand as well the electrophile/nucleophile pair to achieve the correct balance of relative rates.

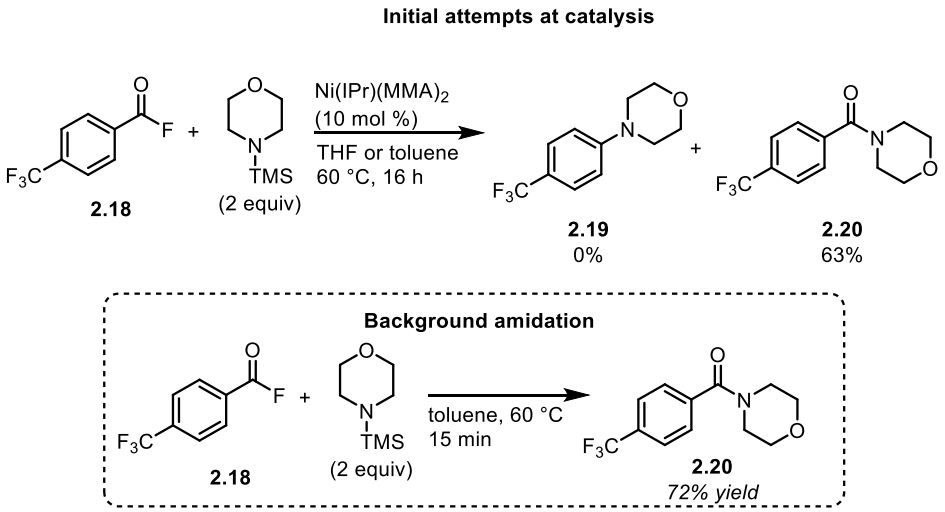

Figure 2-22. Initial catalytic attempts only yielded amide due to a background reaction of the acid fluoride and TMS-morpholine.

Early experiments focused on finding a suitable nucleophilic partner. While our initial stoichiometric reactions used TMS-morpholine, catalytic studies with this nucleophile under a wide variety of conditions only yielded the amide byproduct **2.20**. Ultimately, we discovered that this was due to an uncatalyzed background reaction between TMS-morpholine and the aroyl-fluoride electrophile under the reaction conditions (Figure 2-22). The less nucleophilic silyl amine TMS-(*N*-methyl)aniline **2.21** did not undergo the same background reaction and was thus utilized moving forward (Figure 2-23). Stoichiometric transmetallation studies between (IPr)Ni^{II}(Ar)(F) and **2.21** afforded the desired C–N coupled product **2.22**, providing further support that NHCs are effective ligands for C–N reductive elimination at nickel(II). However, we were never able to achieve successful catalytic decarbonylative coupling with the NHC-ligand system due to poor relative rates of carbonyl de-insertion, and all attempts at catalysis resulted in amide formation (Figure 2-24).

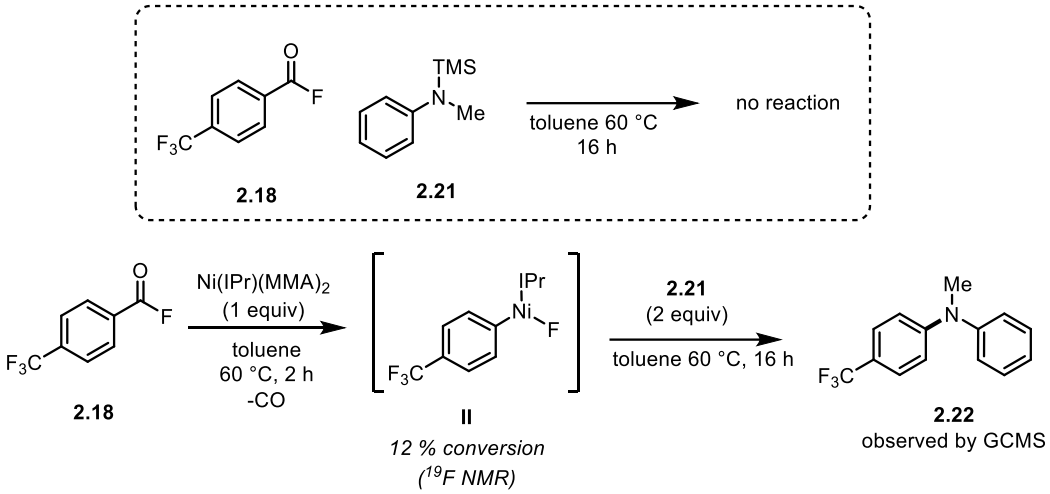

Figure 2-23. Less nucleophilic TMS-(N-methyl)aniline avoids background amidation, yet still transmetallates with Ni-F.

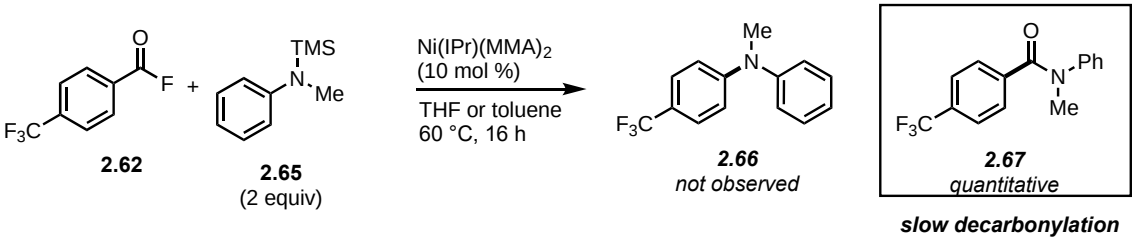

Figure 2-24. Aniline substrate still selective for amide due to slow decarbonylation.

We next hypothesized that a cooperative combination of NHC and phosphine ligands might enhance the rate of carbonyl de-insertion. Using a mixed NHC (IPr)/phosphine (PPh_2Me) system in an analogous stoichiometric reaction, we observed a faster rate of carbonyl de-insertion and higher yields of aryl-Ni-F (Figure 2-25). Oxidative addition of the aroyl fluoride appears to be slightly faster in the absence of phosphine, but we consistently saw higher yields of aryl-Ni-F when 1 equiv of phosphine ligand was used. The higher yield may result from a stabilizing effect of the phosphine ligand. Tracking the reaction by ^{19}F NMR spectroscopy revealed that the rate of carbonyl de-insertion was faster in the presences of PPh_2Me. ^{19}F NMR showed signals diagnostic

for (IPr)Ni(PPh$_2$Me)(Ph)F at -346 ppm (d, J = 58.6 Hz) which was the only Ni-F complex observed.

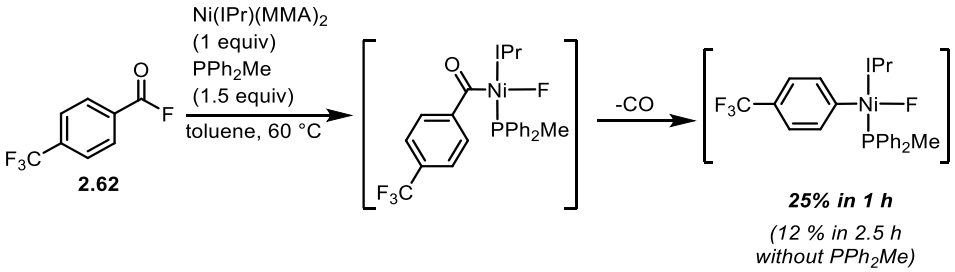

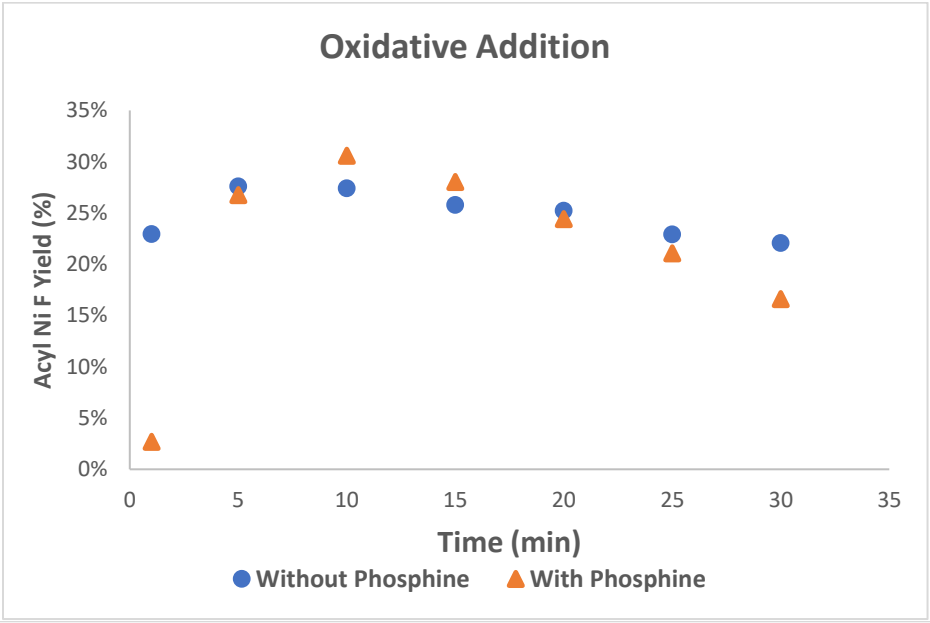

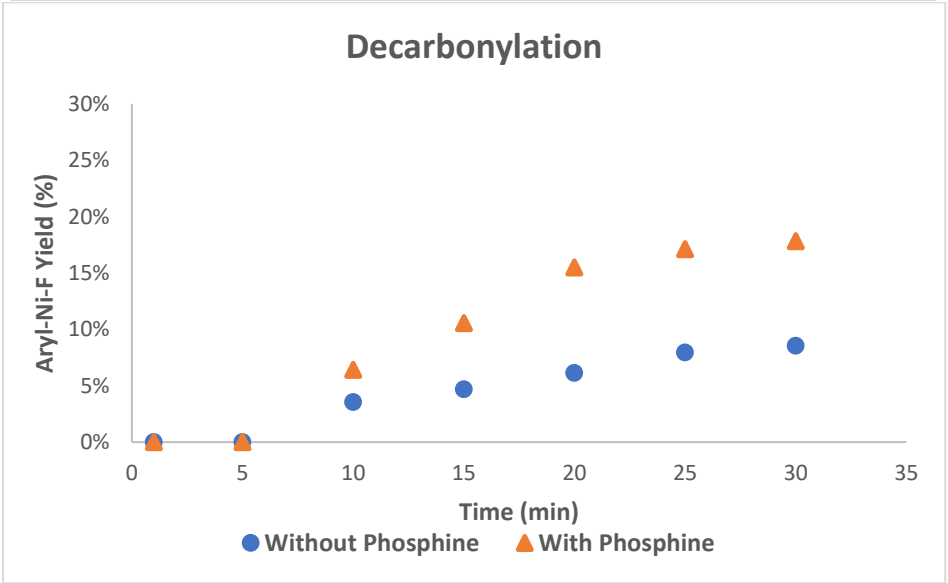

Figure 2-25. Rate of decarbonylation increased with PPh2Me.

We next tested to see how this higher rate of decarbonylation may impact our observed selectivity in catalysis. We hoped that by increasing the rate of carbonyl de-insertion, a higher concentration of decarbonylated intermediate would favor a C–N coupling to form the desired aryl amine. When benzoyl fluoride and TMS(*N*-methyl)aniline are subjected to a Ni-IPr catalyst in the presence of PPh_2Me, we were delighted to see the target aryl amine product in 7% yield (Figure 2-25). Ultimately, however, Ni-NHC ligands never showed sufficient decarbonylation reactivity for a fully catalytic system.

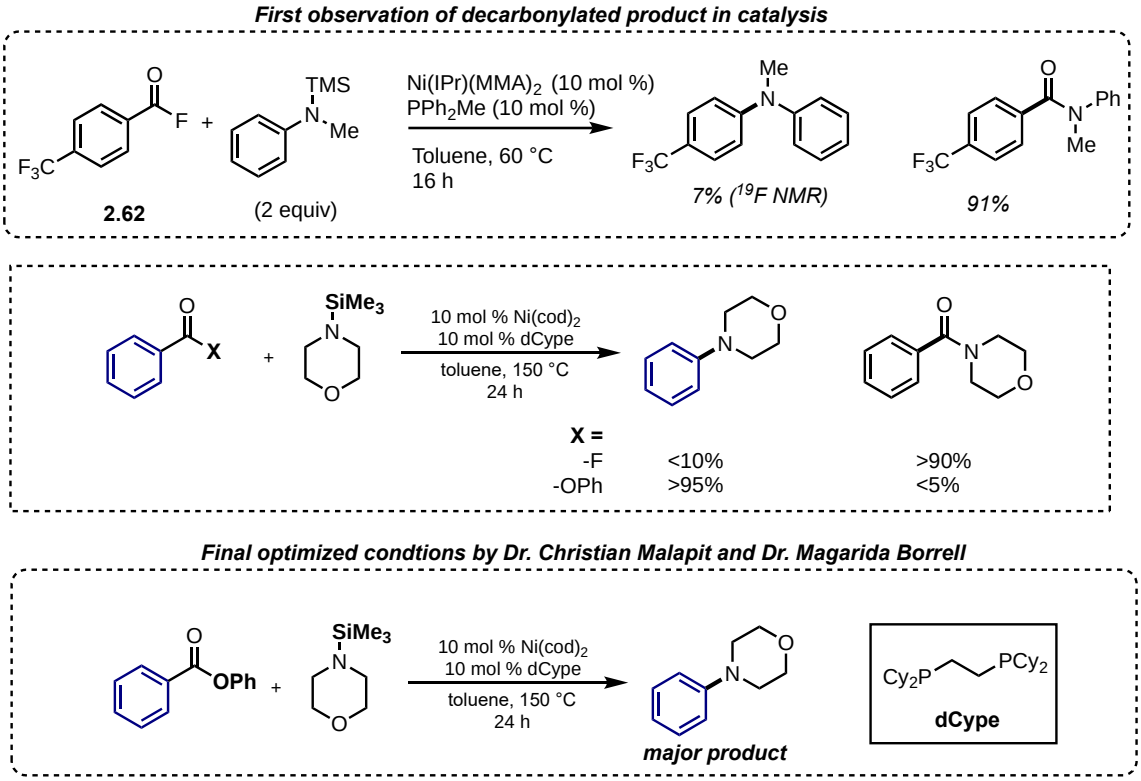

Figure 2-26. First observation of decarbonylated aryl amine in catalysis observed with PPh2Me; Optimized conditions with.

Further optimization by Dr. Christian Malapit and visiting researcher Dr. Margarida Borrell identified a bidentate phosphine ligand, bis(dicyclohexylphosphino)ethane (dCype), that induces C–N reductive elimination (Figure 2-26). Importantly, this phosphine ligand promotes carbonyl de-insertion more efficiently than the NHC, allowing for greater selectivity for transmetallation at

the decarbonylated aryl-Ni^{II}-X. Another significant optimization of this reaction was switching from aroyl fluorides to an aroyl phenyl esters. This limited uncatalyzed amidation, while retaining transmetallation activity with silyl amines, allowing for a greater scope of the amine.

We found that this reaction is general for a variety of electron-deficient and electron neutral carboxylic acid esters (Figure 2-27A). Substituents such as trifluoromethyl, methyl ester, nitrile, ketone, and phenyl ether are well tolerated. Various N-containing heteroaryl carboxylic acid esters such as pyridine, quinoline, and quinoxaline derivatives are converted to N-heteroaryl amines in moderate to excellent yields. S- and O-containing heteroaryl esters such as benzothiophene, benzofuran, and thiazoles are also converted to the desired amine products. Esters derived from carboxylic acid containing drugs such as probenecid, bexarotene, and febuxostat afford good to excellent yields.

This transformation is also general with respect to the amine coupling partner (Figure 2.27B). Utilizing the probenecid ester as the electrophile, various TMS-amines react smoothly. More stable triethylsilyl (TES)- and triisopropylsilyl (TIPS)-protected amines are also effective coupling partners but afford lower yields. We also identified the commercial silyl transfer reagent *N*-methyl-*N*-(trimethylsilyl)trifluoroacetamide (MSTFA) as effective for the rapid, room-temperature conversion of diverse HNR_2 to TMS-NR_2. Indeed, the direct addition of HNR_2 and MSTFA to the standard coupling conditions resulted in effective Ni-catalyzed decarbonylative coupling. Secondary dialkyl and diaryl *N*-heterocycles such as morpholines, piperidines, piperazines, pyrrolidines, indoles, and carbazoles underwent coupling in good to excellent yields under these conditions. Furthermore, both primary aryl and alkyl amines afforded secondary aryl amine products in good yields. the current method eliminates the need for an exogenous base for

$C_{(sp2)}$–N coupling. As such, base-sensitive amine substrates are well tolerated and deliver aryl amine products in good yields.

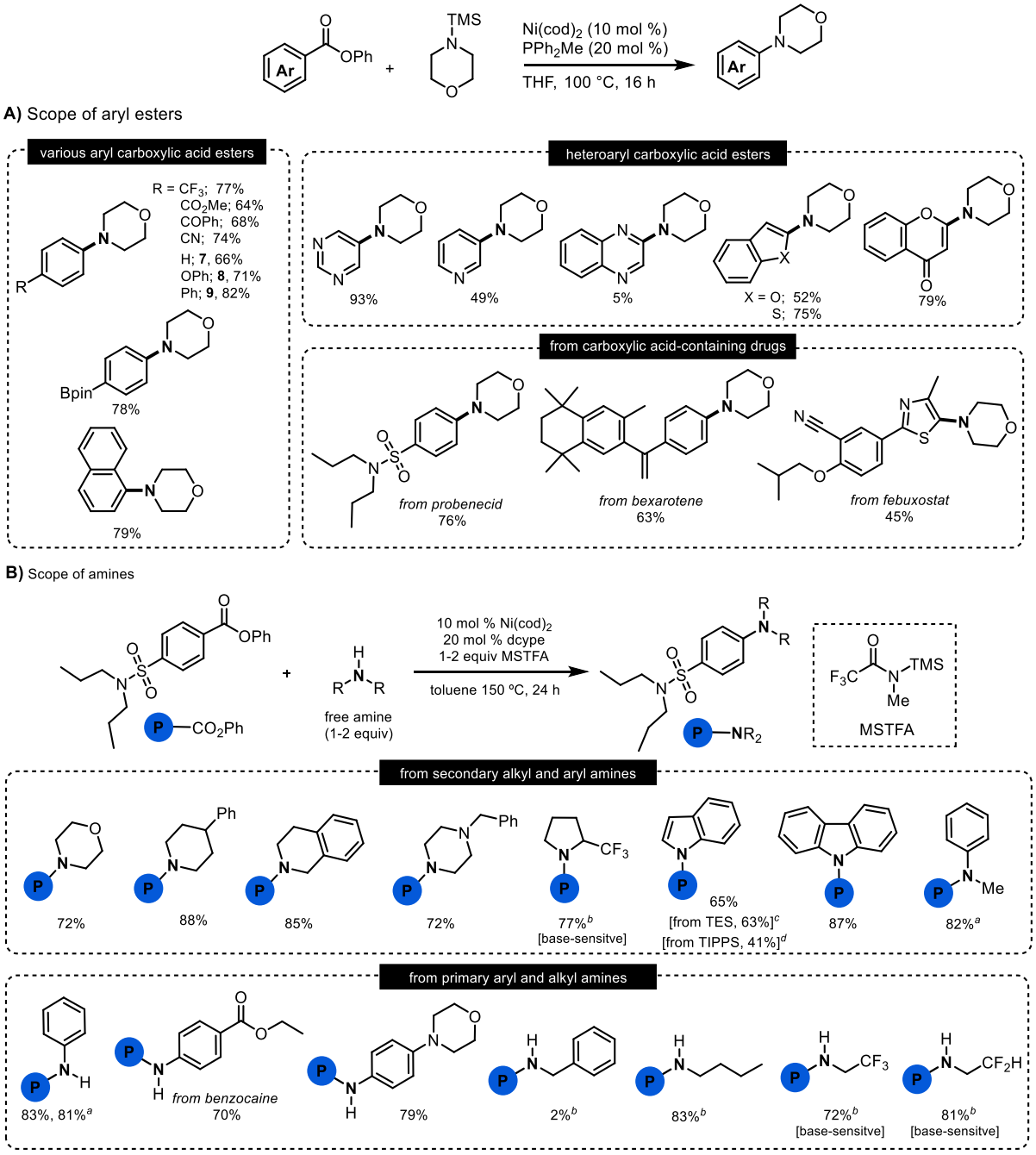

Figure 2-27. Scope of decarbonylative amination.

2.4 Conclusions

Systematic investigations into the decarbonylation of aroyl fluorides has led to the development of Ni-catalyzed cross coupling methodologies with these electrophiles. Stoichiometric studies identified monodentate phosphine ligands, specifically PPh_2Me, that promote fast carbonyl de-insertion at Ni(II). While C–F reductive elimination was unsuccessful even under forcing conditions, we found that Ni-F intermediates are reactive with organometallic nucleophiles to engage in transmetallation. Taking advantage of this reactivity, we developed two methodologies for the decarbonylative cross coupling of carboxylic acid derivatives. Acid fluoride electrophiles were successfully coupled with boronic acids under base-free conditions. This report led to successful coupling of base-sensitive boronic acids. Further, we found that aryl phenyl esters can be coupled with silyl-protected amines. Free amines can be protected *in situ*, and, again, catalysis is achieved under base-free conditions. The work from this chapter serves as a foundation for using a combination of stoichiometric studies and catalytic screens to develop decarbonylative cross coupling reactions. The following chapters expand on this work to develop decarbonylative fluoroalkyl coupling.

2.5 Experimental Procedures

2.5.1 General Information

All manipulations were performed inside an N_2-filled glovebox unless otherwise noted. NMR spectra were obtained on a Varian VNMR 700 (699.76 MHz for 1 H; 175.95 MHz for ^{13}C), Varian VNMR 500 (500.09 MHz for ^{1}H; 470.56 MHz for ^{19}F; 125.75 MHz for ^{13}C), or Varian VNMR 400 (401 MHz for ^{1}H; 376 MHz for ^{19}F; 123 MHz for ^{13}C) spectrometer. ^{1}H and ^{13}C NMR chemical shifts are reported in parts per million (ppm) relative to TMS, with the residual solvent

peak used as an internal reference. ^{19}F NMR chemical shifts are reported in ppm and are referenced to 4-fluorotoluene (–118.00 ppm). Abbreviations used in the NMR data are as follows: s, singlet; d, doublet; t, triplet; q, quartet; m, multiplet; br, broad signal. Yields of reactions that generated fluorinated products were determined by ^{19}F NMR spectroscopic analysis using a relaxation delay of 25 s with a 90º pulse angle. Mass spectral data were obtained on a Micromass Magnetic Sector Mass Spectrometer in electrospray ionization mode. Flash chromatography was performed using a Biotage Isolera One system with cartridges containing high performance silica gel.

2.5.2 Experimental Procedures

2.5.2.1 Stoichiometric decarbonylation of o-toluoyl fluoride

Using *o*-toloyl fluoride **2.6** as substrate, we conducted various decarbonylation studies with $Ni(cod)_2$ and phosphine ligands (PCy_3 or PPh_2Me). we found that decarbonylation is much faster with PPh_2Me compared to PCy_3 as the ligand. $Ni(cod)_2$ (1.5 equiv., 0.03 mmol, 8.4 mg) and ligand (0.06 mmol) were combined in a 4 mL vial and dissolved in 0.25 mL THF. The solution was stirred for 15 minutes at room temperature. A solution of acid fluoride **2.6** (0.02 mmol, 2.8 mg) and internal standard (4-fluorotoluene) in 0.25 mL THF was combined with Ni/ligand solution. The reaction was transferred to a J-Young tube and ^{19}F NMR was used to monitor the reaction. To prevent the reaction from proceeding to quickly, the NMR tube was sometimes cooled in liquid nitrogen while transferring to the NMR. The tube would then be allowed to warm to room temperature before the scans began. Reaction progress was monitored over several hours in 5-minute intervals.

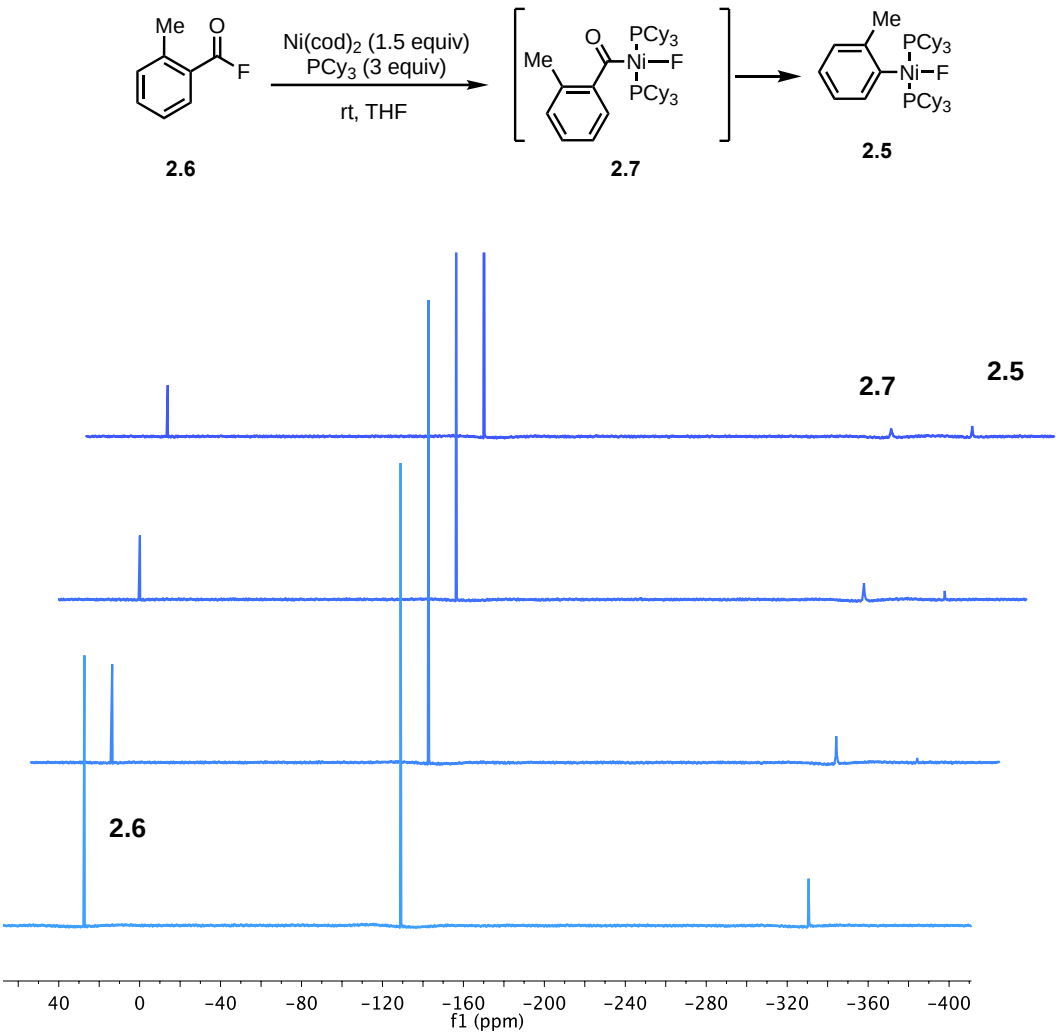

Figure S2.1 ^{19}F NMR spectrum of decarbonylation with PCy_3

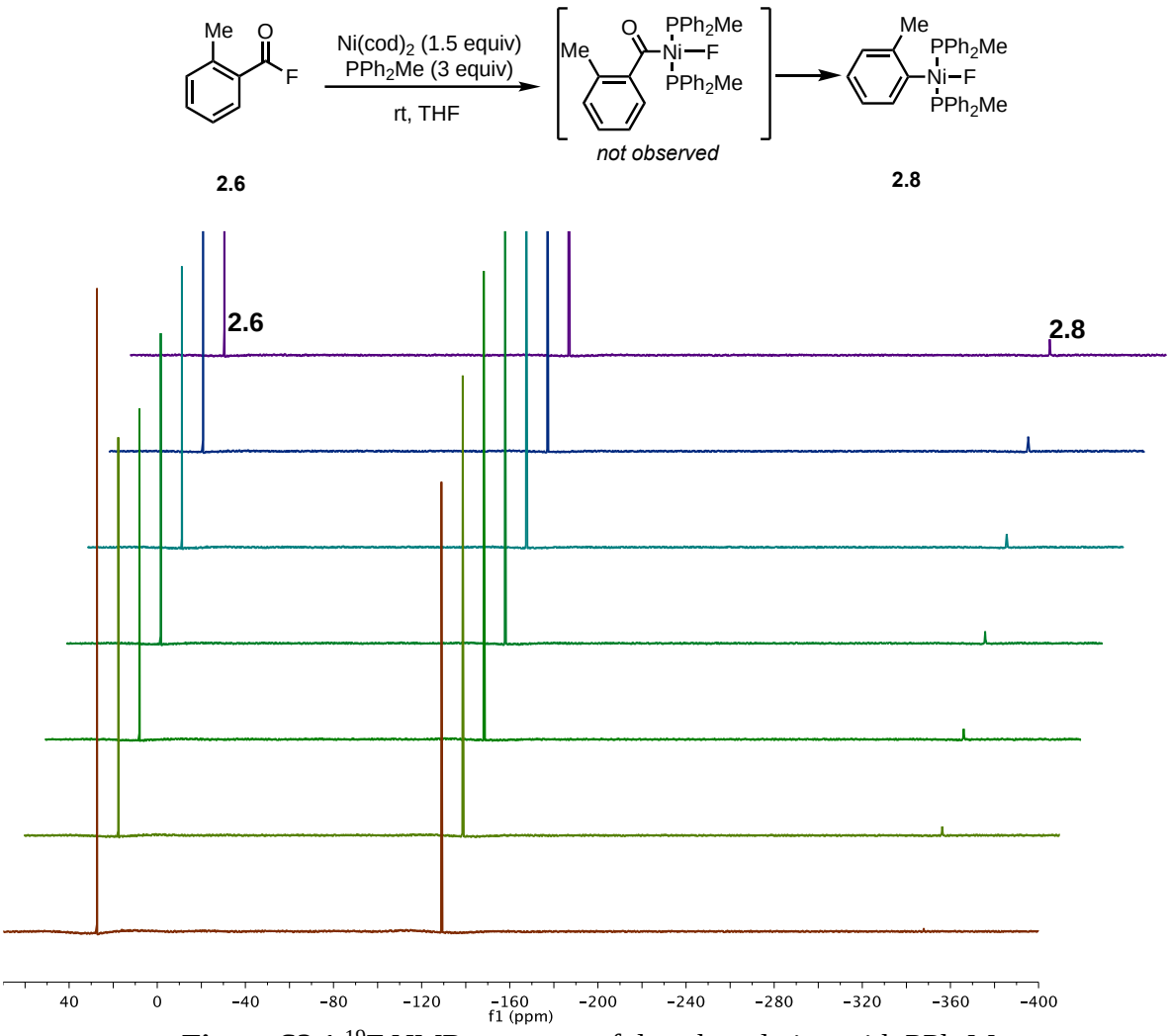

Figure S2.1 ^{19}F NMR spectrum of decarbonylation with PPh_2Me

2.5.2.2 Synthesis of 2.3

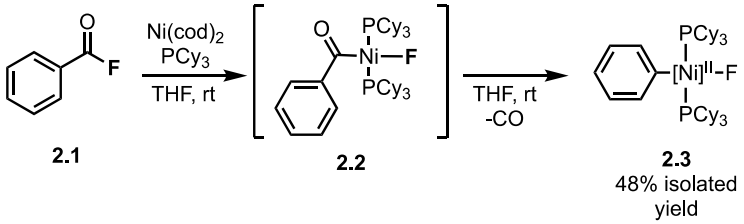

2.1 **2.2** **2.3** 48% isolated yield

In a glovebox, a 50 mL round bottom flask was charged with $Ni(cod)_2$ (300 mg, 1.10 mmol, 1 equiv), PCy_3 (665 mg, 2.37 mmol, 2.15 equiv), THF (20 mL), and a magnetic stir bar. The solution was stirred at room temperature for 25 min until all of the $Ni(cod)_2$ was dissolved. A rubber septum was added to the flask, and the solution was placed in a –35 ºC freezer for 20 min. While the Ni solution cooled, a 4 mL vial was charged with PhCOF **2.1** (165 mg, 1.33 mmol, 1.20 equiv) and THF (1 mL). This solution was added in one portion to the rapidly stirring solution of $Ni(cod)_2/PCy_3$. Upon mixing, the solution rapidly changed from a dark orange to a bright vibrant orange. After stirring for 5 min, an additional 30 mL of THF was added to the round bottom flask. The flask was then sealed with a rubber septum, removed from the glovebox, and placed in a preheated (50 ºC) oil bath. While still in the oil bath, the solution was sparged with a gentle stream of N_2 for 1 h. The flask was removed from the oil bath, allowed to cool to room temperature, and brought back into the glovebox. The volatiles were removed under reduced pressure until the volume was approximately 15 mL total at which point Et_2O (20 mL) was added to precipitate a yellow solid. The yellow precipitate was collected on a frit, washed with of Et_2O (2 x 10 mL) and pentanes (10 mL), and dried under vacuum to yield 2.3 as a bright yellow powder (376 mg, 48% yield): ^{1}H NMR (700 MHz, C_6D_6) 7.68 (d, J = 7.3 Hz, 2H), 6.88 (t, J = 7.3 Hz, 2H), 6.73 (t, J = 7.3 Hz, 2H), 2.18-2.07 (br, 12H), 1.89-1.60 (multiple peaks, 36H), 1.27-1.04 (multiple peaks, 18H); ^{13}C NMR (176 MHz, C_6D_6) 150.22 (m), 140.52, 125.41, 120.74, 32.98 (t, J = 8.2 Hz), 30.44, 28.49 (t, J = 5.1 Hz), 27.40; ^{31}P NMR (283 MHz, C_6D_6) 15.77 (d, J = 42.0 Hz); Elemental

analysis calculated for $C_{42}H_{71}FP_2Ni$, C: 70.49 H: 10.00; Found C: 70.18 H: 9.92; X-ray quality crystals of 3 were obtained by vapor diffusion of diethyl ether into at RT.

2.5.2.3 Attempts at aryl fluorination from 2.3 via oxidation

Compound **2.3** (3.6 mg, 0.005 mmol) was dissolved in 0.95 mL THF and combined with a 0.25 mL solution of oxidant (2 equiv, 0.01 mmol). The solution was stirred for 15 minutes at room temperature. The reaction was transferred to a J-young tube and ^{19}F NMR was used to monitor the reaction. ^{19}F NMR reveleaed either no reaction due to insolubility of the oxidant (Selectfluor) or a loss of starting material signal resulting in a mixture of organic and inorganic products. No aryl fluorides were observed.

2.5.2.4 Attempts at aryl fluorination from 2.3 via ligand exchange

Compound **2.3** (3.6 mg, 0.005 mmol) was dissolved in 0.95 mL THF and combined with a 0.25 mL solution of ligand (2 equiv, 0.01 mmol). The solution was stirred for 15 minutes at room temperature. The reaction was transferred to a J-young tube and ^{19}F NMR was used to monitor the reaction. ^{19}F NMR revealed no ligand exchange occurred with bulky Brettphos-ligands.

2.5.2.4 . Stoichiometric Transmetalation and Reductive Elimination Studies for C-C coupling

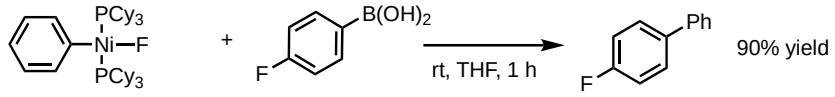

2.3

In a glovebox, $PhNi(PCy_3)_2F$ **2.3** (7.2 mg, 0.01 mmol) was weighed into a 4 mL vial. (4-Fluorophenyl)boronic acid (0.015 mmol, 1.5 equiv) and 2-fluoromesitylene (0.01 mmol, 1.0 equiv) were added from a stock solution in THF resulting in a total volume of 0.6 mL. The reaction mixture was stirred at room temperature. After 1 h, the reaction mixture was transferred to an NMR tube and then analyzed by ^{19}F NMR spectroscopy. Complete consumption of **2.3** was observed along with in high yields of biaryl product after 1 hour (–115.8 ppm).

2.5.2.5 Synthesis of 2.9

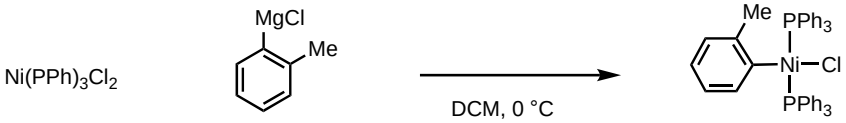

2.9

On the benchtop, $Ni(PPh_3)_2Cl_2$ was added with a stir bar to a 100 mL dried flask with 45 mL DCM. The solution was cooled to 0°C and stirred under N_2. (*o*Tolyl)MgCl (1.4 M in THF) was added dropwise while stirring for 15-20 minutes. DCM was removed en vaco, and MeOH was added (15 mL). Solution was sonicated for 5 minutes than cooled to 0 °C. Collected yellow precipitate by vaccum filtration and wash two times with 15 mL EtO_2. Dried under vaccum to yield **2.9** (0.90 g, 24 %).

2.5.2.6 In situ generation of 2.8 authentic standard

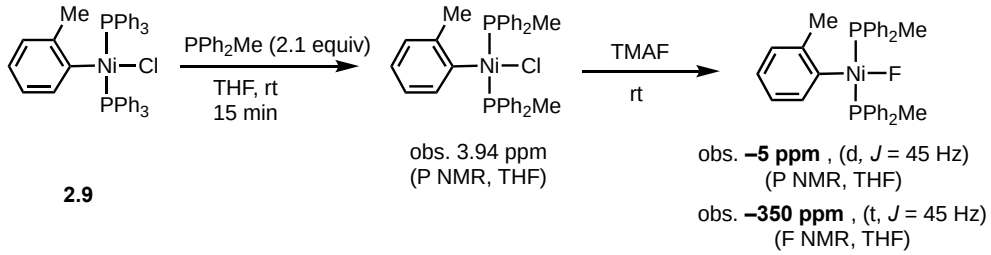

2.9 (7.1 mg, 0.01 mmol) was dissolved in 1.0 mL THF and combined with PPh_2Me (2 equiv, 4.0 mg, 0.02 mmol). The solution was stirred for 15 minutes at room temperature. After some elapsed time, tetrametthylaminoum fluoride (TMAF) was added (1.3 equiv, 1.2 mg, 0.013 mmol). The reaction was transferred to a J-young tube and ^{19}F NMR was used to monitor the reaction. ^{19}F and ^{31}P NMR revealed the Ni-F signal for **2.8** (-348 ppm. t, J = 45 Hz; -5ppm d, J = 45 Hz), identical to when accessed through decarbonylation of **2.6**. Notably, similar when **2.8** is generated via decarbonylation, we again see decomposition of product during isolation attempts.

2.5.2.7 Synthesis of acid fluorides

General procedure for the synthesis of acid fluorides from carboxylic acids (Method A): Based on a modified literature procedure,[50,51] a 20-mL vial equipped with a magnetic stir bar was charged with carboxylic acid (2.0 mmol, 1.0 equiv), TFFH (2.2 mmol, 1.1 equiv), and triethylamine (6.0 mmol, 3.0 equiv) in anhydrous THF (10 mL). The reaction mixture was stirred at room temperature. Within 5 min, the carboxylic acid and TFFH completely dissolve to form a homogeneous colorless solution. After 15-30 min, the reaction mixture was diluted with EtOAc (10 mL) and washed with ice-cold water (10 mL x 2). The organic layer was dried over Na_2SO_4, filtered, and concentrated *in vacuo* to form the acid fluoride. Based on ^1H NMR spectroscopic analysis, the resulting product was typically ~95% pure and was thus used without further

purification. If purification was necessary, silica gel column chromatography was performed using 5% EtOAc/hexanes.

General procedure for the synthesis of acid fluorides from acid chlorides (Method B): Based on a modified literature procedure,[52] a 20-mL vial equipped with a magnetic stir bar was charged with CsF (3.0 mmol, 1.5 equiv), and the appropriate carboxylic acid chloride (2.0 mmol, 1.0 equiv) in anhydrous MeCN (6 mL). The reaction mixture was stirred at 50 ºC until complete conversion (usually 4 to 16 h). The reaction suspension was allowed to settle, and the MeCN solution decanted from the precipitate and then filtered. The precipitate was rinsed with MeCN (6 mL), and the washes was filtered. The combined MeCN washes was concentrated *in vacuo*. Based on ^{1}H NMR spectroscopic analysis, the resulting product was typically ~95% pure and was thus used without further purification. If purification was necessary, silica gel column chromatography was performed using 5% EtOAc/hexanes.

2.5.2.8 Procedure for decarbonylative Suzuki-Miyuara coupling

General procedure for decarbonylative Suzuki reaction (Method A, from acid fluoride): In a nitrogen-filled glovebox, acid fluoride (1 equiv, 0.2 mmol) was weighed into a 10 mL tall vial equipped with a 10 □m magnetic stir bar. A pre-mixed solution of $Ni(cod)_2$ (0.1 equiv, 0.02 mmol) and PPh_2Me (0.2 equiv, 0.04 mmol) in THF (0.6 mL) was added. The boronic acid **10** (2 equiv, 0.4 mmol) was added, and the reaction mixture was capped and removed from the glovebox. The reaction mixture was stirred at 100 ºC for 16 h. The reaction was then cooled to room temperature, and EtOAc (5 mL) and brine (5 mL) were added. The organic layer was collected, and the aqueous solution was further extracted with EtOAc (2 x 5 mL). The combined organic extracts were dried over Na_2SO_4 and concentrated *in vacuo*. The crude product was purified by flash column chromatography on silica gel using EtOAc in hexanes.

General procedure for decarbonylative Suzuki reaction (Method B, in situ, from carboxylic acid): In a nitrogen-filled glovebox, carboxylic acid (1 equiv, 0.2 mmol), TFFH (1 equiv, 0.2 mmol), and proton sponge (1 equiv, 0.2 mmol) were weighed into a 10 mL tall vial equipped with a 10 □m magnetic stir bar. THF (0.4 mL) was added, and the reaction mixture was stirred at room temperature for 15 to 30 min. A pre-mixed solution of $Ni(cod)_2$ (0.1 equiv, 0.02 mmol) and PPh_2Me (0.2 equiv, 0.04 mmol) in THF (0.2 mL) was added. The boronic acid **10** (2 equiv, 0.4 mmol) was added, and the reaction mixture was capped and removed from the glovebox. The reaction mixture was stirred at 100 ºC for 16 h. The reaction was then cooled to room temperature, and EtOAc (5 mL) and brine (5 mL) were added. The organic layer was collected, and the aqueous solution was further extracted with EtOAc (2 x 5 mL). The combined organic extracts were dried over Na_2SO_4 and concentrated *in vacuo*. The crude product was purified by flash column chromatography on silica gel using EtOAc in hexanes. Characterization of product can be found in our published article.

2.5.2.9 General procedure for stoichiometric decarbonylation with Ni-NHC precatalysts

In a nitrogen-filled glovebox, Ni-NHC precatalysts were weighed in a tared 4 mL vial (0.01 mmol) followed by acid fluoride **2.62** (0.011 mmol) and internal standard 2-fluoromesetilene. The mixture was then dissolved in 0.7 mL of THF and transferred into a J Young tube. The J Young was then gently heated in an oil bath at 60 °C for 24 hours. ^{19}F NMR revealed conversion to a single Ni-F intermediate and unreacted starting material.

2.5.2.10 Stoichiometric amination via Ni(IPr)MMA$_2$

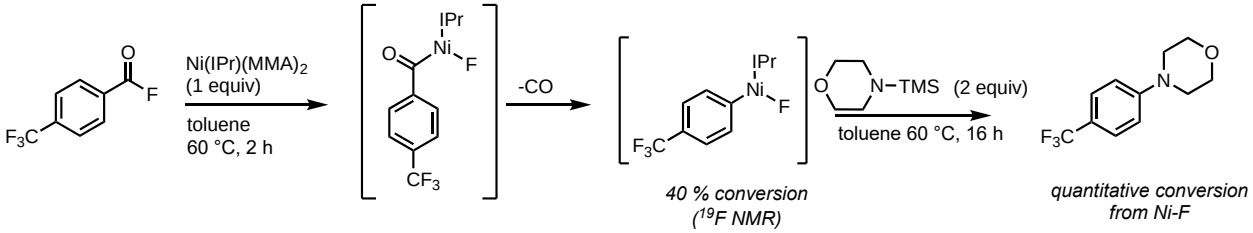

Ni(IPr)aryl(F) was generated *in situ* via decarbonylation procedure outlined in **2.5.2.9**. After confirming conversion to aryl Ni-fluoride by NMR, the solution was returned into the glovebox and transferred into a 4 mL vial charged with TMS-morpholine and a stirbar. After stirring at 60 °C overnight outside of the glovebox sealed with electrical tape, the reaction was filtered and GC/GCMS analaysis was performed. GC/GCMS revealed both aminated arene as well as amide by product in a 3.2:1 ratio. This result suggested to us that arly-NR_2 reductive elimination was possible from Ni(II)-NHC catalysts. Amide byproduct likely originated from uncatalyzed background reaction of **2.63** and the amine.

2.5.2.11 Catalytic amination attempts with Ni(IPr)MMA$_2$

Acid fluoride **2.63** (0.025 mmol) and Ni(IPr)MMA_2 (0.005 mmol, 3.4 mg) we combined in a tall 10 mL vial with a stir bar and dissolved in 0.3 mL toluene. In cases were additional phosphine ligand was used, PPh_2Me would be added (0.005 mmol) prior to solvent. No prestir with the catalyst was necessary. TMS-amine was then added (0.05 mmol, 2 equiv). 0.4 mL of internal standard solution in toluene (0.125 M, 0.05 mmol) was added. The reaction was then taken out of the glovebox and heated in the sealed reaction vial at 60°C overnight. After cooling the reaction to room temperature, and sample was taken and diluted with DCM for GC/GCMS analysis. Quantitative analysis of GCMS revealed relative ratios of aryl amine and amide products.

2.5.2.12 Synthesis of carboxylic acid phenyl esters

A 20 mL vial equipped with a magnetic stir bar was charged with the corresponding carboxylic acid (2.0 mmol, 1.0 equiv), phenol (2.0 mmol, 1.0 equiv), and 1-ethyl-3-(3-dimethylaminopropyl)carbodiimide (EDC) (3.0 mmol, 1.5 equiv) in DCM (8 mL). The reaction mixture was stirred at rt for 20 h. The reaction mixture was then diluted with dichloromethane (10 mL) and washed with ice-cold water (10 mL x 2). The organic extracts were collected, dried over Na_2SO_4, and concentrated in vacuo. The crude product was purified by flash column chromatography on silica gel using EtOAc in hexanes.

2.5.2.13 Procedure for decarbonylative amination of aryl esters

General procedure for decarbonylative amination of esters (Method A, using TMS-amine): In a nitrogen-filled glovebox, the corresponding carboxylic acid ester (0.2 mmol, 1.0 equiv) and TMS-morpholine (0.2 mmol, 1.0 equiv) were weighed into a 10 mL tall vial equipped with a 10 µm magnetic stir bar. A pre-mixed solution of $Ni(cod)_2$ (0.02 mmol, 0.1 equiv) and dcype (0.02 mmol, 0.1 equiv) in toluene (0.3 mL) was added. The resulting solution was diluted further with toluene (0.7 mL). The reaction vial was capped and removed from the glovebox. The reaction mixture was stirred at 150 ºC for 24 h. The reaction was then cooled to rt, and Et_2O (10 mL) and saturated $NaHCO_3$ (10 mL) were added. The organic layer was collected, and the aqueous solution was further extracted with Et_2O (2 x 10 mL). The combined organic extracts were dried over Na_2SO_4 and concentrated in vacuo. The crude product was purified by flash column chromatography on silica gel using EtOAc in hexanes.

General procedure for decarbonylative amination of esters (Method B, using free amine): In a nitrogen-filled glovebox, probenecid phenyl ester (0.2 mmol, 1.0 equiv) was weighed into a 10 mL tall vial equipped with a 10 µm magnetic stir bar. Pre-mixed solutions of $Ni(cod)_2$ (0.02 mmol, 0.1 equiv) and dcype (0.02 mmol, 0.1 equiv) in toluene (0.3 mL) and free amine (0.2–0.4 mmol, 1.0–2.0 equiv) in toluene (0.3 mL) were added. N-Methyl-N-(trimethylsilyl) trifluoroacetamide, MSTFA (0.2–0.4 mmol, 0.2–0.4 equiv) was added using a microsyringe, and the resulting solution was diluted with toluene (0.4 mL). The reaction vial was capped and removed from the glovebox. The reaction mixture was stirred at 150 ºC for 24 h. The reaction was then cooled to rt, and Et_2O (10 mL) and saturated $NaHCO_3$ (10 mL) were added. The organic layer was collected, and the aqueous solution was further extracted with Et_2O (2 x 10 mL). The combined organic extracts were dried over Na2SO4 and concentrated in vacuo. The crude product was purified by flash column chromatography on silica gel using EtOAc in hexanes.

General procedure for decarbonylative amination of esters (Method C, via in situ formation of TMS-amine):

In situ formation of TMS-amine: In a nitrogen-filled glovebox, free amine (0.2–0.4 mmol, 0.2– 0.4 equiv) was weighed into a 4 mL vial. MSTFA (0.2–0.4 mmol, 0.2–0.4 equiv) was added using a microsyringe and diluted with toluene (0.5 mL). The reaction vial was capped and removed from the glovebox. The reaction mixture was stirred at 35 or 60 ºC for 1 h and brought back into the glovebox.

Decarbonylative amination: In a nitrogen-filled glovebox, probenecid phenyl ester (0.2 mmol, 1.0 equiv) was weighed into a 10 mL tall vial equipped with a 10 µm magnetic stir bar. Pre-mixed solutions of $Ni(cod)_2$ (0.02 mmol, 0.1 equiv) and dcype (0.02 mmol, 0.1 equiv) in toluene (0.3 mL) and the in situ generated TMS-amine (0.2–0.4 mmol, 1.0–2.0 equiv) in toluene (0.5 mL) were

added. The resulting solution was then further diluted with toluene (0.2 mL). The reaction vial was capped and removed from the glovebox. The reaction mixture was stirred at 150 ºC for 24 h. The reaction was then cooled to rt, and Et_2O (10 mL) and saturated $NaHCO_3$ (10 mL) were added. The organic layer was collected, and the aqueous solution was further extracted with Et2O (2 x 10 mL). The combined organic extracts were dried over Na_2SO_4 and concentrated in vacuo. The crude product was purified by flash column chromatography on silica gel using EtOAc in hexanes.

2.6 References

1) Biffis, A.; Centomo, P.; Del Zotto, A.; Zecca, M. *Chemical Reviews,* **2018** *118* (4), 2249–2295.
2) Brown, D. G.; Boström, J., *J. Med. Chem.* **2016**, *59*, 4443–4458.
3) Ananikov, V. P., *ACS Catalysis*, **2015** *5* (3), 1964–1971.
4) Han, F.-S., ***Chem. Soc. Rev.***, **2013**,***42***, 5270–5298.
5) Gooßen, L. J,; Gooßen, K.; Rodríguez, N.; Blanchot, M.; Linder, C.; Zimmermann, B. *Pure Appl. Chem*., **2008**, *80*, 1725–1733.
6) Liu, C.; Szostak, M., *Org. Biomol. Chem*., **2018**, *16*, 7998–8010.
7) Guo, L.; Reuping, M.; *Chem. Eur. J*. **2018**, *24*, 7794–7809.
8) Guo, L.; Reuping, M.; *Acc. Chem. Res*. **2018**, *51*, 1185–1195.
9) Rodriguez.; Gooßen, L. J., *Chem. Soc. Rev*. **2011**, *40*, 5030–5048.
10) Dzik, W. I.; Lange, P. P.; Gooßen, L. J., *Chem. Sci.* **2012**, *3*, 267 –2678.
11) Dermenci, A.; Dong, G. B. *Sci. China Chem.* **2013**, *56*, 685–701.
12) Takise, R.; Muto, K.; Yamaguchi, J., *Chem. Soc. Rev.* **2017**, *46*, 5864 – 5888.
13) Lu, H.; Yu, T.-Y.; Xu, P.-F.; Wei, H., *Chem. Rev*. **2021**, *121*, 365–411.
14) Furuya, T.; Kamlet, A. S.; Tobias, R. *Nature* **2011**, *473*, 470–477.
15) Campbell, M. G.; Tobias, R. *Chem. Rev*. **2014**, *115*, 612–633.
16) Purser, S.; Moore, P. R.; Swallow, S.; Gouverneur, V. *Chem. Soc. Rev*. **2008**, *37*, 320–330.
17) Yerien, D. E.; Bonesi, S.; Postigo, A., *Org. Biomol. Chem*., **2016**, *14*, 8398-8427.
18) Wang, J.; Sánchez-Roselló, M.; Aceña, J. L.; del Pozo, C.; Sorochinsky, A. E.; Fustero, S.; Soloshonok, V. A.; Liu, H. *Chem. Rev*. **2014**, *114*, 2432–2506.
19) Y. Zhou, J. Wang, Z. Gu, S. Wang, W. Zhu, J. L. Aceña, V. A. Soloshonok, K. Izawa and H. Liu, Chem. Rev., 2016,116, 422–528
20) Q. A. Huchet, B. Kuhn, B. Wagner, N. A. Kratochwil, H. Fischer, M. Kansy, D. Zimmerli, E. M. Carreira and K. Müller, J. Med. Chem., 2015, 58(22), 9041–9060.
21) E. P. Gillis, K. J. Eastman, M. D. Hill, D. J. Donnelly and N. A. Meanwell, J. Med. Chem., 2015, 58, 8315–8359;
22) Patterson, J.C., Mosley, M.L. How Available is Positron Emission Tomography in the United States?. Mol Imaging Biol 7, 197–200 (2005)
23) Stéphane Caron Organic Process Research & Development **2020,** *24*, 470-480
24) Xiaowei Li Xiaolin Shi Xiangqian Li and Dayong Shi *Beilstein J. Org. Chem*. **2019**, *15*, 2213–2270.
25) Sather, A.C.; Stephen L. Buchwald, S.L., *Accounts of Chemical Research,* **2016,** *49*, 2146-2157.
26) Keaveney, S. T.; Schoenebeck, F., *Angew. Chem., Int. Ed*. **2018**, *57*, 4073−4077.
27) Malapit, C. A.; Ichiishi, N.; Sanford, M. S., *Org. Lett*. **2017**, *19*, 4142–4145.
28) Zhang, Y.; Rovis, T. *J. Am. Chem. Soc*. **2004,** *126*, 15964–15965.
29) Wang, Z.; Wang, X.; Nishihara, Y. *Chem. Asian. J.*, **2020**, *15*, 1234–1247.
30) Lee, H.; Borgel, J.; Ritter. T., *Angew. Chem. Int. Ed.* **2017**, *56*, 6966–6969.
31) Lennox, A. J. J. & Lloyd-Jones, G. C.. Angew. Chem. Int. Ed. 52, 7362–7370 (2013).
32) Cox, P. A. et J. Am. Chem.Soc. 139, 13156–13165 (2017)
33) Cox, P. A., Leach, A. G., Campbell, A. D. & Lloyd-Jones, G. C. J. Am. Chem. Soc. 138, 9145–9157(2016)

34) Yue, H.; Guo, L.; Liao, H.-H.; Cai, Y.; Zhu, C.; Rueping, M.. Angew. Chem., Int. Ed. 2017, 56, 4282.
35) Lee, S.-C.; Guo, L.; Yue, H.; Liao, H.-H.; Rueping, M. Synlett 2017, 28, 2594
36) Ruiz-Castillo, P.; Buchwald, S. L., *Chem. Rev.* **2016,** *116*, 12564-12649.
37) Ogata, T.; Hartwig, J. F. J. Am. Chem. Soc. 2008, 130, 13848−13849.
38) Gao, C.-Y.; Yang, L.-M. J. Org. Chem. 2008, 73, 1624−1627. (c) Fors, B. P.; Watson, D. A.; Biscoe, M. R.; Buchwald, S. L. J. Am. Chem. Soc. 2008, 130, 13552−13554.
39) Tobisu, M.; Shimasaki, T.; Chatani, N. Chem. Lett. 2009, 38, 710−711.
40) Shimasaki, T.; Tobisu, M.; Chatani, N. Angew. Chem., Int. Ed. 2010, 49, 2929−2932.
41) Mesganaw, T.; Silberstein, A. L.; Ramgren, S. D.; Fine Nathel, N. F.; Hong, X.; Liu, P.; Garg, N. K. Chem. Sci.2011, 2, 1766−1771.
42) Ramgren, S. D.; Silberstein, A. L.; Yang, Y.;Garg, N. K. Angew. Chem., Int. Ed. 2011, 50, 2171−2173.
43) Ackermann, L.; Sandmann, R.; Song, W. Org. Lett. 2011, 13,1784−1786.
44) Huang, J.-H.; Yang, L.-M. Org. Lett. 2011, 13, 3750−3753.
45) Hie, L.; Ramgren, S. D.; Mesganaw, T.; Garg, N. K. Org. Lett.2012, 14, 4182−4185.
46) Marin, M.; Rama, R. J.; Nicasio, M. C. *Chem. Rev*., **2016**, *16* 1819-1832.
47) Gradel, B.; Brenner, E.; Schneider, R.; Fort, Y.; *Tetrahedron Letters*, **2001**, *42*, 5689–5692.
48) Nagao, S.; Matsumoto, T.; Koga, Y.; Matsubara, K. *Chem. Lett*. **2011**, *40*, 1036-1038
49) Nett, A. J.; Cañellas, S.;Higuchi, Y.; Robo, M. T.; Kochkodan, J. M.; Haynes, M. T.; Kampf, J. W.; Montgomery, J., *ACS Catal*. 2018 8 (7), 6606-6611.
50) Carpino, L. A. & El-Faham, A.. A. J. Am. Chem. Soc. 117, 5401–5402 (1995).
51) Carpino, L. A., Beyermann, M., Wenschuh, H. & Bienert, M.. Acc. Chem. Res. 29, 268–274 (1996).
52) Cismesia, M. A., Ryan, S. J., Bland, D. C. & Sanford, M. S. J. Org. Chem. 2017, 82, 5020.

Chapter 3 - Nickel-Catalyzed Fluoroalkylation of Thiols via Decarbonylation of (Fluoroalkyl)thioesters

*Portions of this work have been published in:

Brigham, C. E.; Malapit, C. A.; Lalloo, N.; Sanford, M. S. Nickel-catalyzed Decarbonylative Synthesis of Fluoroalkyl Thioethers. *ACS. Catal.* **2020**, *10*, 8315–8320.

3.1 Background

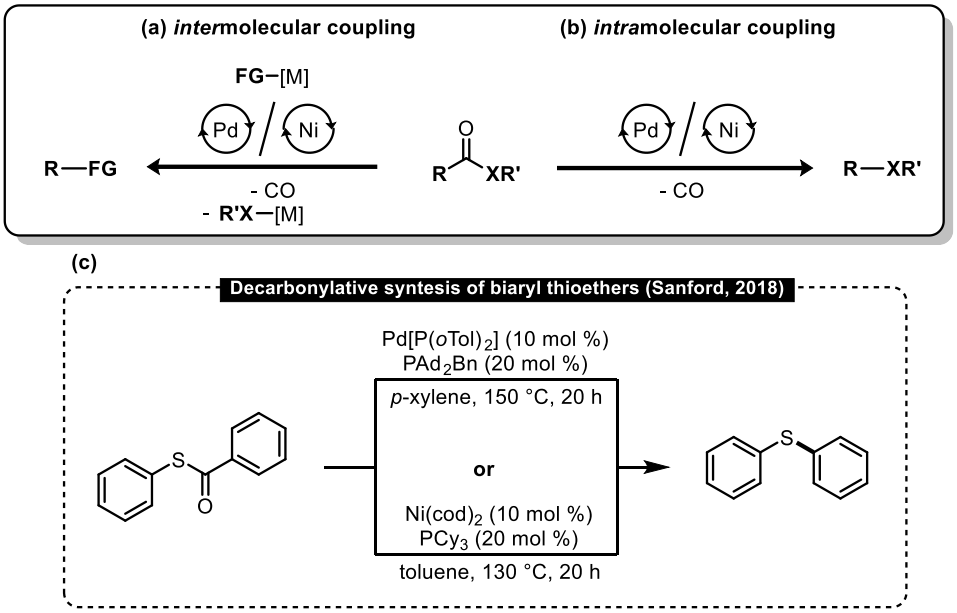

Figure 3-1.(a) Intermolecular decarbonylative coupling. (b) Intramolecular decarbonylative coupling. (c) Decarbonylative synthesis of biaryl thioethers.

Our investigations into decarbonylative methodologies to this point had largely focused on the development for intermolecular cross couplings, utilizing carboxylic acid derivatives as electrophilic coupling partners (Figure 3-1a). A major component of the development of these reactions is identifying the optimal pairing of electrophile and nucleophile. While they need to be

unreactive enough to avoid uncatalyzed acylation, they also require sufficient transmetallation activity of the acid XR' leaving group and the organometallic nucleophile. An alternative type of decarbonylative reaction would be an intramolecular transformation in which C-X bond formation occurs after decarbonylation. This approach offers a simple pathway for forging new C-X bonds from widely available carboxylic acid starting materials (Figure 3-1b).

Previously our group reported an intramolecular decarbonylative thioether synthesis, which included two catalytic methods, one with palladium and the other with nickel (Figure 3-1c).[1] In both cases, biaryl thioesters were converted to the corresponding thioethers. Notably, the nickel and palladium catalysts offered some complementary reactivity. For example, substrates such as electron rich acyl arenes often showed lower yields for palladium due to more challenging oxidative addition and carbonyl deinsertion. In contrast, these substrates perform very well with nickel. The goal of the work in this Chapter was to expand this reactivity to the synthesis of new types of thioethers, specifically (fluoroalkyl) thioethers.

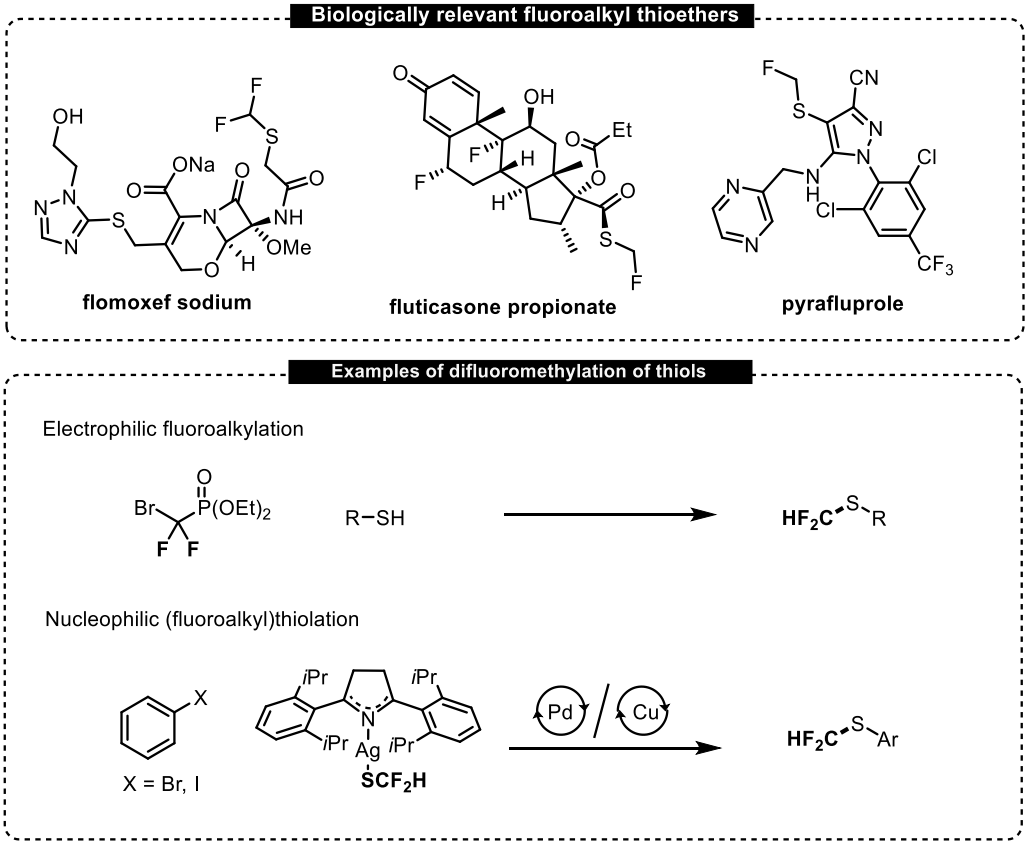

Figure 3-2. (Fluoroalkyl)thioethers in biologically relevant compounds. Synthetic approaches to fluoroalkyl thioethers

Fluoroalkyl thioethers (R_FSR) have emerged as increasingly common motifs in bioactive molecules due to their unique physiochemical properties.[2-6] As shown in Figure 3-2, thioethers bearing diverse fluoroalkyl substituents (for example, CF_2H, CFH_2, and CH_2CF_3) appear in lead structures relevant to both medicinal and agricultural chemistry.[7-8] The most common synthetic routes to R_FSR involve either the electrophilic fluoroalkylation of thiols or the coupling of aryl/alkyl electrophiles with $[M]-SR_F$ nucleophiles.[8-25] Both approaches have significant limitations with respect to the breadth of R_F substituents that can be introduced, since very few of the necessary R_F-containing electrophiles/nucleophiles are commercially available. Furthermore, many of these methods require other toxic, unstable, or expensive reagents.[8-11,20-25] Overall, more general synthetic approaches to fluoroalkyl thioethers are of high interest, and the use of readily

available fluoroalkyl carboxylic acids as R_F precursors would be particularly enabling in this context.

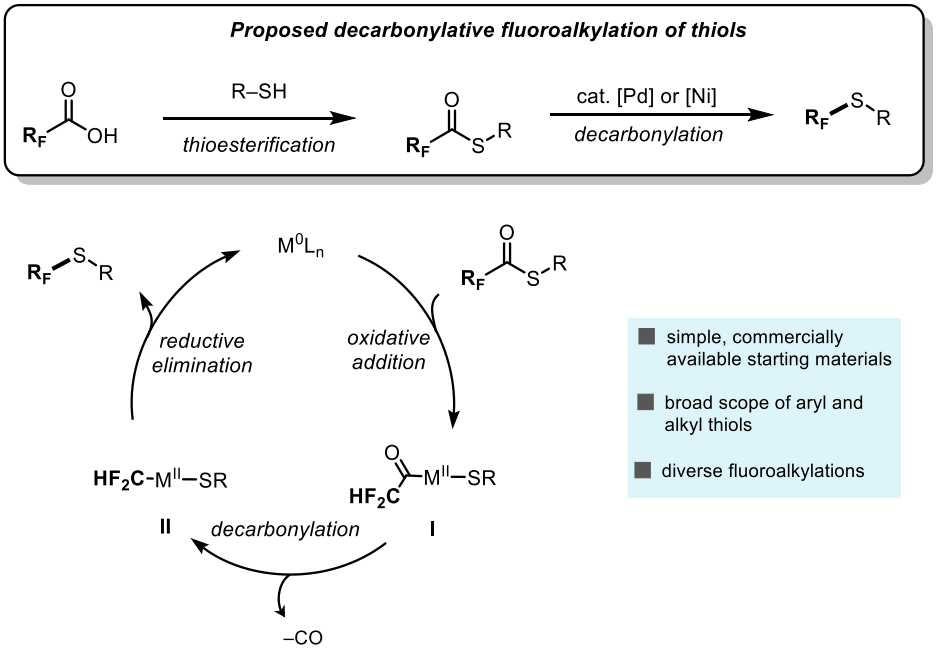

Figure 3-3. Proposed catalytic cycle for decarbonylative fluoroalkylation.

This Chapter describes the development of a Ni-catalyzed reaction for constructing fluoroalkyl thioethers from the corresponding thioesters. Our approach leverages fluoroalkyl carboxylic acids as inexpensive, stable, and commercially available R_F precursors.[26-35] As such, it enables the construction of a variety of different fluoroalkyl thioethers from a single thiol starting material.

We hypothesized that an analogous pathway to our previous decarbonylative C-S coupling, now using fluoroalkyl thioesters as starting materials, could offer a route to R_FSR products. The proposed catalytic cycle (Figure 3-3) involves initial oxidative addition of the fluoroalkyl thioester at a M(0) catalyst (M = Ni or Pd) to form the acyl M(II)-intermediate, **I**. Carbonyl deinsertion then generates the M(II)(fluoroalkyl)(thiolate) intermediate **II**. Finally, **II** undergoes C−S bond-

forming reductive elimination to yield the target fluoroalkyl thioether product and regenerate the M(0) catalyst.

3.2 Reaction optimization

We started these studies by evaluating palladium-based catalysts. Literature precedent suggeste that these should be particularly effective at promoting the reductive elimination step of the catalytic cycle, while oxidative addition and CO de-insertion would be more challenging.[1, 36-37] Initial screening focused on palladium(0) catalysts with bulky phosphine ligands (Table 3-1). However, the Pd-catalyzed reactions of the napthyl thioester **3.1f** never gave more than trace yields of decarbonylated product **3.2f** The fluoroalkylthioesters appear to be sufficiently electrophilic to engage in oxidative addition at palladium(0), as suggested by the significant color change of the reaction (from light yellow to a dark orange) at room temperature as well as by a 10-20% loss of starting material. Thus, we hypothesize that the carbonyl de-insertion reaction is likely kinetically and/or thermodynamically disfavored in this system, thus precluding the desired decarbonylation and thioether formation. To circumvent this issue, we next evaluated nickel-based catalysts, which are well-precedented to undergo fast carbonyl deinsertion.[36]

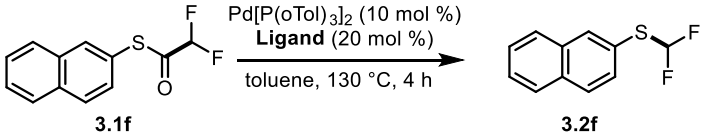

3.1f **3.2f**

entry	ligand	**3.2f** (% yield)	% remaining **3.1f**
1	Brettphos	<1	81
2	dppe	0	75
3	dppf	0	36
4	PAd_2Bu	<1	73
5	PAd_2Bn	<1	88
6	Sphos	0	83

Table 3-1. Initial catalytic optimization of decarbonylative difluoromethylation with palladium.

We initially examined catalysts based on a combination of $Ni(cod)_2$ and monodentate phosphine ligands (PR_3), which were previously employed for the transformation in Figure 3.5a[1,39-49]. However, only traces (<1%) of product **3.2a** were detected using PPh_3, P(*o*-Tol)$_3$, PCy_3, or P^{n}Bu$_3$ (Figure 3-4a). In these systems, the remaining mass balance was the unreacted starting material **3.1a**.

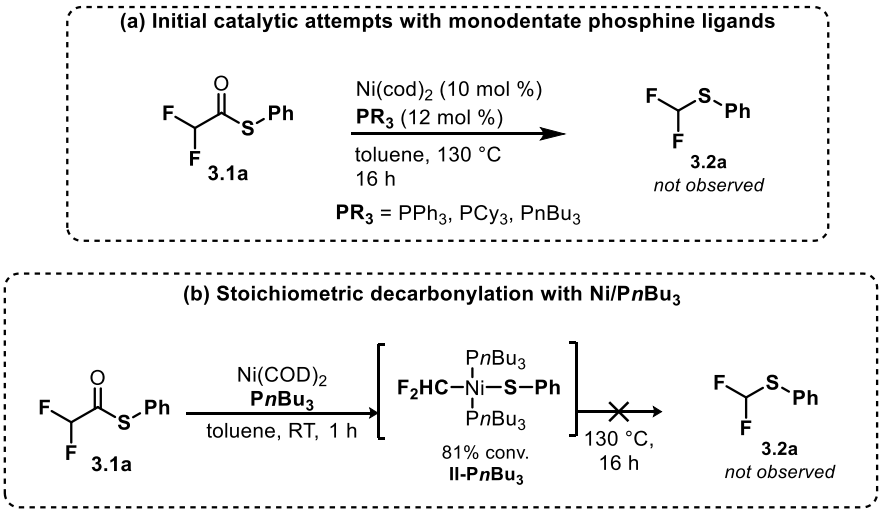

Figure 3-4. (a) Catalytic attempts with monodentate phosphine ligands. (b) Stoichiometric decarbonylation with $Ni(cod)_2$/P^{n}Bu$_3$.

We next conducted stoichiometric studies to identify the challenging step(s) in this sequence. The treatment of a toluene solution of $Ni(cod)_2$/P^{n}Bu$_3$ with 1 equiv of **3.1a** resulted in the formation of (P^{n}Bu$_3$)$_2$Ni(SPh)(CF$_2$H) (**II-P^{n}Bu$_3$**) within 1 h at ambient temperature (Figure 3.4b). Complex **II-P^{n}Bu$_3$** was characterized in situ via ^{19}F and ^{31}P NMR spectroscopy, which show resonances indicative of a *trans* configuration, with three-bond coupling between the CF_2H and P^{n}Bu$_3$ ligands (J_{PF} = 26.5 Hz). The formation of **II-P^{n}Bu$_3$** implicates the feasibility of two key steps of the catalytic cycle: oxidative addition (step i) and carbonyl de-insertion (step ii). However, when *in situ*-generated **II-P^{n}Bu$_3$** was heated at 130 °C for 2 h, none of the thioether product **3.2a** was formed (step iii, reductive elimination). Instead, the resonances associated with **II-P^{n}Bu$_3$** slowly decayed, without the observation of identifiable organic products. This suggests that

F_2HC-S bond-forming reductive elimination is challenging in this system and that alternative ligands are required to enable this step.

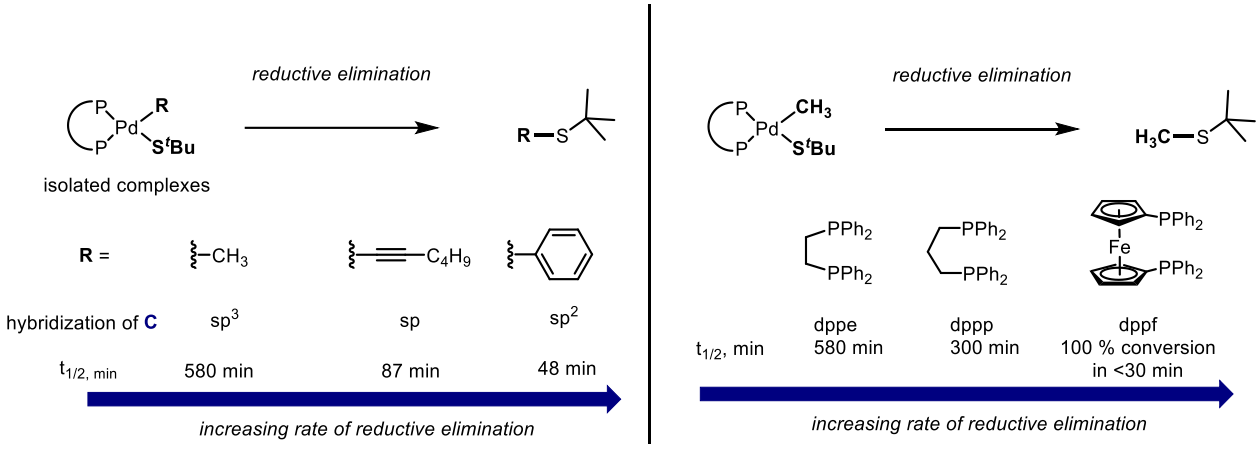

Figure 3-5. Hartwig's stoichiometric C-S reductive elimination studies from palladium complexes

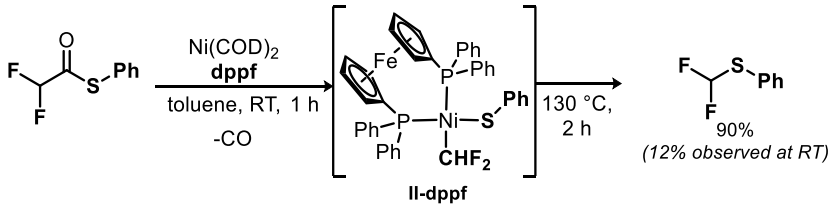

Figure 3-6. Stoichiometric decarbonylation of 3.1a with Ni/dppf.

Literature reports have shown that 1,1′-bis-(diphenylphosphino)ferrocene (dppf) is particularly effective for promoting challenging reductive elimination reactions at group 10 metal centers.[50-53] For example, Hartwig and coworkers reported C-S bond-forming reductive elimination studies of organopalladium complexes (Figure 3-5). They found that hybridization of the carbon directly involved in reductive elimination had a large impact on the rate of bond formation. Notably, sp^3-hybridized carbons reacted significantly slower than those with sp- or sp^2-hybridization. Furthermore, Hartwig noted that large, bidentate phosphine ligands could promote

C(sp^3)-S coupling, with dppf performing particularly well (Figure 3-6). Based on this precedent, we next conducted stoichiometric experiments with $Ni(cod)_2$/dppf. As shown in Figure 3-7 the treatment of a toluene solution of $Ni(cod)_2$/dppf with 1 equiv of **3.1a** resulted in 70% consumption of **3.1a** within 1 h at 50 °C. This was accompanied by the formation of **3.2a** (in 12% yield) along with broad signals in the ^{19}F NMR spectrum. Based on previous reports, these broad signals are indicative of fluxional (dppf)Ni^{II} intermediates.[50] Subsequent heating at 130 °C for 1 h resulted in S−CF_2H bond formation to generate **3.2a** in 90% yield by ^{19}F NMR spectroscopy.

We next revisited the optimization of the catalytic reaction, focusing on using dppf and other bidentate phosphine ligands. Supported by our stoichiometric studies, dppf afforded the highest yield for the conversion of **3.1a** to **3.2a**. As shown in Table 3-2, the combination of 10 mol % $Ni(cod)_2$ and 12 mol % dppf afforded **3.2a** in 58% yield over 20 h at 130 °C in toluene. Other bidentate phosphine ligands, such as Xantphos and DPEphos, also performed well, though yields were generally slightly lower. Some other ligands commonly used in nickel-catalyzed decarbonylative thioetherification such as dcype and dppp afforded low yields of product. Furthermore, monodentate phosphine ligands never gave more than trace yields of product. Further optimization of the reaction solvent and time resulted in nearly quantitative yield over 4 h in THF. High reaction temperatures were required, as is typically the case in nickel-catalyzed decarbonylative reactions. Previous work from our group identified dicarbonyl nickel side products that are unreactive at low temperatures.[54] However, at elevated temperatures, CO is liberated from the Ni(0) and activity is reestablished, suggesting that these high temperatures are likely required in decarbonylation reactions to limit product inhibition. The optimal yields were obtained in etheral solvents (THF and dioxane), while lower yields were observed in toluene. One

possible rationale for this is that the more coordinating ether-based solvents solvent could play a role in accelerating this removal of CO from nickel.

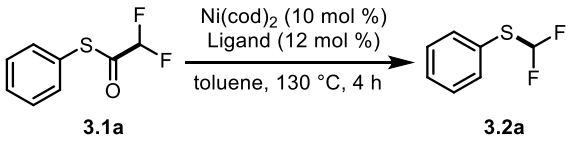

3.1a **3.2a**

entry	ligand	**3.2a** (% yield)[b]
1	PCy_3[a]	0
2	$PnBu_3$[a]	0
3	PPh_3[a]	1
4	P(*o*-Tol)$_3$[a]	<1

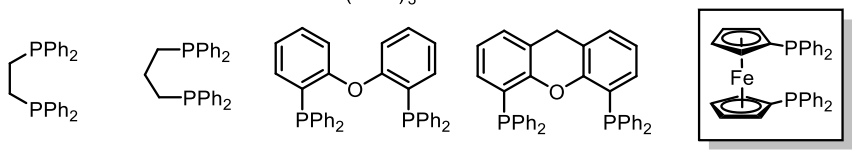

dppe 0% | dppp 5% | dpePhos 41% | Xantphos 52% | dppf 58% (94% in THF, 80% in 1,4-dioxane)

Table 3-2. Optimization of phosphine ligand for Ni-catalyzed decarbonylative fluoroalkylation. [a]20 mol % used for monodentate phosphines. [b]Yields determined by 19F NMR.

3.3 Synthesis of substrates

A series of difluoromethyl thioester substrates **3.1a−w** were prepared as outlined in Figure 3.7A. Aryl and alkyl thiols were treated with excess difluoroacetic anhydride in the presence of pyridine and catalytic dimethylaminopyridine (DMAP) in dichloromethane at room temperature. These reactions were typically completion within an hour. Aqueous washes removed any unreacted starting material, leaving the pure product in the organic layer. Thus, the difluoromethyl thioesters were isolated by simply evapoarting the solvent, without the need for chromatography. Captopril, an ACE inhibitor, required protection of a carboxylic acid group prior to addition of the difluoracetyl group (Figure 3-7B). Protection using TMS-diazomethane in methanol forms the

methyl ester. At this point, some racemization occurs at the alpha carbon of the newly formed methyl ester (typically ~10-20 %). From here, standard conditions with difluoroacetic anhydride are carried out. Base was not used to prevent further racemization of the substrate.

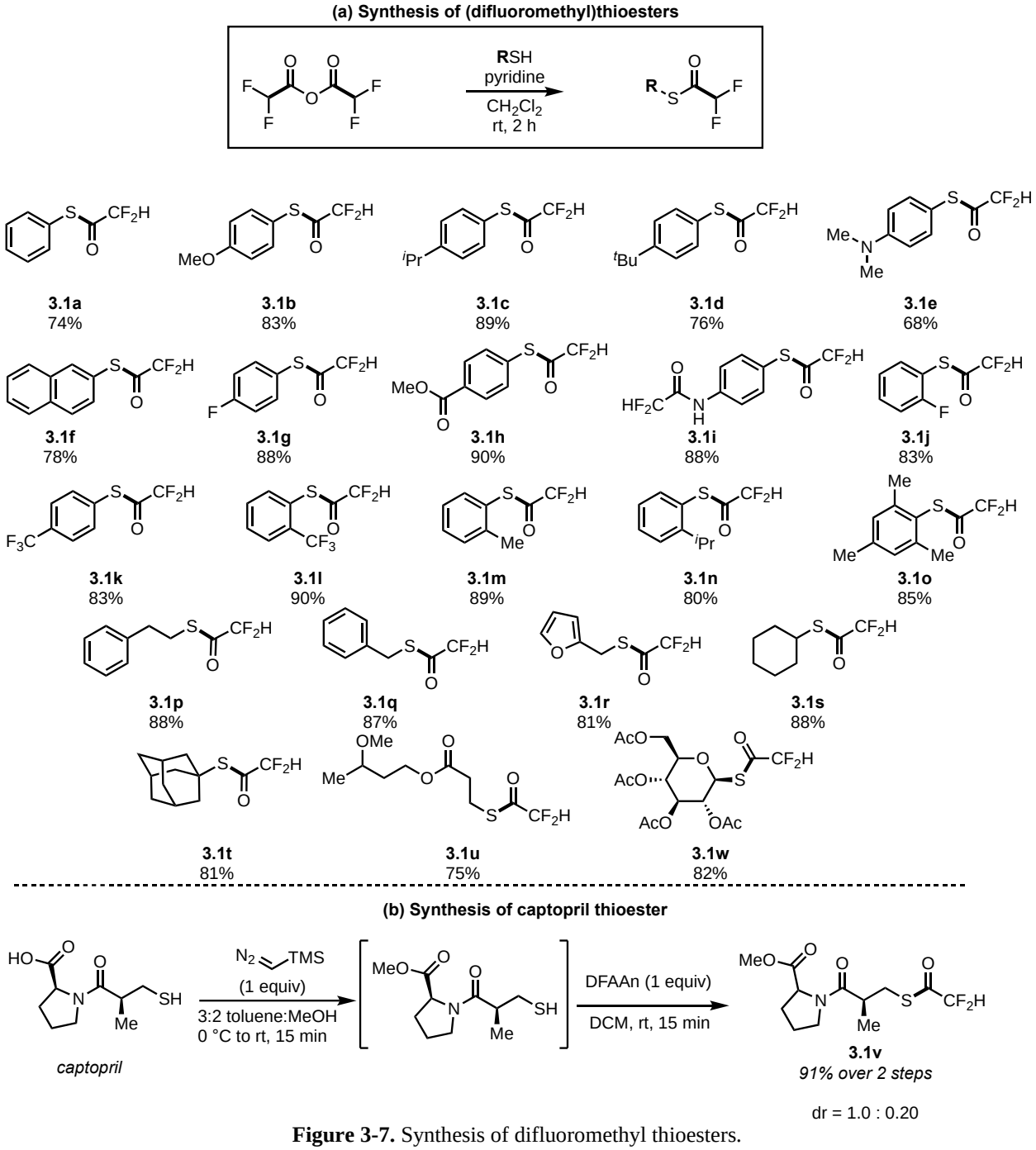

Figure 3-7. Synthesis of difluoromethyl thioesters.

In addition to difluoromethyl thioesters, we also synthesized thioesters derived from other (Figure 3-8a) EDC-mediated coupling or (Figure 3-8b) a two-step chlorination of the acid followed by addition of the thiol.[55] In these cases, 4-methoxy thiophenol or 4-isopropyl thiophenol was used, since the electron rich aryl thiols typically exhibited higher reactivity. Following literature procedures, flash chromatography enabled isolation of the fluoroalkyl thioesters.

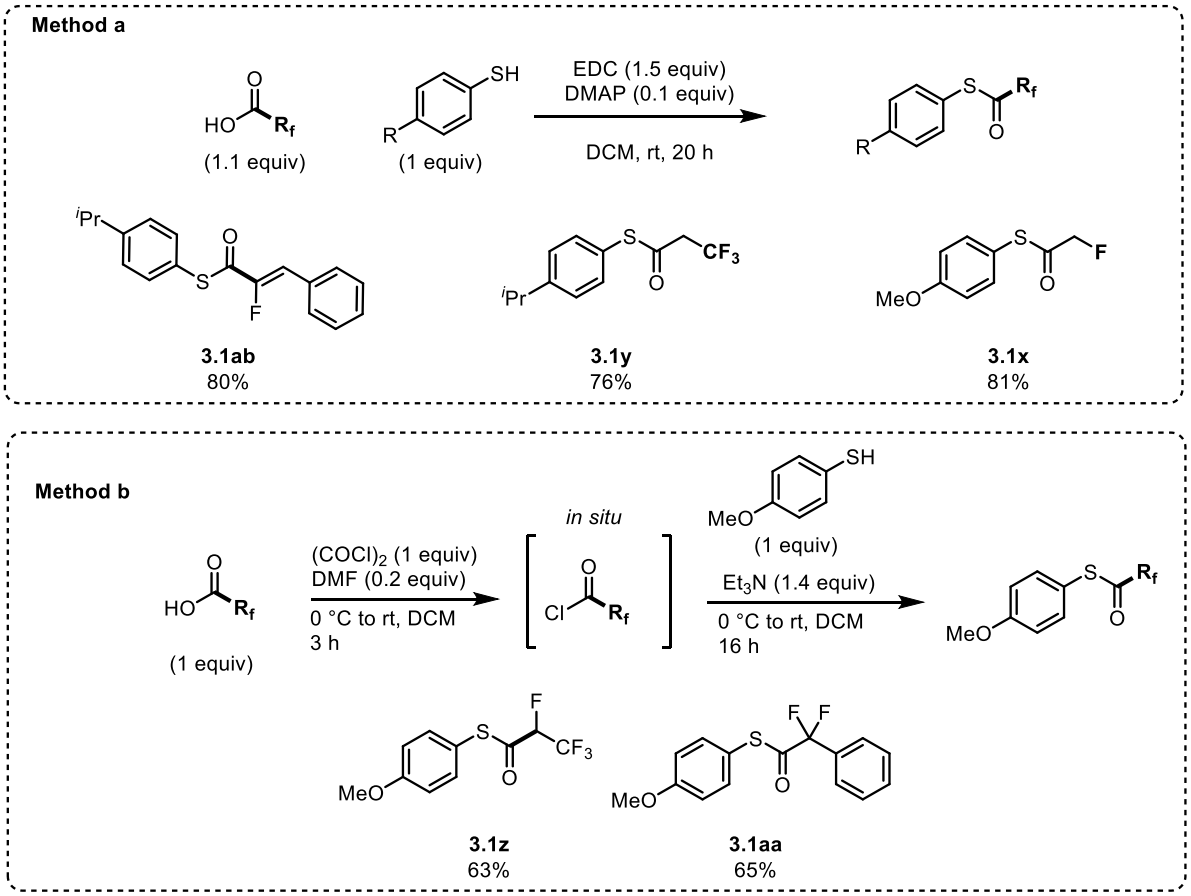

Figure 3-8. Synthesis of fluoroalkyl thioesters from carboxylic acids.

3.4 Substrate scope

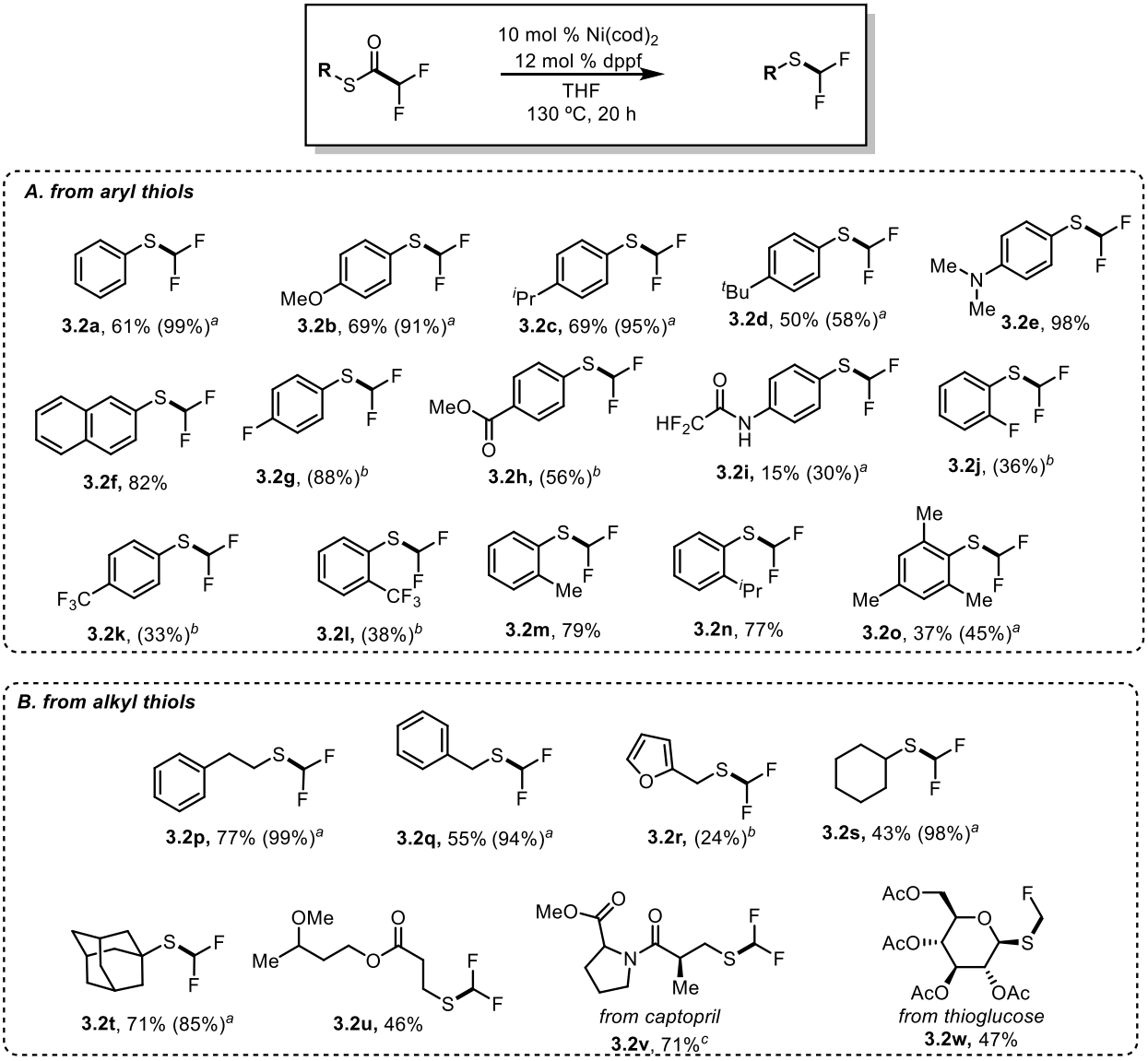

Figure 3-9. Synthesis of fluoroalkyl thioesters from carboxylic acids.

The scope of decarbonylative R_F–S coupling was first explored with respect to the substitution on sulfur (Figure 3-9). Aryl thioesters bearing electron-donating and -neutral substituents (**3.1b**–**1f**) afforded good yields of the difluoromethyl thioether products. Substituents such as ethers, amines, and amides were compatible. Aryl thioesters bearing electron-withdrawing groups resulted in lower yields (see products **3.2h**–**3.2l**), apart from 4-fluorothiophenol derivative,

3.2g. In these systems, the major side products were diarylthioethers, which are likely formed via competing activation of the aryl−S bond of the product by the Ni(0) catalyst.

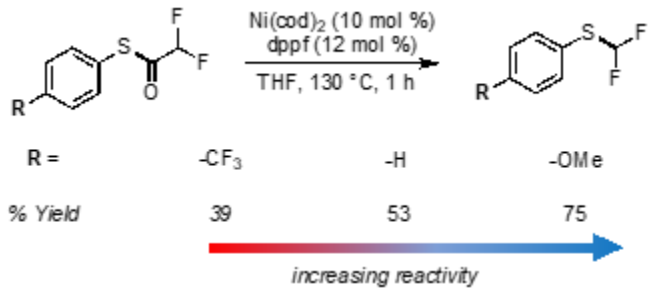

Figure 3-10. Higher yields observed with thiols bearing electron donating groups.

This transformation showed modest sensitivity to steric bulk on the aryl ring, and substrates containing either one or two electron-donating ortho-substituents afforded **3.2m**−**3.2o** in moderate to good yields. Primary, secondary, and tertiary alkyl thiols were also effective substrates for this transformation (for example **3.2p, 3.2s**, and **3.2t**). Thiol-containing biologically active compounds such as captopril (**3.2v**) and thioglucose (**3.2w**) underwent conversion to the corresponding difluoromethyl thioethers in good yields. In cases where the yields were modest, unreacted starting material accounted for the remaining mass balance. Importantly, the catalytic cycle for this transformation does not require an exogenous base. This limited racemization of substrates such as **3.2v** during catalysis. Some trends observed included electronic effects of the thiol. While electron poor thioesters engaged in oxidative addition more readily, faster turnover of the catalyst was observed for electron rich thiols (Figure 3.10). Literature reports suggest that increased electron density in the thiolate ligand increased the rate of C-S reductive elimination from palladium.[53] This trend is consistent with the hypothesis that reductive elimination is the rate-limiting step.

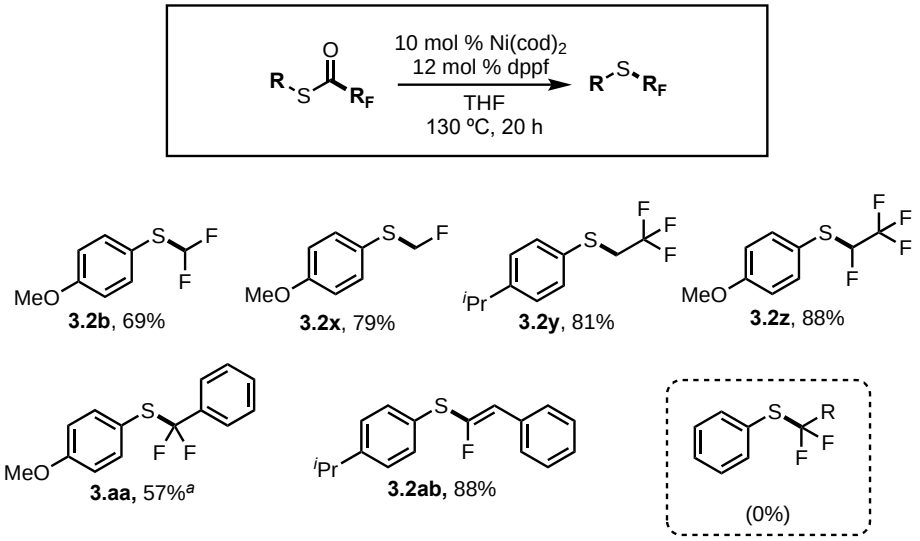

Figure 3-11. Scope of RF groups in Ni-catalyzed decarbonylative fluoroalkylation.

Finally, we used this approach to synthesize a series of different fluoroalkyl thioethers. As shown in Figure 3-11, the substrates for this transformation were synthesized from commercially available R_FCO_2H and thiols. Catalytic decarbonylation then provided the partially fluorinated thioether products **3.2x**−**3.2ab** in good to excellent yields. Notably, these products are challenging to synthesize using most existing thiol fluoroalkylation approaches (Figure 3-2), because of the inaccessibility of the required fluoroalkylating reagents. Only thioester **3.1aa** required a change to the catalytic system, using Xantphos as the optimized ligand. This change was required because the dppf-based catalyst afforded only trace yield of the desired product.

One current limitation of is that fully fluorinated derivatives (e.g., SCF_3, SCF_2CF_3) afford none of the fluoroalkyl thioether product. A stoichiometric study of the CF_3 system (Figure 3-12) showed the formation of Ni−CF_3 intermediates; however, no thioether product was detected upon heating these species. This preliminary result suggests that the S−R_F reductive elimination step remains a challenge in these systems. Catalyst and ligand optimization will likely be required to achieve these challenging transformations.

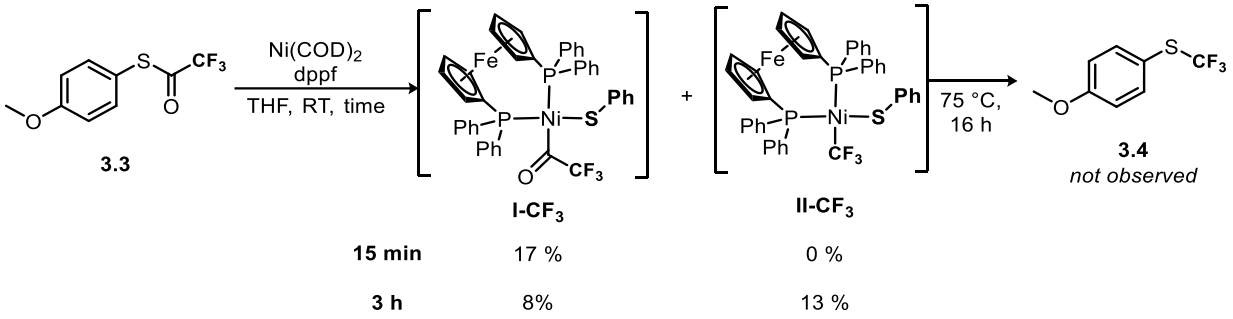

Figure 3-12. Stoichiometric reaction of trifluoromethyl thioesters.

3.5 Conclusions

In summary, a nickel-catalyzed decarbonylative coupling reaction was developed to convert fluoroalkyl thioesters to the analogous thioethers. Difluoromethyl thioesters were used as model substrates for the optimization. We found that a sterically large bidentate phosphine ligand, dppf, was required to promote S–R_F reductive elimination at Ni(II). This method leverages readily available fluorocarboxylic acids as commercial and stable fluoroalkyl sources to install these functional groups, which are increasingly prevalent in biologically active molecules. This project was a valuable first demonstration of decarbonylative fluoroalkylation from fluoroalkyl carboxylic acid derivatives. The next chapter discusses investigations into further decarbonylative (fluoro)alkyl cross coupling methodologies.

3.6 Experimental Procedures and Supplemental Information

3.6.1 *General Information*

All manipulations were performed inside an N_2-filled glovebox unless otherwise noted. NMR spectra were obtained on a Varian VNMR 700 (699.76 MHz for 1 H; 175.95 MHz for ^{13}C), Varian VNMR 500 (500.09 MHz for ^{1}H; 470.56 MHz for ^{19}F; 125.75 MHz for ^{13}C), or Varian VNMR 400 (401 MHz for ^{1}H; 376 MHz for ^{19}F; 123 MHz for ^{13}C) spectrometer. ^{1}H and ^{13}C NMR

chemical shifts are reported in parts per million (ppm) relative to TMS, with the residual solvent peak used as an internal reference. ^{19}F NMR chemical shifts are reported in ppm and are referenced to 4-fluorotoluene (–118.00 ppm). Abbreviations used in the NMR data are as follows: s, singlet; d, doublet; t, triplet; q, quartet; m, multiplet; br, broad signal. Yields of reactions that generated fluorinated products were determined by ^{19}F NMR spectroscopic analysis using a relaxation delay of 25 s with a 90^{o} pulse angle. Mass spectral data were obtained on a Micromass Magnetic Sector Mass Spectrometer in electrospray ionization mode. Flash chromatography was performed using a Biotage Isolera One system with cartridges containing high performance silica gel.

3.6.2 *Methods*

All commercially available reagents were used as received unless otherwise stated. Ni(cod)$_2$ (Strem) and phosphine ligands (Alfa Aesar, Acros Organics, Oakwood Scientific) were stored in a glovebox. Difluoroacetic anhydride (Oakwood Chemicals) and pyridine (Sigma) were purchased and used as received. Thiol reagents and carboxylic acids were purchased from commercial sources (Sigma, Alfa Aesar, Matrix Scientific, Frontier Scientific, Synquest, TCI America) and used as received. Deuterated solvents were purchased from Cambridge Isotope Laboratories, Inc.

Stoichiometric reaction of Ni(cod)$_2$/P^{n}Bu$_3$ with 3.1a. Ni(cod)$_2$ (20.6 mg, 0.075 mmol, 1.5 equiv) and P^{n}Bu$_3$ (30.3 mg, 0.15 mmol, 3.0 equiv) were dissolved in 0.5 mL of toluene-d_8. The solution was stirred at room temperature for 15 min, at which point it was transferred to a pre-weighed mixture of 3.**1a** (9.4 mg, 0.05 mmol, 1.0 equiv) and the internal standard 4-fluorotoluene (5.5 mg, 0.05 mmol, 1.0 equiv). The reaction was allowed to stir at ambient temperature for 1 h, at which point the solution was transferred to a screw cap NMR tube and sealed with a Teflon-lined cap. ^{19}F NMR and ^{31}P NMR spectra were then recorded (Figures S1 and S2, respectively). ^{19}F and ^{31}P NMR spectroscopic analysis showed high conversion of the thioester starting material to

intermediate **II-P^{n}Bu$_3$** [^{19}F NMR: δ –91.49 (dt, *J* = 51.6, 26.0 Hz); ^{31}P NMR: δ 11.85 (t, *J* = 27.0 Hz)]. The observed three-bond P–F coupling, is consistent with a *trans* ligand configuration. The temperature of the reaction was then elevated to 130 °C for 16 h. ^{19}F and ^{31}P NMR spectroscopic analysis revealed complete decomposition of **II-P^{n}Bu$_3$**, but the formation of **3.2a** was not observed.

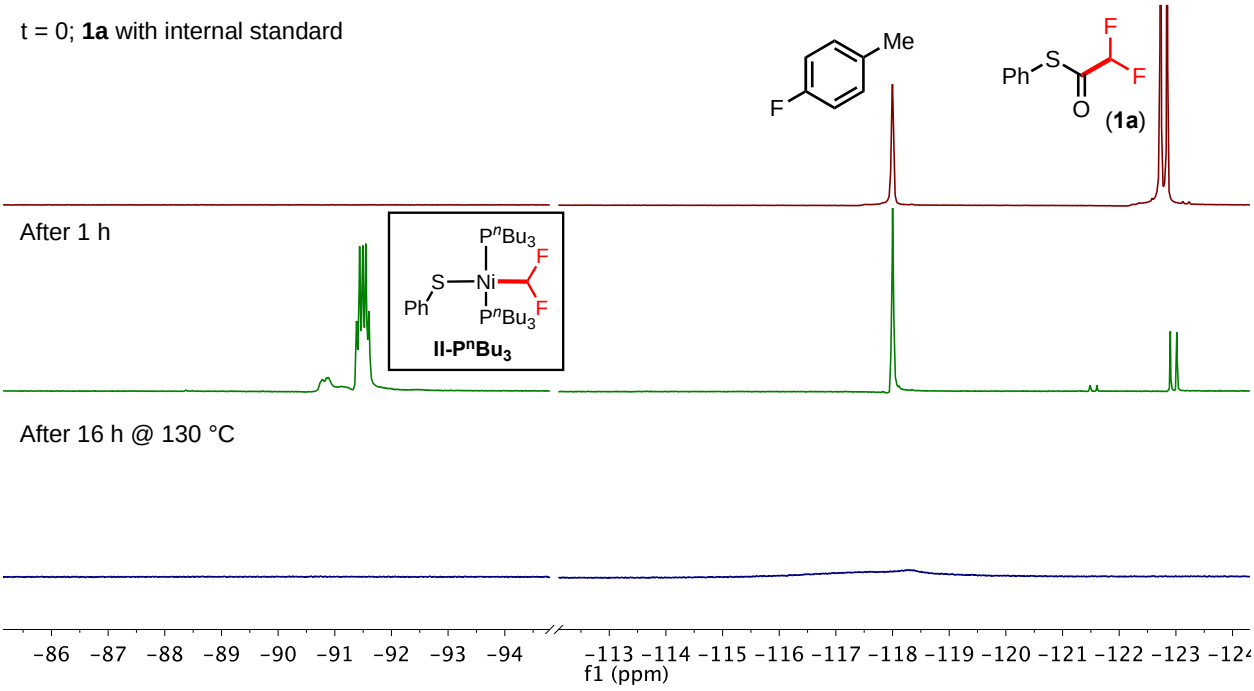

Figure 3.S1. ^{19}F NMR spectral data for *in situ* generated **II-P^{n}Bu$_3$**.

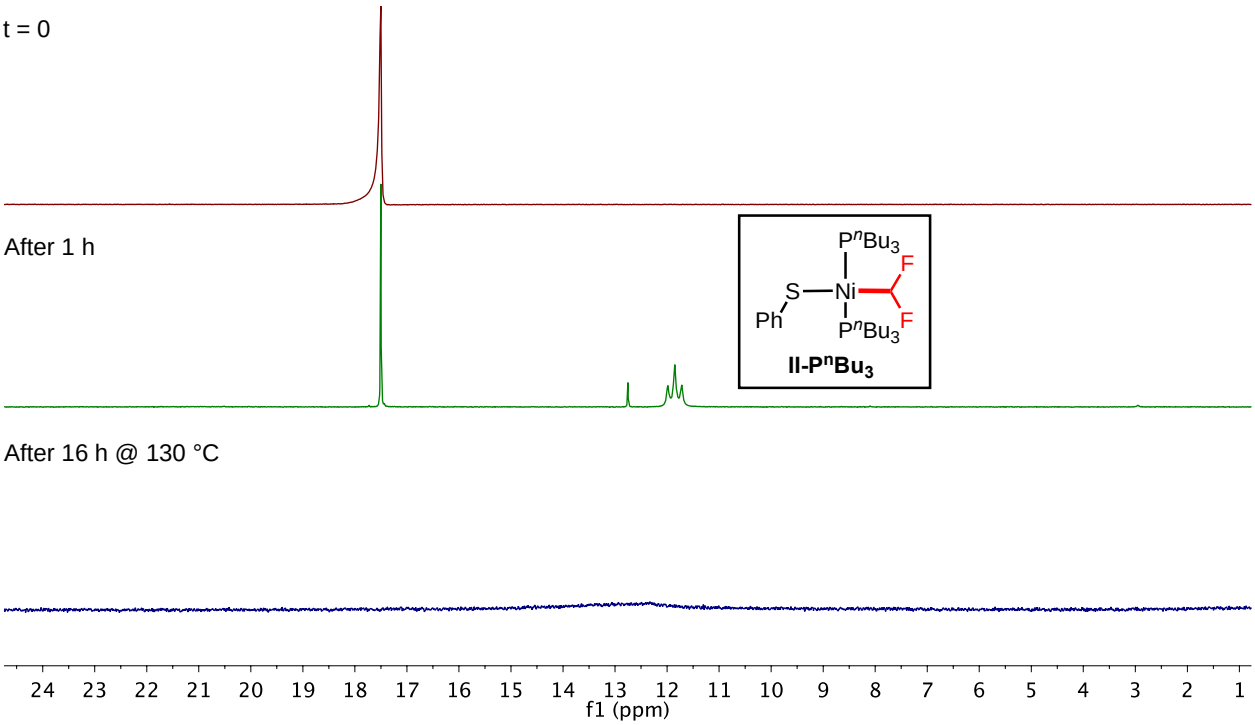

Figure 3.S2. ^{31}P NMR spectral data of *in situ* generated **II-P^{n}Bu$_3$.**

Stoichiometric reaction of Ni(cod)$_2$/dppf with 3.1a. Ni(cod)$_2$ (20.6 mg, 0.075 mmol, 1.5 equiv) and dppf (30.3 mg, 0.075 mmol, 1.5 equiv) were dissolved in 0.5 mL of toluene. The solution was stirred at room temperature for 15 min, at which point it was transferred to a pre-weighed mixture of **3.1a** (9.4 mg, 0.05 mmol, 1.0 equiv) and the internal standard 4-fluorotoluene (0.05 mmol, 1.0 equiv). After mixing, the solution was transferred to a screw cap NMR tube and sealed with a Teflon-lined cap. The reaction mixture was heated at 50 °C for 1 h, at which point the ^{19}F NMR spectrum was recorded. At this time point, ^{19}F NMR spectroscopic analysis (Figure S3) revealed some formation of the target product **3.2a**. Furthermore, broad signals were present in the region between –86 and –93 ppm. While these species could not be fully characterized, the broad resonances are consistent with fluxional (dppf)Ni^{II} complexes (likely **II-dppf**).[50] Additional heating up to 130 °C accelerated the reaction further, and all starting material was converted to **3.2a** within 2 h.

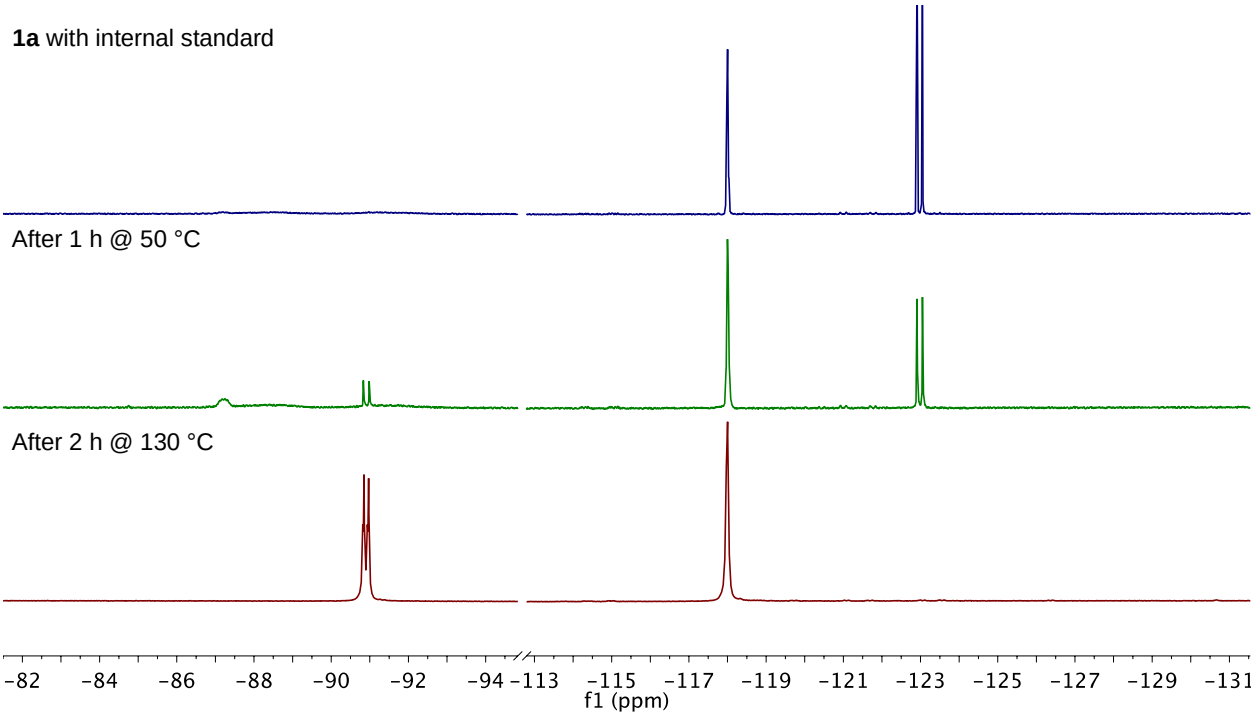

Figure 3.S3. ^{19}F NMR spectral data for stoichiometric reaction between Ni/dppf and **3.1a**.

General procedure for optimizing the catalytic decarbonylation of difluoromethyl thiophenol ester 1a. $Ni(cod)_2$ (4.1 mg, 0.015 mmol, 0.1 equiv) and the appropriate phosphine ligand (0.036 mmol, 0.24 equiv for monodentate ligands; 0.018 mmol, 0.12 equiv for bidentate ligands) were dissolved in 0.2 mL of solvent. The solution was stirred at room temperature for 15 min in a tall 10 mL vial (Figure S4), at which point **3.1a** (28.2 mg, 0.15 mmol, 1.0 equiv) was added via syringe in 0.1 mL of solvent. The vial was sealed with a Teflon-lined screw cap, brought out of the glovebox, and stirred at 130 °C. After 4 h of heating, the reaction mixture was allowed to cool to room temperature. A stock solution of 4-fluorotoluene was prepared (0.3 M in toluene) and added to the cooled reaction mixture (0.5 mL, 0.15 mmol, 1 equiv). A sample of the crude reaction mixture with internal standard was removed for NMR analysis. Yields of **3.2a** reported were determined by ^{19}F NMR spectroscopy.

Figure 3.S4. Reaction set-up of a 0.15 mmol scale in a capped 10-mL tall vial.

General procedure for the synthesis of difluoromethyl thioesters from difluoromethylacetic anhydride. The appropriate thiol (3.0 mmol, 1.0 equiv) was weighed into a 20 mL vial and dissolved in CH_2Cl_2 (8 mL). DMAP (5.0 mg, 0.04 mmol) was added, followed by pyridine (0.24 mL, 3 mmol, 1.0 equiv). The solution was then cooled to 0 °C, at which point difluoroacetic anhydride (6.0 mmol, 2.0 equiv) was slowly added while stirring. The reaction was allowed to warm to room temperature and stir for 1 h. At the end of the reaction, the solution was diluted with CH_2Cl_2 (30 mL) and washed with cold water (3 x 10 mL). The organic layer was collected and dried over $MgSO_4$. Solvent was removed *in vacuo* to afford the difluoromethylthioester product. The difluoromethylthioester products were characterized and used in catalysis without further purification, unless stated otherwise.

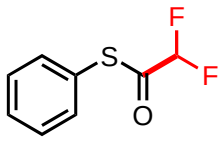

***S*-Phenyl 2,2-difluoroethanethioate (3.1a).** The general method was followed using 2 mmol of the corresponding thiol. This afforded **3.1a** as a clear oil (274 mg, 74% yield). **^{1}H NMR** (500 MHz, $CDCl_3$) δ 7.51–7.38 (multiple peaks, 5H), 5.98 (t, *J* = 54.0 Hz, 1H). **^{13}C NMR** (126 MHz, $CDCl_3$) δ 189.81 (t, *J* = 29.2 Hz), 134.62, 130.39, 129.67, 123.96, 109.31 (t, *J* = 255.5 Hz). **^{19}F NMR** (377 MHz, $CDCl_3$) δ –123.62 (d, *J* = 54.0 Hz, 2F). **HRMS** (ES) calcd. for $C_8H_6F_2OS$ [M+] *m/z* 188.0107, found 188.0103.

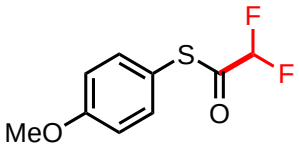

***S*-(4-Methoxyphenyl) 2,2-difluoroethanethioate (3.1b).** The general method was followed using 2 mmol of the corresponding thiol. This afforded **3.1b** as a clear oil (363 mg, 83% yield). **^{1}H NMR** (500 MHz, $CDCl_3$) δ 7.35 (d, *J* = 8.8 Hz, 2H), 6.99 (d, *J* = 8.8 Hz, 2H), 5.96 (t, *J* = 54.0 Hz, 1H), 3.84 (s, 3H). **^{13}C NMR** (126 MHz, $CDCl_3$) δ 190.67 (t, *J* = 28.9 Hz), 161.37, 136.17, 115.36, 114.19, 109.35 (t, *J* = 255.4 Hz), 55.39. **^{19}F NMR** (377 MHz, $CDCl_3$) δ –123.54 (d, *J* = 54.0 Hz, 2F). **HRMS** (ES) calcd. for $C_9H_8F_2OS$ [M+] *m/z* 218.0213, found 218.0207.

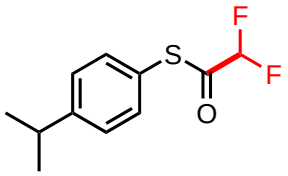

***S*-(4-Isopropylphenyl) 2,2-difluoroethanethioate (3.1c).** The general method was followed using 2 mmol of the corresponding thiol. This afforded **3.1c** as a clear oil (410 mg, 89% yield). **^{1}H NMR** (500 MHz, $CDCl_3$) δ 7.42–7.28 (multiple peaks, 4H), 5.97 (t, *J* = 54.0 Hz, 1H), 2.97 (hept, *J* = 6.9 Hz, 1H), 1.29 (d, *J* = 6.9 Hz, 6H). **^{13}C NMR** (126 MHz, $CDCl_3$) δ 190.16 (t, *J* = 29.0 Hz),

151.52, 134.53, 127.90, 120.59 (d, *J* = 1.7 Hz), 109.33 (t, *J* = 255.5 Hz), 34.00, 23.73. **^{19}F NMR** (471 MHz, $CDCl_3$) δ –123.48 (d, *J* = 54.0 Hz, 2F). **HRMS** (ES) calcd. for $C_{11}H_{12}F_2OS$ [M+] *m/z* 230.0577, found 230.0570.

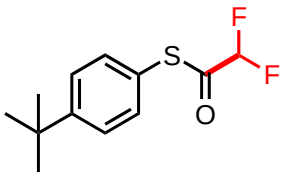

***S*-(4-(*Tert*-butyl)phenyl) 2,2-difluoroethanethioate (3.1d).** The general method was followed using 2 mmol of the corresponding thiol. This afforded **3.1d** as a clear oil (350 mg, 76% yield). **^{1}H NMR** (500 MHz, $CDCl_3$) δ 7.49 (d, *J* = 8.0 Hz, 2H), 7.38 (d, *J* = 8.3 Hz, 2H), 5.96 (t, *J* = 54.0 Hz, 1H), 1.35 (s, 9H). **^{13}C NMR** (126 MHz, $CDCl_3$) δ 190.15 (t, *J* = 29.0 Hz), 153.79, 134.22, 126.82, 120.35, 109.32 (t, *J* = 255.6 Hz), 34.88, 31.15. **^{19}F NMR** (377 MHz, $CDCl_3$) δ –123.74 (d, *J* = 54.0 Hz, 2F). **HRMS** (ES) calcd. for $C_{12}H_{14}F_2OS$ [M+] *m/z* 244.0733, found 244.0725.

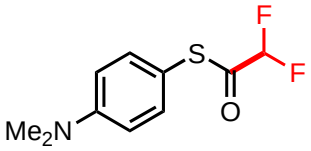

***S*-(4-(Dimethylamino)phenyl) 2,2-difluoroethanethioate (3.1e).** The general method was followed using 2 mmol of the corresponding thiol. This afforded a crude yellow oil. **3.1e** was purified via flash chromatography (hexanes/EtOAc, 80:20) to afford a light yellow solid (313 mg, 68% yield). **mp** 43.8–46.9 °C. **^{1}H NMR** (500 MHz, $CDCl_3$) δ 7.25 (d, *J* = 7.6 Hz, 2H), 6.74 (d, *J* = 7.5 Hz, 2H), 5.94 (t, *J* = 54.1 Hz, 1H), 3.01 (s, 6H). **^{13}C NMR** (126 MHz, $CDCl_3$) δ 191.60 (t, *J* = 28.5 Hz), 151.56, 135.69, 112.82, 109.46 (t, *J* = 255.4 Hz), 107.57, 40.10. **^{19}F NMR** (376 MHz, $CDCl_3$) δ –123.54 (d, *J* = 54.1 Hz, 2F). **HRMS** (ES) calcd. for $C_{12}H_{14}F_2OS$ [M+H] *m/z* 232.0629, found 232.0611.

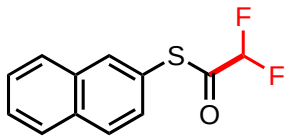

***S*-(Naphthalen-2-yl) 2,2-difluoroethanethioate (3.1f).** The general method was followed using 3 mmol of the corresponding thiol. This afforded **3.1f** as a white solid (559 mg, 78% yield). **mp** 50.7–52.1 °C. **^{1}H NMR** (500 MHz, $CDCl_3$) δ 8.02 (s, 1H), 7.94 (d, *J* = 8.6 Hz, 1H), 7.90 (d, *J* = 7.9 Hz, 1H), 7.87 (d, *J* = 7.8 Hz, 1H), 7.63–7.52 (multiple peaks, 2H), 7.47 (dt, *J* = 8.6, 1.4 Hz, 1H), 6.02 (t, *J* = 54.0 Hz, 1H). **^{13}C NMR** (126 MHz, $CDCl_3$) δ 190.02 (t, *J* = 29.4 Hz), 134.99, 133.71, 133.59, 130.36, 129.41, 128.02, 127.89, 127.73, 126.93, 121.12, 109.34 (t, *J* = 255.7 Hz). **^{19}F NMR** (376 MHz, $CDCl_3$) δ –123.39 (d, *J* = 54.0 Hz, 2F). **HRMS** (ES) calcd. for $C_{12}H_8F_2OS$ [M+] *m/z* 238.0264, found 238.0260.

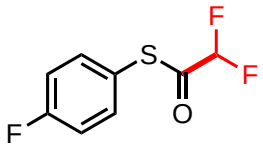

***S*-(4-fluorophenyl) 2,2-difluoroethanethioate (3.1g).** The general method was followed using 2 mmol of the corresponding thiol. This afforded **3.1g** as a clear oil (365 mg, 88% yield). **^{1}H NMR** (500 MHz, $CDCl_3$) δ 7.47 – 7.41 (m, 2H), 7.18 (t, *J* = 8.6 Hz, 2H), 5.98 (t, *J* = 53.9 Hz, 1H). **^{13}C NMR** (126 MHz, $CDCl_3$) δ 189.88 (t, *J* = 29.3 Hz), 164.05 (d, *J* = 251.7 Hz), 136.77 (d, *J* = 8.7 Hz), 119.17, 117.06 (d, *J* = 22.4 Hz), 109.23 (t, *J* = 255.7 Hz). **^{19}F NMR** (471 MHz, $CDCl_3$) δ -109.38 (ddd, *J* = 13.8, 8.6, 5.2 Hz), -123.54 (d, *J* = 54.1 Hz). **HRMS** (GC-APCI) calcd. for $C_8H_5F_3OS$ [M+] *m/z* 206.0013, found 206.0008

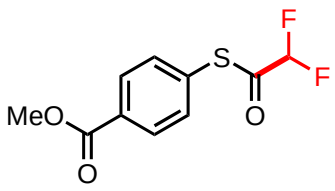

methyl 4-((2,2-difluoroacetyl)thio)benzoate (3.1h). The general method was followed using 2 mmol of the corresponding thiol. This afforded **3.1h** as a white solid (444 mg, 90% yield). **^{1}H NMR** (500 MHz, $CDCl_3$) δ 8.13 (d, *J* = 8.5 Hz, 1H), 7.55 (d, *J* = 8.4 Hz, 1H), 5.99 (t, *J* = 53.9 Hz, 1H), 3.96 (s, 3H). **^{13}C NMR** (176 MHz, $CDCl_3$) δ 188.85 (t, *J* = 29.7 Hz), 166.11, 134.36, 131.85, 130.53, 129.51, 109.15 (t, *J* = 256.0 Hz), 52.45. **^{19}F NMR** (376 MHz, $CDCl_3$) δ -123.46 (d, *J* = 54.0 Hz). **HRMS** (GC-APCI) calcd. for $C_8H_5F_3OS$ [M+H]+ *m/z* 247.0262, found 247.0241.

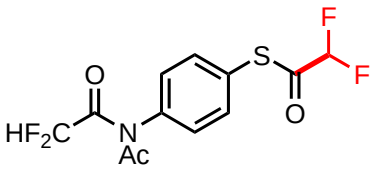

***S*-(4-(*N*-(2,2-Difluoroacetyl)acetamido)phenyl) 2,2-difluoroethanethioate (3.1i).** The general method was followed using 2 mmol of the corresponding thiol. This afforded **1i** as a clear oil (568 mg, 88% yield). **mp** 101.3–103.3 °C. **^{1}H NMR** (500 MHz, $CDCl_3$) δ 7.63 (d, *J* = 7.9 Hz, 2H), 7.33 (d, *J* = 8.0 Hz, 2H), 6.65 (t, *J* = 53.2 Hz, 1H), 6.01 (t, *J* = 54.0 Hz, 1H), 2.19 (s, 3H). **^{13}C NMR** (126 MHz, $CDCl_3$) δ 188.75 (t, *J* = 29.8 Hz), 171.97, 164.84 (t, *J* = 27.9 Hz), 138.41, 136.10, 129.84, 126.57, 109.12 (t, *J* = 255.9 Hz), 107.12 (t, *J* = 247.6 Hz), 25.74. **^{19}F NMR** (377 MHz, $CDCl_3$) δ –123.56 (d, *J* = 54.0 Hz), –125.58 (d, *J* = 53.2 Hz). **HRMS** (ESI) calcd. for $C_{12}H_9F_4NO_3S$ [M+H] *m/z* 324.0339, found 324.0312.

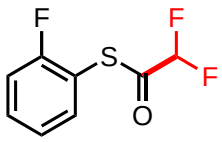

***S*-(2-fluorophenyl) 2,2-difluoroethanethioate (3.1j).** The general method was followed using 2 mmol of the corresponding thiol. This afforded **1j** as a clear oil (343 mg, 83% yield). **^{1}H NMR** (500 MHz, $CDCl_3$) δ δ 7.53 (dddd, *J* = 8.0, 7.2, 5.0, 1.5 Hz, 1H), 7.46 (ddd, *J* = 8.1, 6.9, 1.7 Hz, 1H), 7.31 – 7.21 (m, 2H), 6.00 (t, *J* = 53.9 Hz, 1H). **^{13}C NMR** (126 MHz, $CDCl_3$) δ 188.03 (t, *J* =

29.7 Hz), 163.23, 161.23, 136.49, 133.15 (d, *J* = 8.0 Hz), 125.09 (d, *J* = 4.0 Hz), 116.61 (d, *J* = 22.2 Hz), 109.13 (t, *J* = 255.7 Hz). **^{19}F NMR** (471 MHz, $CDCl_3$) δ -105.79 – -106.12 (m, 1F), -123.43 (dd, *J* = 53.9, 19.1 Hz, 2F). **HRMS** (GC-APCI) calcd. for $C_8H_5F_3OS$ [M+] *m/z* 206.0013, found 206.0007.

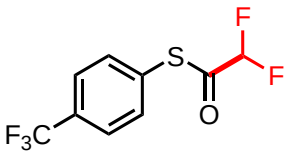

***S*-(4-(trifluoromethyl)phenyl) 2,2-difluoroethanethioate (3.1k).** The general method was followed using 2 mmol of the corresponding thiol. This afforded **1k** as a clear oil (425 mg, 83% yield). **^{1}H NMR** (400 MHz, $CDCl_3$) 7.71 (d, *J* = 8.1 Hz, 1H), 7.57 (d, *J* = 8.0 Hz, 1H), 5.97 (t, *J* = 53.9 Hz, 1H). **^{13}C NMR** (176 MHz, $CDCl_3$) δ 188.82 (t, *J* = 29.8 Hz), 134.85, 132.41 (q, *J* = 33.0 Hz), 128.67, 126.45 (q, *J* = 3.8 Hz), 123.55 (q, *J* = 272.7 Hz), 109.12 (t, *J* = 256.0 Hz). **^{19}F NMR** (376 MHz, $CDCl_3$) δ -63.10, -123.48 (d, *J* = 54.3 Hz). **HRMS** (GC-APCI) calcd. for $C_9H_5F_5OS$ [M+] *m/z* 255.9981, found 255.9983.

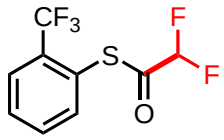

***S*-(2-(trifluoromethyl)phenyl) 2,2-difluoroethanethioate (3.1l).** The general method was followed using 2 mmol of the corresponding thiol. This afforded **1l** as a clear oil (462 mg, 90% yield). **^{1}H NMR** (500 MHz, $CDCl_3$) δ 7.87 (d, *J* = 7.1 Hz, 1H), 7.73 – 7.58 (*multiple peaks*, 3H), 6.00 (t, *J* = 53.9 Hz, 1H). **^{13}C NMR** (126 MHz, $CDCl_3$) δ 188.70 (t, *J* = 29.9 Hz), 138.91, 133.66 (q, *J* = 30.7 Hz), 132.68, 130.91, 127.61 (q, *J* = 5.4 Hz), 122.90 (q, *J* = 273.7 Hz), 122.61, 109.09 (t, *J* = 255.7 Hz). **^{19}F NMR** (471 MHz, $CDCl_3$) δ -60.65 (s, 3F), -123.45 (d, *J* = 53.3 Hz, 2F). **HRMS** (GC-APCI) calcd. for $C_9H_5F_5OS$ [M+] *m/z* 255.9981, found 255.9980.

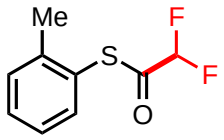

***S*-(*o*-Tolyl) 2,2-difluoroethanethioate (3.1m).** The general method was followed using 3 mmol of the corresponding thiol. This afforded **3.1m** as a clear oil (466 mg, 89% yield). **^{1}H NMR** (401 MHz, $CDCl_3$) δ 7.45–7.31 (m, 3H), 7.25 (d, *J* = 3.6 Hz, 1H), 5.95 (t, *J* = 53.7 Hz, 1H), 2.34 (s, 3H). **^{13}C NMR** (176 MHz, $CDCl_3$) δ 189.26 (t, *J* = 29.2 Hz), 142.43, 135.89, 131.18, 131.00, 127.03, 123.41, 109.33 (t, *J* = 255.5 Hz), 20.46. **^{19}F NMR** (471 MHz, $CDCl_3$) δ –123.35 (d, *J* = 53.7 Hz, 2F). **HRMS** (ES) calcd. for $C_9H_8F_2OS$ [M+] *m/z* 202.0264, found 202.0257.

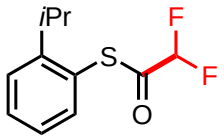

***S*-(2-Isopropylphenyl) 2,2-difluoroethanethioate 3. (1n).** The general method was followed using 2 mmol of the corresponding thiol. This afforded **1n** as a clear oil (370 mg, 80% yield). **^{1}H NMR** (500 MHz, $CDCl_3$) δ 7.52–7.42 (m, 2H), 7.40 (d, *J* = 7.8 Hz, 1H), 7.26 (d, *J* = 7.5 Hz, 1H), 5.97 (t, *J* = 54.1 Hz, 1H), 3.25 (hept, *J* = 6.6 Hz, 1H), 1.22 (d, *J* = 6.9 Hz, 6H). **^{13}C NMR** (176 MHz, $CDCl_3$) δ 189.80 (t, *J* = 29.1 Hz), 152.41, 136.33, 131.35, 126.91, 126.76, 122.18, 109.35 (t, *J* = 255.6 Hz), 31.33, 23.58. **^{19}F NMR** (471 MHz, $CDCl_3$) δ –123.06 (d, *J* = 54.1 Hz, 2F). **HRMS** (ES) calcd. for $C_{11}H_{12}F_2OS$ [M+] *m/z* 230.0577, found 230.0571.

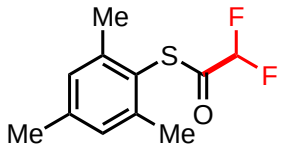

***S*-Mesityl 2,2-difluoroethanethioate (3.1o).** The general method was followed using 2 mmol of the corresponding thiol. This afforded **3.1o** as white solid (393 mg, 85% yield). **mp** 69.3–72.0 °C. **^{1}H NMR** (500 MHz, $CDCl_3$) δ 7.02 (s, 2H), 5.95 (t, *J* = 54.1 Hz, 1H), 2.32 (s, 9H). **^{13}C NMR** (126

MHz, $CDCl_3$) δ 189.02 (t, *J* = 29.0 Hz), 142.71, 140.90, 129.61, 119.70, 109.37 (t, *J* = 255.4 Hz), 21.29. **^{19}F NMR** (470 MHz, $CDCl_3$) δ –122.89 (d, *J* = 54.1 Hz, 2F). **HRMS** (GC-APCI) calcd. for $C_{11}H_{12}F_2OS$ [M+]+ *m/z* 231.0677, found 231.0649.

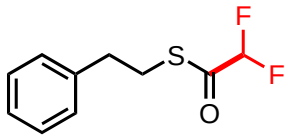

***S*-Phenethyl 2,2-difluoroethanethioate (3.1p).** The general method was followed using 2 mmol of the corresponding thiol. This afforded **3.1p** as a clear oil (379 mg, 88% yield). **^{1}H NMR** (700 MHz, $CDCl_3$) δ 7.34 (t, *J* = 7.5 Hz, 2H), 7.27 (t, *J* = 6.9 Hz, 1H), 7.24 (d, *J* = 7.6 Hz, 2H), 5.86 (t, *J* = 54.1 Hz, 1H), 3.26 (t, *J* = 7.7 Hz, 2H), 2.94 (t, *J* = 7.7 Hz, 2H). **^{13}C NMR** (176 MHz, $CDCl_3$) δ 191.32 (t, *J* = 29.0 Hz), 139.07, 128.66, 128.55, 126.86, 108.98 (t, *J* = 254.5 Hz), 35.12, 29.83. **^{19}F NMR** (377 MHz, $CDCl_3$) δ –123.80 (d, *J* = 54.1 Hz, 2F). **HRMS** (ES) calcd. for $C_{10}H_{10}F_2OS$ [M+] *m/z* 216.0420, found 216.0419.

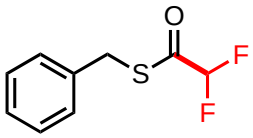

***S*-Benzyl 2,2-difluoroethanethioate (3.1q).** The general method was followed using 2 mmol of the corresponding thiol. This afforded **3.1q** as a clear oil (350 mg, 87% yield). **^{1}H NMR** (700 MHz, $CDCl_3$) δ 7.39–7.27 (m, 5H), 5.88 (t, *J* = 54.0 Hz, 1H), 4.25 (s, 2H). **^{13}C NMR** (176 MHz, $CDCl_3$) δ 190.99 (t, *J* = 29.1 Hz), 135.60, 128.97, 128.85, 127.89, 109.02 (t, *J* = 254.6 Hz), 32.77 (d, *J* = 1.5 Hz). **^{19}F NMR** (377 MHz, $CDCl_3$) δ –123.79 (d, *J* = 54.0 Hz, 2F). **HRMS** (ES) calcd. for $C_9H_8F_2OS$ [M+] *m/z* 202.0264, found 202.0264.

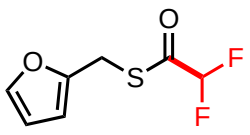

***S*-(Furan-2-ylmethyl) 2,2-difluoroethanethioate (3.1r).** The general method was followed using 3 mmol of the corresponding thiol. This afforded **3.1r** as a clear oil (467 mg, 81% yield). **^{1}H NMR** (700 MHz, $CDCl_3$) δ 7.35 (d, *J* = 1.0 Hz, 1H), 6.33–6.29 (m, 1H), 6.29 (d, *J* = 3.2 Hz, 1H), 5.88 (t, *J* = 54.0 Hz, 1H), 4.27 (s, 2H). **^{13}C NMR** (176 MHz, $CDCl_3$) δ 190.52 (t, *J* = 29.4 Hz), 148.49, 142.76, 110.74, 108.99, 108.90 (t, *J* = 254.6 Hz), 25.24. **^{19}F NMR** (377 MHz, $CDCl_3$) δ –123.73 (d, *J* = 54.0 Hz, 2F). **HRMS** (ES) calcd. for $C_7H_6F_2O_2S$ [M+] *m/z* 192.0057, found 192.0056.

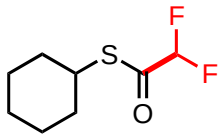

***S*-Cyclohexyl 2,2-difluoroethanethioate (3.1s).** The general method was followed using 2 mmol of the corresponding thiol. This afforded **3.1s** as a clear oil (341 mg, 88% yield). **^{1}H NMR** (500 MHz, $CDCl_3$) δ 5.82 (t, *J* = 54.3 Hz, 1H), 3.67 (dp, *J* = 10.0, 4.0 Hz, 1H), 2.02–1.93 (m, 2H), 1.74 (dt, *J* = 8.0, 4.1 Hz, 2H), 1.66–1.58 (m, 1H), 1.57–1.42 (multiple peaks, 4H), 1.39–1.27 (m, 1H). **^{13}C NMR** (176 MHz, $CDCl_3$) δ 191.03 (t, *J* = 28.6 Hz), 109.03 (t, *J* = 254.6 Hz), 42.51, 32.57, 25.70, 25.33. **^{19}F NMR** (377 MHz, $CDCl_3$) δ –123.90 (d, *J* = 54.3 Hz, 2F). **HRMS** (ES) calcd. for $C_8H_{12}F_2OS$ [M+] *m/z* 194.0577, found 194.0578.

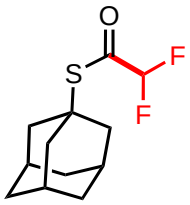

***S*-((3*s*,5*s*,7*s*)-Adamantan-1-yl) 2,2-difluoroethanethioate (3.1t).** The general method was followed using 2 mmol of the corresponding thiol. This afforded **3.1t** as a clear oil (397 mg, 81% yield). **mp** 45.0–47.2°C. **^{1}H NMR** (500 MHz, $CDCl_3$) δ 5.69 (t, *J* = 54.4 Hz, 1H), 2.20 (d, *J* = 2.9 Hz, 6H), 2.14–2.06 (m, 3H), 1.87–1.67 (m, 6H). **^{13}C NMR** (176 MHz, $CDCl_3$) δ 190.76 (t, *J* = 27.5 Hz), 108.88 (t, *J* = 255.5 Hz), 52.42, 41.60, 36.07, 29.83. **^{19}F NMR** (377 MHz, $CDCl_3$) δ –

123.38 (d, *J* = 54.4 Hz, 2F). **HRMS** (ES) calcd. for $C_{12}H_{16}F_2OS$ [M+] *m/z* 246.0890, found 246.0882.

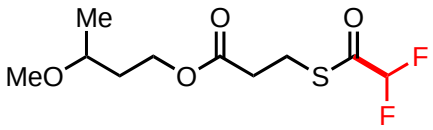

3-Methoxybutyl 3-((2,2-difluoroacetyl)thio)propanoate (3.1u). The general method was followed using 2 mmol of the corresponding thiol. This afforded **3.1u** as a light brown oil (404 mg, 75% yield). **^{1}H NMR** (500 MHz, $CDCl_3$) δ 5.85 (t, *J* = 54.0 Hz, 1H), 4.20 (t, *J* = 6.9 Hz, 2H), 3.39 (q, *J* = 6.4 Hz, 1H), 3.30 (s, 3H), 3.23 (t, *J* = 7.0 Hz, 2H), 2.66 (t, *J* = 7.0 Hz, 2H), 1.83–1.70 (m, 2H), 1.15 (d, *J* = 6.0 Hz, 3H). **^{13}C NMR** (126 MHz, $CDCl_3$) δ 191.29 (t, *J* = 29.2 Hz), 171.01, 108.87 (t, *J* = 254.6 Hz), 73.56, 62.10, 56.06, 35.42, 33.59, 23.46, 18.99. **^{19}F NMR** (377 MHz, $CDCl_3$) δ –123.61 (d, *J* = 54.0 Hz, 2F). **HRMS** (ESI) calcd. for $C_{10}H_{16}F_2O_4S$ [M+H] *m/z* 271.0837, found 271.0830.

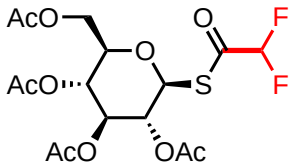

(2*R*,3*R*,4*S*,5*R*,6*S*)-2-(Acetoxymethyl)-6-((2,2-difluoroacetyl)thio)tetrahydro-2*H*-pyran-3,4,5-triyl triacetate (3.1w). The general method was followed using 1.5 mmol of the corresponding thiol. Washing, drying, and removal of solvent afforded **3.1w** as a sticky white solid (543 mg, 82% yield). **mp** 75.1–78.5 °C. **^{1}H NMR** (700 MHz, $CDCl_3$) δ 5.87 (t, *J* = 53.7 Hz, 1H), 5.24 (dd, *J* = 22.8, 9.9 Hz, 2H), 5.12 (t, *J* = 9.9 Hz, 1H), 5.06 (t, *J* = 9.8 Hz, 1H), 4.19 (dd, *J* = 12.6, 4.4 Hz, 1H), 4.03 (d, *J* = 12.5 Hz, 1H), 3.82 (d, *J* = 8.3 Hz, 1H), 2.00 (s, 3H), 1.96 (s, 3H), 1.95 (s, 3H), 1.93 (s, 3H). **^{13}C NMR** (176 MHz, $CDCl_3$) δ 188.63 (t, *J* = 30.3 Hz), 170.44, 169.87, 169.24, 169.11, 108.57 (t, *J* = 255.0 Hz), 79.12, 76.55, 73.58, 68.89, 67.63, 61.45, 20.40. **^{19}F NMR** (376

MHz, $CDCl_3$) δ –123.26 (dd, *J* = 308.5, 53.7 Hz, 1F), –124.66 (dd, *J* = 308.5, 53.7 Hz, 1F). **HRMS** (ESI) calcd. for $C_9H_8F_2OS$ [M+Na] *m/z* 465.0642, found 465.0637.

General procedure for the synthesis of methyl ((S)-3-((difluoromethyl)thio)-2-methylpropanoyl)prolinate *(3.1v)*. In an oven dried round bottom flask, captopril (217 mg, 1.0 mmol, 1.0 equiv) was dissolved in 10 mL of solvent (3:2 anhydrous toluene:MeOH). Under a flow of N_2 at 0 °C, 2.0 M TMS-diazomethane in diethyl ether (0.5 mL, 1.0 mmol, 1.0 equiv) was added dropwise to the stirring reaction until a yellow color persisted in solution. Once the reaction turned yellow, it was allowed to warm to room temperature. The volatiles were then removed *in vacuo*, leaving behind the methyl ester thiol as a viscous, maroon-colored oil. The oil was dissolved in 6 mL of CH_2Cl_2, and difluoroacetic anhydride was added dropwise (0.13 mL, 1.0 mmol, 1.0 equiv) to the solution at room temperature. After stirring the solution at ambient temperature for 15 min, the solution was diluted with CH_2Cl_2 (30 mL) and washed with cold water (3 x 10 mL). The organic layer was collected and dried over $MgSO_4$. The solvent was removed *in vacuo* to afford difluoromethylthioester **1v**. During the reaction, isomerization of the tertiary pyrrolidine proton resulted in an inseparable mixture of diastereomers (dr = 1.0 : 0.2). Removal of solvent afforded **1v** as a clear, sticky solid (255 mg, 83% yield, dr = 1.0 : 0.2). **mp** 57.5–60.3 °C. **^{1}H NMR** (500 MHz, $CDCl_3$) δ 5.86 (t, *J* = 54.1 Hz, 1H), 4.54 (dd, *J* = 8.7, 4.0 Hz, 1H), 3.73 (s, 3H), 3.67–3.50 (m, 2H), 3.26 (dd, *J* = 13.4, 8.4 Hz, 1H), 3.13 (dd, *J* = 13.6, 5.9 Hz, 1H), 2.85 (h, *J* = 6.9 Hz, 1H), 2.32–2.14 (m, 1H), 2.08 (ddd, *J* = 14.1, 6.9, 2.3 Hz, 1H), 2.05–1.96 (m, 2H), 1.30 (d, *J* = 6.9 Hz, 3H) *for the major diastereomer*. **^{13}C NMR** (126 MHz, $CDCl_3$) δ 191.91 (t, *J* = 29.0 Hz), 172.75, 172.54, 108.92 (t, *J* = 254.6 Hz), 58.67, 52.21, 46.90, 38.07, 31.25, 29.00, 24.82, 16.85 *for the*

major diastereomer. **^{19}F NMR** (471 MHz, $CDCl_3$) δ –122.91 *to* –125.63 (multiple peaks, 2F). **HRMS** (ESI) calcd. for $C_9H_8F_2OS$ [M+H] *m/z* 310.0946, found 310.0919.

General procedure for the synthesis of fluoroalkylated thioesters from fluoroalkyl carboxylic acids (Method A). The respective thiol (2.0 mmol, 1.0 equiv), fluorocarboxylic acid (2.2 mmol, 1.1 equiv), EDC (3.0 mmol, 1.5 equiv), pyridine (2.0 mmol, 1 equiv), and DMAP (0.2 mmol, 0.1 equiv) were weighed into a 20 mL vial and dissolved in CH_2Cl_2 (6 mL). The reaction was stirred at room temperature for 20 h. After this time, the solution was diluted with CH_2Cl_2 (20 mL) and washed with cold water (3 x 10 mL). The organic layer was collected and dried over $MgSO_4$. Solvent was removed *in vacuo* to afford the crude reaction mixture. Purification was performed by silica column chromatography using an ethyl acetate/hexane solvent mixture.

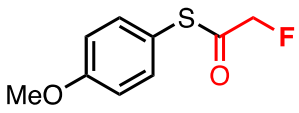

***S*-(4-Methoxyphenyl) 2-fluoroethanethioate (3.1x). Method A** was followed using 4-methoxythiophenol (1.0 mmol) and 2-fluoroacetic acid (1.1 mmol). Purification by flash chromatography on silica gel (hexanes/EtOAc, 95:5) afforded **3.1x** as a colorless oil (162 mg, 81% yield). **^{1}H NMR** (400 MHz, $CDCl_3$) δ 7.33 (d, *J* = 7.8 Hz, 2H), 6.96 (d, *J* = 7.8 Hz, 2H), 4.96 (d, *J* = 47.1 Hz, 2H), 3.81 (s, 3H). **^{13}C NMR** (126 MHz, $CDCl_3$) δ 196.49 (d, *J* = 24.9 Hz), 161.19, 136.54, 115.62 (d, *J* = 4.9 Hz), 115.31, 84.87 (d, *J* = 187.9 Hz), 55.50. **^{19}F NMR** (377 MHz, $CDCl_3$) δ –225.59 (t, *J* = 47.1 Hz, 1F). **HRMS** (ESI) calcd. for $C_9H_{10}FO_2S$ [M+H] *m/z* 201.0386, found 201.0389.

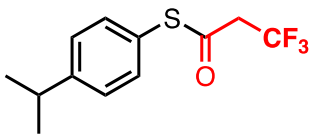

***S*-(4-Isopropylphenyl) 3,3,3-trifluoropropanethioate (3.1y). Method A** was followed using 4-isopropylthiophenol (2.0 mmol) and 3,3,3-trifluoropropionic acid (2.2 mmol). Purification by flash chromatography on silica gel (hexanes/EtOAc, 95:5) afforded **3.1y** as a colorless oil (398 mg, 76% yield). **^{1}H NMR** (500 MHz, $CDCl_3$) δ 7.36 (d, *J* = 8.3 Hz, 2H), 7.32 (d, *J* = 8.3 Hz, 2H), 3.45 (q, *J* = 9.9 Hz, 2H), 2.96 (septet, *J* = 6.9 Hz, 1H), 1.28 (d, *J* = 6.9 Hz, 6H). **^{13}C NMR** (176 MHz, $CDCl_3$) δ 187.63 (q, *J* = 3.1 Hz), 151.28, 134.41, 127.70, 122.94 (d, *J* = 277.8 Hz), 122.78, 46.42 (q, *J* = 29.6 Hz), 33.99, 23.73. **^{19}F NMR** (377 MHz, $CDCl_3$) δ –62.66 (t, *J* = 9.9 Hz, 3F). **HRMS** (ESI) calcd. for $C_{12}H_{14}F_3OS$ [M+H] *m/z* 263.0717, found 263.0717.

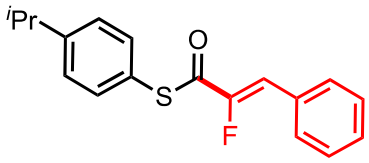

***S*-(4-Isopropylphenyl)-(*Z*)-2-fluoro-3-phenylprop-2-enethioate (3.1ab).** The general method was followed using 4-isopropylthiophenol (2.0 mmol) and (*Z*)-2-fluoro-3-phenylacrylic acid (2.2 mmol). Purification by flash chromatography on silica gel (hexanes/EtOAc, 95:5) afforded **1ab** as a white solid (480 mg, 80% yield). **mp** 92–94 °C. **^{1}H NMR** (500 MHz, $CDCl_3$) δ 7.70 (dd, *J* = 7.9, 1.8 Hz, 2H), 7.48–7.38 (multiple peaks, 5H), 7.34 (d, *J* = 8.2 Hz, 2H), 6.86 (d, *J* = 36.6 Hz, 1H), 2.97 (septet, *J* = 6.9 Hz, 1H), 1.30 (d, *J* = 6.9 Hz, 6H). **^{13}C NMR** (126 MHz, $CDCl_3$) δ 185.51 (d, *J* = 37.5 Hz), 152.31 (d, *J* = 271.8 Hz), 151.13, 135.09, 131.04 (d, *J* = 8.1 Hz), 130.99, 130.27 (d, *J* = 2.6 Hz), 129.14, 127.86, 122.79 (d, *J* = 4.4 Hz), 114.03 (d, *J* = 4.4 Hz), 34.23, 24.03. **^{19}F NMR** (471 MHz, $CDCl_3$) δ –125.26 (d, *J* = 36.6 Hz, 1F). **HRMS** (ESI) calcd. for $C_{18}H_{18}FOS$ [M+H] *m/z* 301.1062, found 301.1065.

Fluoroalkyl thioester synthesis via in situ generated acid chlorides (Method B).[55] The corresponding carboxylic acid (4.25 mmol, 1 equiv) was dissolved in 8 mL of CH_2Cl_2 and DMF

(0.07 mL, 0.85 mmol, 0.2 equiv) was added. At 0 °C, $(COCl)_2$ was added dropwise (0.36 mL, 4.25 mmol, 1 equiv) to the stirring solution. The reaction was then allowed to warm to room temperature and stir for 3 h. After this time, the acid chloride solution was added dropwise to a 0 ºC solution of thiol (595 mg, 4.25 mmol, 1 equiv) and Et_3N (0.83 mL, 6 mmol, 1.4 equiv) in 8 mL of CH_2Cl_2. The resulting mixture was allowed to warm to room temperature and stir overnight, after which the volatiles were removed *in vacuo*. The thioester product was purified via flash column chromatography on silica gel.

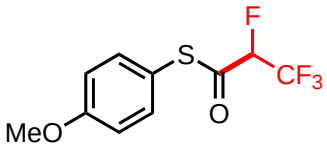

***S*)-(4-Methoxyphenyl)(1,2,2,2-tetrafluoroethyl)sulfane (1z). Method B** was followed using 4-(methoxy)thiophenol (3.5 mmol) and 2,3,3,3-(tetrafluoro)propionic acid (3.5 mmol). Purification by flash chromatography on silica gel (hexanes/EtOAc, 90:10) afforded **1z** as a clear oil (591 mg, 63% yield). **^{1}H NMR** (401 MHz, $CDCl_3$) δ 7.32 (d, *J* = 8.9 Hz, 1H), 6.97 (d, *J* = 8.9 Hz, 1H), 5.16 (dq, *J* = 46.1, 6.4 Hz, 1H), 3.83 (s, 2H). **^{13}C NMR** (126 MHz, $CDCl_3$) δ 190.31 (d, *J* = 27.3 Hz), 161.41, 136.29, 119.95 (dd, *J* = 283.1, 25.7 Hz), 115.35, 114.29 (d, *J* = 5.3 Hz), 88.94 (dq, *J* = 204.3, 33.9 Hz), 55.39. **^{19}F NMR** (377 MHz, $CDCl_3$) δ –75.70 (dd, *J* = 11.8, 6.4 Hz, 3F), –202.79 (dq, *J* = 46.1, 11.8 Hz, 1F). **HRMS** (GC-APCI) calcd. for $C_{10}H_8F_4O_2S$ [M+H]+ *m/z* 269.0281, found 269.0262.

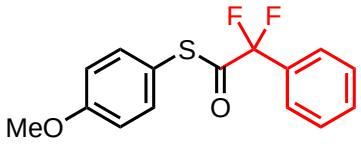

***S*-(4-Isopropylphenyl) 2,2-difluoro-2-phenylethanethioate (1aa). Method B** was followed using 4-isopropylthiophenol (1.0 mmol) and 2,2-difluoro-2-phenylacetic acid (1.1 mmol). Purification by flash chromatography on silica gel (hexanes/EtOAc, 95:5) afforded **1aa** as a

colorless oil (199 mg, 65 % yield). **Mp** 75.0 °C–77.6°C **^{1}H NMR** (500 MHz, $CDCl_3$) δ 7.68 (d, *J* = 7.0 Hz, 2H), 7.55–7.47 (*multiple peaks*, 3H), 7.32 (d, *J* = 8.8 Hz, 2H), 6.96 (d, *J* = 8.8 Hz, 2H), 3.83 (s, 3H). **^{13}C NMR** (176 MHz, $CDCl_3$) δ 191.98 (t, *J* = 36.8 Hz), 161.19, 136.16, 132.65, 132.07 (t, *J* = 25.3 Hz), 131.12, 128.68, 125.72 (t, *J* = 6.1 Hz), 116.01 (t, *J* = 256.7 Hz), 115.18, 55.38. **^{19}F NMR** (471 MHz, $CDCl_3$) δ -101.48. **HRMS** (ESI) calcd. for $C_{15}H_{12}F_2O_2S$ [M+H]+ *m/z* 295.0626, found 295.0599.

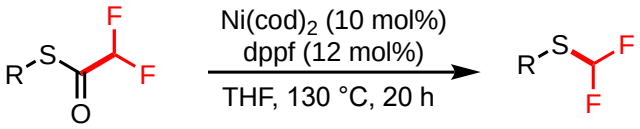

General procedure for the decarbonylation of fluorinated thioesters: $Ni(cod)_2$ (13.8 mg, 0.05 mmol, 0.1 equiv) and dppf (30.9 mg, 0.06 mmol, 0.12 equiv) were dissolved in anhydrous THF (1 mL), and this mixture was stirred for 15 min at room temperature. The resulting solution was then transferred to a tall 10 mL vial with a stir bar containing the respective, pre-weighed thioester (0.5 mmol, 1 equiv). The vial was sealed with a Teflon-lined screw cap and taken outside the glovebox. The vial was heated at 130 °C for 20 h with stirring. The reaction was then allowed to cool to room temperature, and the solvent was removed *in vacuo*. The resulting crude brown residue was purified via flash chromatography on silica gel.

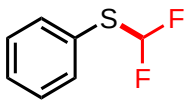

(Difluoromethyl)(phenyl)sulfane (3.2a). The general decarbonylation procedure was followed using 0.5 mmol of the corresponding thioester. Purification by flash chromatography on silica gel (hexanes/EtOAc, 97:3) afforded the product as a clear oil (49 mg, 61% yield). **^{1}H NMR** (500 MHz, $CDCl_3$) δ 7.60 (d, *J* = 7.6 Hz, 2H), 7.48–7.37 (multiple peaks, 3H), 6.85 (t, *J* = 57.0 Hz, 1H). **^{13}C**

NMR (176 MHz, $CDCl_3$) δ 135.30, 129.74, 129.34, 126.10, 120.99 (t, *J* = 275.0 Hz). **^{19}F NMR** (377 MHz, $CDCl_3$) δ –91.23 (d, *J* = 57.0 Hz, 2F). **HRMS** (EI) calcd. for $C_7H_6F_2S$ [M+] *m/z* 160.0158, found 160.0163.

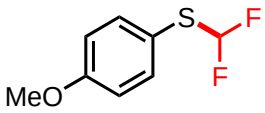

(Difluoromethyl)(4-methoxyphenyl)sulfane (3.2b). The general decarbonylation procedure was followed using 0.5 mmol of the corresponding thioester. Purification by flash chromatography on silica gel (hexanes/EtOAc, 97:3) afforded the product as a clear oil (65 mg, 69% yield). **^{1}H NMR** (500 MHz, $CDCl_3$) δ 7.52 (d, *J* = 8.7 Hz, 2H), 6.91 (d, *J* = 8.6 Hz, 2H), 6.75 (t, *J* = 57.2 Hz, 1H), 3.83 (s, 3H). **^{13}C NMR** (176 MHz, $CDCl_3$) δ 161.17, 137.57, 120.94 (t, *J* = 275.1 Hz), 116.15, 114.89, 55.36. **^{19}F NMR** (471 MHz, $CDCl_3$) δ –105.48 (d, *J* = 57.2 Hz, 2F). **HRMS** (GC-APCI) calcd. for $C_8H_8F_2S$ [M+] *m/z* 190.0264, found 190.0258.

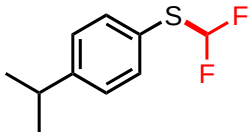

(Difluoromethyl)(4-isopropylphenyl)sulfane (3.2c). The general decarbonylation procedure was followed using 0.5 mmol of the corresponding thioester. Purification by flash chromatography on silica gel (hexanes/EtOAc, 97:3) afforded the product as a clear oil (65 mg, 64% yield). **^{1}H NMR** (700 MHz, $CDCl_3$) δ 7.51 (d, *J* = 8.0 Hz, 2H), 7.25 (d, *J* = 7.8 Hz, 2H), 6.80 (t, *J* = 57.1 Hz, 1H), 2.93 (p, *J* = 6.9 Hz, 1H), 1.26 (d, *J* = 6.9 Hz, 6H). **^{13}C NMR** (176 MHz, $CDCl_3$) δ 150.97, 135.58, 127.55, 121.17 (t, *J* = 274.8 Hz), 33.91, 23.79. **^{19}F NMR** (377 MHz, $CDCl_3$) δ –91.81 (d, *J* = 57.1 Hz, 2F). **HRMS** (GC-APCI) calcd. for $C_{10}H_{12}F_2S$ [M+] *m/z* 202.0628, found 202.0622.

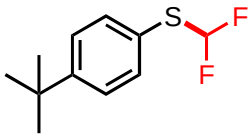

(4-(*Tert*-butyl)phenyl)(difluoromethyl)sulfane (3.2d). The general decarbonylation procedure was followed using 0.5 mmol of the corresponding thioester. Purification by flash chromatography on silica gel (hexanes/EtOAc, 97:3) afforded the product as a clear oil (55 mg, 51% yield). **^{1}H NMR** (500 MHz, $CDCl_3$) δ 7.53 (d, *J* = 8.4 Hz, 2H), 7.43 (d, *J* = 8.2 Hz, 2H), 6.82 (t, *J* = 57.2 Hz, 1H), 1.35 (s, 9H). **^{13}C NMR** (126 MHz, $CDCl_3$) δ 153.22, 135.19, 126.45, 122.53, 121.19 (t, *J* = 274.9 Hz), 34.75, 31.16. **^{19}F NMR** (377 MHz, $CDCl_3$) δ –91.79 (d, *J* = 57.2 Hz, 2F). **HRMS** (GC-APCI) calcd. for $C_{11}H_{14}F_2S$ [M+] *m/z* 216.0784, found 216.0779.

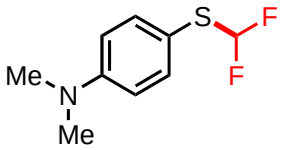

4-((Difluoromethyl)thio)-*N*,*N*-dimethylaniline (3.2e). The general decarbonylation procedure was followed using 0.5 mmol of the corresponding thioester. Purification by flash chromatography on silica gel (hexanes/EtOAc, 90:10) afforded the purified product as a yellow oil (99 mg, 98% yield). **^{1}H NMR** (700 MHz, $CDCl_3$) δ 7.54 (d, *J* = 8.9 Hz, 2H), 6.81 (t, *J* = 57.5 Hz, 1H), 6.79 (d, *J* = 8.5 Hz, 2H), 3.11 (s, 6H). **^{13}C NMR** (176 MHz, $CDCl_3$) δ 151.55, 137.49, 121.52 (t, *J* = 274.9 Hz), 112.61, 109.96, 40.28. **^{19}F NMR** (471 MHz, $CDCl_3$) δ –92.60 (d, *J* = 57.5 Hz, 2F). **HRMS** (ESI) calcd. for $C_9H_{11}F_2NS$ [M+H]+ *m/z* 204.0680, found 204.0653.

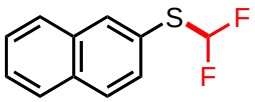

(Difluoromethyl)(naphthalen-2-yl)sulfane (3.2f). The general decarbonylation procedure was followed using 0.5 mmol of the corresponding thioester. Purification by flash chromatography on silica gel (hexanes/EtOAc, 97:3) afforded the product as a light brown oil (82 mg, 86% yield). **^{1}H NMR** (500 MHz, $CDCl_3$) δ 8.13 (s, 1H), 7.90–7.81 (multiple peaks, 3H), 7.63 (d, *J* = 8.5 Hz, 1H), 7.56 (ddd, *J* = 6.8, 3.7, 1.8 Hz, 2H), 6.92 (t, *J* = 56.9 Hz, 1H). **^{13}C NMR** (176 MHz, $CDCl_3$) δ

135.41, 133.50, 133.42, 131.38, 129.04, 127.92, 127.76, 127.40, 126.88, 123.30, 121.12 (t, J = 275.3 Hz). **^{19}F NMR** (377 MHz, $CDCl_3$) δ –91.59 (d, J = 56.9 Hz, 2F). **HRMS** (GC-APCI) calcd. for $C_{11}H_8F_2S$ [M+] *m/z* 210.0315, found 210.0309.

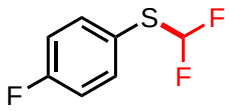

(difluoromethyl)(4-fluorophenyl)sulfane (3.2g). The general decarbonylation procedure was followed using 0.3 mmol of the corresponding thioester, and the yield was determined by ^{19}F NMR spectroscopy with 4-fluorotoluene as the internal standard (88% yield). ^{19}F NMR shifts were consistent with formation of decarbonylated (difluoromethyl)thioether, ^{19}F NMR (377 Hz, $CDCl_3$) δ 91.50 ppm (d, J = 56.7Hz, 2F). Due to the high volatility of the product, attempts at isolation were unsuccessful.

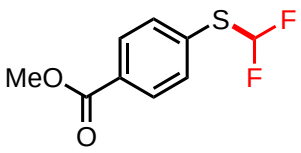

methyl 4-((difluoromethyl)thio)benzoate (3.2h). The general decarbonylation procedure was followed using 0.3 mmol of the corresponding thioester, and the yield was determined by ^{19}F NMR spectroscopy with 4-fluorotoluene as the internal standard (54% yield). ^{19}F NMR shifts were consistent with formation of decarbonylated (difluoromethyl)thioether, ^{19}F NMR (471 Hz, $CDCl_3$) δ –92.13 ppm (d, J = 56.5 Hz, 2F).

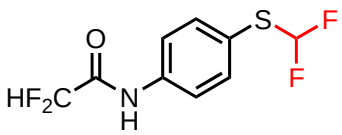

***N*-(4-((Difluoromethyl)thio)phenyl)-2,2-difluoroacetamide (3.2i).** The general decarbonylation procedure was followed using 0.5 mmol of the corresponding thioester. Purification by flash chromatography on silica gel (hexanes/EtOAc, 80:20) afforded the product as a white solid (19

mg, 15% yield). During the work up, the acetyl group was cleaved, affording the difluoromethylacetamide as the isolated product. **mp** 101.8–102.8 °C. **^{1}H NMR** (500 MHz, $CDCl_3$) δ 8.03 (b, 1H), 7.63 (d, *J* = 8.5 Hz, 2H), 7.60 (d, *J* = 8.3 Hz, 2H), 6.80 (t, *J* = 56.9 Hz, 1H), 6.03 (t, *J* = 54.3 Hz, 1H). **^{13}C NMR** (176 MHz, $CDCl_3$) δ 160.39 (t, *J* = 24.7 Hz), 137.25, 136.65, 122.58, 120.77, 120.45 (t, *J* = 275.7 Hz), 108.36 (t, *J* = 254.4 Hz). **^{19}F NMR** (471 MHz, $CDCl_3$) δ –87.24 (d, *J* = 56.9 Hz, 1F), –121.02 (d, *J* = 54.3 Hz, 1F). **HRMS** (GC-APCI) calcd. for $C_9H_7F_4OS$ [M+H] *m/z* 254.0284, found 254.0265.

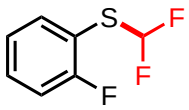

(difluoromethyl)(2-fluorophenyl)sulfane (3.2j). The general decarbonylation procedure was followed using 0.3 mmol of the corresponding thioester, and the yield was determined by ^{19}F NMR spectroscopy with 4-fluorotoluene as the internal standard (36% yield). ^{19}F NMR shifts were consistent with formation of decarbonylated (difluoromethyl)thioether, ^{19}F NMR (377 Hz, $CDCl_3$) –91.17 ppm (d, *J* = 56.9 Hz, 2F).). Due to the high volatility of the product, attempts at isolation were unsuccessful.

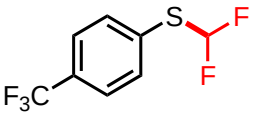

(Difluoromethyl)(4-(trifluoromethyl)phenyl)sulfane (3.2k). The general decarbonylation procedure was followed using 0.15 mmol of the corresponding thioester. The final yield (33%) was determined by ^{19}F NMR spectroscopic analysis with 4-fluorotoluene as an internal standard. ^{19}F NMR shifts were consistent with formation of decarbonylated (difluoromethyl)thioether. ^{19}F NMR (377 Hz, $CDCl_3$) δ –61.77 (s, 3F), –91.32 ppm (d, *J* = 56.0 Hz, 2F).

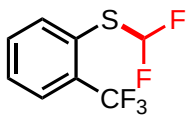

(Difluoromethyl)(4-(trifluoromethyl)phenyl)sulfane (3.2l). The general decarbonylation procedure was followed using 0.15 mmol of the corresponding thioester. The final yield (38%) was determined by ^{19}F NMR spectroscopic analysis with 4-fluorotoluene as an internal standard. ^{19}F NMR shifts were consistent with formation of decarbonylated (difluoromethyl)thioether. ^{19}F NMR (377 Hz, $CDCl_3$) δ –58.59 (s, 3F), –91.22 ppm (d, *J* = 55.8 Hz, 2F).

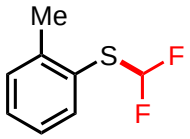

(Difluoromethyl)(*o*-tolyl)sulfane (3.2m). The general decarbonylation procedure was followed using 0.5 mmol of the corresponding thioester. Purification by flash chromatography on silica gel (hexanes/EtOAc, 97:3) afforded the product as a clear oil (69 mg, 79% yield). **^{1}H NMR** (700 MHz, $CDCl_3$) δ 7.58 (d, *J* = 7.7 Hz, 1H), 7.35–7.28 (m, 2H), 7.21 (t, *J* = 7.5 Hz, 1H), 6.79 (t, *J* = 56.9 Hz, 1H), 2.51 (s, 3H). **^{13}C NMR** (176 MHz, $CDCl_3$) 142.97, 136.83, 130.87, 130.18, 126.77, 125.53, 121.23 (t, *J* = 275.0 Hz), 21.24. **^{19}F NMR** (377 MHz, $CDCl_3$) δ –91.32 (d, *J* = 56.9 Hz, 2F). **HRMS** (GC-APCI) calcd. for $C_8H_8F_2S$ [M+] *m/z* 174.0315, found 174.0309.

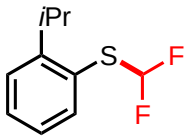

(Difluoromethyl)(2-isopropylphenyl)sulfane (3.2n). The general decarbonylation procedure was followed using 0.5 mmol of the corresponding thioester. Purification by flash chromatography on silica gel (hexanes/EtOAc, 97:3) afforded the product as a clear oil (78 mg, 77% yield). **^{1}H NMR** (500 MHz, $CDCl_3$) δ 7.60 (d, *J* = 7.9 Hz, 1H), 7.48–7.36 (m, 2H), 7.21 (t, *J* = 7.9 Hz, 1H), 6.78 (t, *J* = 57.0 Hz, 1H), 3.69 (p, *J* = 6.9 Hz, 1H), 1.25 (d, *J* = 7.0 Hz, 6H). **^{13}C NMR** (176 MHz,

$CDCl_3$) δ 153.07, 136.93, 130.52, 126.51, 124.46, 121.38 (t, *J* = 275.2 Hz), 30.80, 23.64. **^{19}F NMR** (471 MHz, $CDCl_3$) δ –91.16 (d, *J* = 57.0 Hz, 2F). **HRMS** (EI) calcd. for $C_{10}H_{12}F_2S$ [M+] *m/z* 202.0628, found 202.0626.

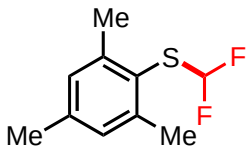

(Difluoromethyl)(mesityl)sulfane (3.2o). The general decarbonylation procedure was followed using 0.5 mmol of the corresponding thioester. Purification by flash chromatography on silica gel (hexanes/EtOAc, 100:0) afforded the product as a clear oil (37 mg, 37% yield). **^{1}H NMR** (500 MHz, $CDCl_3$) δ 7.01 (s, 2H), 6.66 (t, *J* = 57.1 Hz, 1H), 2.52 (s, 6H), 2.31 (s, 3H). **^{13}C NMR** (176 MHz, $CDCl_3$) δ 144.66, 140.38, 129.40, 121.61 (t, *J* = 275.4 Hz), 121.39, 22.24, 21.06. **^{19}F NMR** (471 MHz, $CDCl_3$) δ –90.71 (d, *J* = 57.1 Hz, 2F). **HRMS** (GC-APCI) calcd. for $C_{10}H_{12}F_2S$ [M+H] *m/z* 203.0728, found 203.0701.

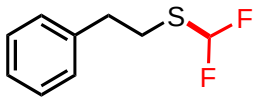

(Difluoromethyl)(phenethyl)sulfane (3.2p). The general decarbonylation procedure was followed using 0.5 mmol of the corresponding thioester. Purification by flash chromatography on silica gel (hexanes/EtOAc, 97:3) afforded the product as a clear oil (72 mg, 77% yield). **^{1}H NMR** (500 MHz, $CDCl_3$) δ 7.34 (t, *J* = 7.4 Hz, 2H), 7.30–7.25 (m, 1H), 7.24 (d, *J* = 7.4 Hz, 2H), 6.80 (t, *J* = 56.1 Hz, 1H), 3.11–3.05 (m, 2H), 3.03–2.98 (m, 2H). **^{13}C NMR** (126 MHz, $CDCl_3$) δ 139.53, 128.62, 128.56, 126.73, 120.63 (t, *J* = 272.9 Hz), 36.75, 28.56. **^{19}F NMR** (377 MHz, $CDCl_3$) δ –93.19 (d, *J* = 56.1 Hz, 2F). **HRMS** (GC-APCI) calcd. for $C_9H_{10}F_2S$ [M+] *m/z* 188.0471, found 188.0466.

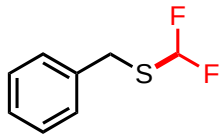

Benzyl(difluoromethyl)sulfane (3.2q). The general decarbonylation procedure was followed using 0.5 mmol of the corresponding thioester. Purification by flash chromatography on silica gel (hexanes/EtOAc, 97:3) afforded the product as a clear oil (48 mg, 55% yield). To demonstrate that the low yield was due to the volatility of the product, the general decarbonylation procedure was followed using 0.15 mmol of the corresponding thioester, and the yield was determined by ^{19}F NMR spectroscopy with 4-fluorotoluene as the internal standard (97% yield). **^{1}H NMR** (500 MHz, $CDCl_3$) δ 7.42–7.32 (multiple peaks, 5H), 6.75 (t, *J* = 56.6 Hz, 1H), 4.04 (s, 2H). **^{13}C NMR** (126 MHz, $CDCl_3$) δ 136.23, 128.87, 128.78, 127.63, 120.22 (t, *J* = 272.9 Hz), 31.74. **^{19}F NMR** (377 MHz, $CDCl_3$) δ –94.78 (d, *J* = 56.6 Hz, 2F). **HRMS** (EI) calcd. for $C_8H_8F_2S$ [M+] *m/z* 174.0315, found 174.0315.

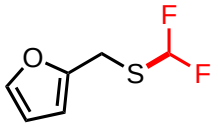

2-(((Difluoromethyl)thio)methyl)furan (3.2r). The general decarbonylation procedure was followed using 0.15 mmol of the corresponding thioester, and the yield was determined by ^{19}F NMR spectroscopy with 4-fluorotoluene as the internal standard (24% yield). ^{19}F NMR shifts were consistent with formation of decarbonylated (difluoromethyl)thioether, ^{19}F NMR (377 Hz, $CDCl_3$) δ –90.86 ppm (d, *J* = 57.1 Hz, 2F). Due to the high volatility of the product, attempts at isolation were unsuccessful.

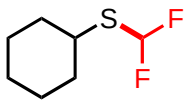

Cyclohexyl(difluoromethyl)sulfane (3.2s). The general decarbonylation procedure was followed using 0.5 mmol of the corresponding thioester. Purification by flash chromatography on silica gel (hexanes/EtOAc, 97:3) afforded the product as a clear oil (38 mg, 43% yield). To demonstrate that the low yield was due to the volatility of the product, the general decarbonylation procedure was followed using 0.15 mmol of the corresponding thioester, and the yield was determined by ^{19}F NMR spectroscopy with 4-fluorotoluene as the internal standard (99% yield). **^{1}H NMR** (^{1}H NMR (500 MHz, $CDCl_3$) δ 6.86 (t, *J* = 56.7 Hz, 1H), 3.20 (tt, *J* = 10.6, 3.8 Hz, 1H), 2.04 (dd, *J* = 13.4, 4.1 Hz, 2H), 1.83–1.74 (m, 2H), 1.66–1.59 (m, 1H), 1.54–1.45 (m, 2H), 1.45–1.34 (m, 2H), 1.35–1.23 (m, 1H). **^{13}C NMR** (126 MHz, $CDCl_3$) δ 120.98 (t, *J* = 271.7 Hz), 41.66, 34.44, 25.83, 25.36. **^{19}F NMR** (377 MHz, $CDCl_3$) δ –91.49 (d, *J* = 56.7 Hz, 2F). **HRMS** (GC-APCI) calcd. for $C_7H_{12}F_2S$ [M-F]+ *m/z* 147.0644, found 147.0638.

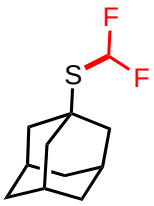

((3*s*,5*s*,7*s*)-Adamantan-1-yl)(difluoromethyl)sulfane (3.2t). The general decarbonylation procedure was followed using 0.5 mmol of the corresponding thioester. Purification by flash chromatography on silica gel (hexanes/EtOAc, 97:3) afforded the product as a clear oil (77 mg, 71% yield). **^{1}H NMR** (500 MHz, $CDCl_3$) δ 6.95 (t, *J* = 56.9 Hz, 1H), 2.10–2.05 (br, 3H), 2.02 (d, *J* = 3.2 Hz, 6H), 1.72 (br, 6H). **^{13}C NMR** (126 MHz, $CDCl_3$) δ 120.37 (t, *J* = 269.3 Hz), 48.29, 44.23, 35.94, 29.76. **^{19}F NMR** (471 MHz, $CDCl_3$) δ –90.16 (d, *J* = 56.9 Hz, 2F). **HRMS** (EI) calcd. for $C_{11}H_{16}F_2S$ [M+] *m/z* 218.0941, found 218.0936.

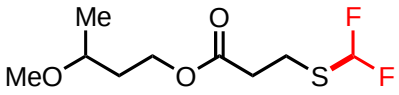

3-Methoxybutyl 3-((difluoromethyl)thio)propanoate (3.2u). The general decarbonylation procedure was followed using 0.5 mmol of the corresponding thioester. Purification by flash chromatography on silica gel (hexanes/EtOAc, 60:40) afforded the product as a clear oil (56 mg, 46% yield). **^{1}H NMR** (500 MHz, $CDCl_3$) δ 6.85 (t, *J* = 56.0 Hz, 1H), 4.23 (t, *J* = 7.0 Hz, 2H), 3.42 (dqd, *J* = 7.7, 6.2, 4.6 Hz, 1H), 3.33 (s, 3H), 3.07 (t, *J* = 7.1 Hz, 2H), 2.74 (t, *J* = 7.1 Hz, 2H), 1.93–1.70 (m, 2H), 1.18 (d, *J* = 6.2 Hz, 3H). **^{13}C NMR** (176 MHz, $CDCl_3$) δ 171.29, 120.52 (t, *J* = 273.0 Hz), 73.58, 61.98, 56.11, 35.58, 35.47, 22.13 (t, *J* = 3.6 Hz), 19.03. **^{19}F NMR** (377 MHz, $CDCl_3$) δ –93.17 (d, *J* = 56.0 Hz, 2F). **HRMS** (EI) calcd. for $C_9H_{16}F_2O_3S$ [M+] *m/z* 242.0788, found 242.0793.

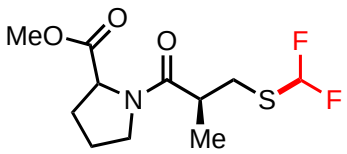

Methyl ((*S*)-3-((difluoromethyl)thio)-2-methylpropanoyl)prolinate (3.2v). The general decarbonylation procedure was followed using 0.3 mmol of the corresponding thioester. Flash chromatography on silica gel (hexanes/EtOAc, 60:40) afforded a mixture of two diastereomer products (dr = 1.0:0.14) as a clear oil (60 mg, 71% yield). The diagnostic peaks of the chiral proton alpha to the ester and amide, as well as both -CH_3 signals, were used to determine the diastereomeric ratio. Relative integrations assisted in determining the remaining signals for the major diastereomer. **NMR** (500 MHz, $CDCl_3$) δ 6.83 (t, *J* = 56.3 Hz, 1H), 4.55 (dd, *J* = 8.6, 4.0 Hz, 1H), 3.73 (s, 3H), 3.65 (t, *J* = 6.6 Hz, 2H), 3.11 (dd, *J* = 13.8, 9.1 Hz, 1H), 2.94 (h, *J* = 6.8 Hz, 1H), 2.82 (dd, *J* = 13.8, 5.2 Hz, 1H), 2.27–2.17 (m, 1H), 2.16–1.96 (m, 3H), 1.26 (d, *J* = 6.8 Hz, 3H) *for the major diastereomer*. **^{13}C NMR** (126 MHz, $CDCl_3$) δ 173.15, 172.60, 121.15 (t, *J* = 272.5 Hz), 58.58, 52.10, 46.80, 39.90, 30.21, 29.01, 24.76, 17.02 *for the major diastereomer*. **^{19}F**

NMR (471 MHz, $CDCl_3$) δ –90.93 *to* –92.97 *(multiple peaks,* 2F). **HRMS** (GC-APCI) calcd. for $C_{11}H_{17}F_2NO_3S$ [M+H]+ *m/z* 282.0997, found 282.0983.

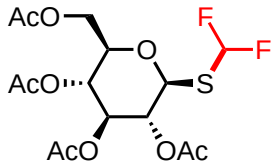

(2*R*,3*R*,4*S*,5*R*,6*S*)-2-(Acetoxymethyl)-6-((difluoromethyl)thio)tetrahydro-2*H*-pyran-3,4,5-triyl triacetate (3.2w). The general decarbonylation procedure was followed using 0.5 mmol of the corresponding thioester. Flash chromatography on silica gel (hexanes/EtOAc, 45:55) afforded the purified product as a white solid (62.6 mg, 47% yield). **mp** 79.9–83.2 °C. **^{1}H NMR** (700 MHz, $CDCl_3$) δ 7.25 (t, *J* = 56.4 Hz, 1H), 5.54 (t, *J* = 9.7 Hz, 1H), 5.37 (dt, *J* = 31.6, 10.0 Hz, 1H), 5.20 (d, *J* = 10.2 Hz, 1H), 4.55 (d, *J* = 12.2 Hz, 1H), 4.42 (d, *J* = 12.5 Hz, 1H), 2.37 (s, 3H), 2.35 (s, 3H), 2.32 (s, 3H), 2.30 (s, 3H). **^{13}C NMR** (176 MHz, $CDCl_3$) δ 170.79, 170.24, 169.51, 169.49, 119.08 (t, *J* = 278.8 Hz), 80.09, 76.52, 73.72, 70.00, 68.09, 61.98, 20.78. **^{19}F NMR** (376 MHz, $CDCl_3$) δ –95.92 (dd, *J* = 248.0, 56.4 Hz, 1F), –99.22 (dd, *J* = 248.0, 56.4 Hz, 1F). **HRMS** (ESI) calcd. for $C_{15}H_{20}F_2O_9S$ [M+Na] *m/z* 437.0694, found 437.0688.

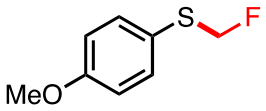

(Fluoromethyl)(4-methoxyphenyl)sulfane (3.2x). The general decarbonylation procedure was followed using 0.3 mmol of the corresponding thioester. Purification by flash chromatography on silica gel (hexanes/EtOAc, 99:1) afforded **3.2x** as a clear oil (41 mg, 71% yield). **^{1}H NMR** (500 MHz, $CDCl_3$) δ 6.85 (t, *J* = 56.0 Hz, 1H), 4.23 (t, *J* = 7.0 Hz, 2H), 3.42 (dqd, *J* = 7.7, 6.2, 4.6 Hz, 1H), 3.33 (s, 3H), 3.07 (t, *J* = 7.1 Hz, 2H), 2.74 (t, *J* = 7.1 Hz, 2H), 1.93–1.70 (m, 2H), 1.18 (d, *J* = 6.2 Hz, 3H). **^{13}C NMR** (176 MHz, $CDCl_3$) δ 171.29, 120.52 (t, *J* = 273.0 Hz), 73.58, 61.98,

56.11, 35.58, 35.47, 22.13 (t, *J* = 3.6 Hz), 19.03. **^{19}F NMR** (377 MHz, $CDCl_3$) δ –93.17 (t, *J* = 56.0 Hz, 1F). **HRMS** (EI) calcd. for C_8H_9FOS [M+] *m/z* 172.0358, found 172.0361.

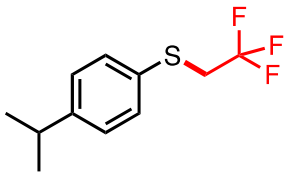

(4-Isopropylphenyl)(2,2,2-trifluoroethyl)sulfane (3.2y). The general decarbonylation procedure was followed using 0.3 mmol of the corresponding thioester. Purification by flash chromatography on silica gel (hexanes/EtOAc, 99:1) afforded **3.2y** as a clear oil (57 mg, 81% yield). **^{1}H NMR** (500 MHz, $CDCl_3$) δ 7.43 (d, *J* = 8.5 Hz, 1H), 7.20 (d, *J* = 8.3 Hz, 1H), 3.40 (q, *J* = 9.8 Hz, 2H), 2.90 (hept, *J* = 6.9 Hz, 1H), 1.24 (d, *J* = 7.0 Hz, 3H). **^{13}C NMR** (176 MHz, $CDCl_3$) δ 149.53, 132.72, 130.61, 127.64, 125.66 (q, *J* = 276.5 Hz), 38.85 (q, *J* = 32.4 Hz), 34.01, 24.04. **^{19}F NMR** (377 MHz, $CDCl_3$) δ –66.39 (t, *J* = 9.7 Hz, 3F). **HRMS** (EI) calcd. for $C_{11}H_{13}F_3S$ [M+] *m/z* 234.0690, found 234.0691.

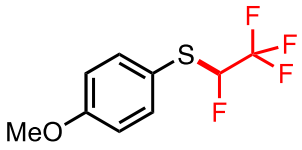

(4-Methoxyphenyl)(1,2,2,2-tetrafluoroethyl)sulfane (3.2z). The general decarbonylation procedure was followed using 0.5 mmol of the corresponding thioester. Purification by flash chromatography on silica gel (hexanes/EtOAc, 99:1) afforded **3.2z** as a light yellow oil (105 mg, 88% yield). **^{1}H NMR** (500 MHz, $CDCl_3$) δ 7.54 (d, *J* = 7.9 Hz, 2H), 6.92 (d, *J* = 7.9 Hz, 2H), 5.72 (dq, *J* = 50.1, 5.8 Hz, 1H), 3.84 (s, 2H). **^{13}C NMR** (126 MHz, $CDCl_3$) δ 161.13, 136.43, 121.42 (dd, *J* = 281.4, 31.0 Hz), 119.27, 115.05, 97.43 (dq, *J* = 231.6, 36.8, 36.4 Hz), 55.39. **^{19}F NMR** (376 MHz, $CDCl_3$) δ –76.38 (dd, *J* = 16.1, 5.8 Hz), –166.99 (dq, *J* = 50.1, 16.1 Hz). **HRMS** (EI) calcd. for $C_9H_8F_4OS$ [M-F] *m/z* 221.0332, found 221.0247.

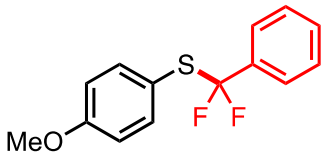

(difluoro(phenyl)methyl)(4-methoxyphenyl)sulfane (3.2aa). The general decarbonylation procedure was followed using 0.5 mmol of the corresponding thioester. Loading of $Ni(cod)_2$ and bidentate phosphine ligand was increased to 20 mol% and 24 mol%, respectively. Xantphos was used instead of dppf. Purification by flash chromatography on silica gel (0%–5% **A**/hexanes; A = 15:85 $CHCl_3$:Et_2O) afforded the product as a white solid (76.4 mg, 57% yield). **^{1}H NMR** (500 MHz, $CDCl_3$) δ 7.57 (d, *J* = 6.8 Hz, 2H), 7.54 (d, *J* = 8.6 Hz, 2H), 7.40–7.47 (*multiple peaks*, 3H), 6.91 (d, *J* = 8.6 Hz, 2H), 3.84 (s, 3H). **^{13}C NMR** (126 MHz, $CDCl_3$) δ 161.18, 138.24, 130.44, 128.27, 127.50, 125.37 (t, *J* = 4.5 Hz), 118.05, 114.51, 55.35. **^{19}F NMR** (376 MHz, $CDCl_3$) δ -72.44. **HRMS** (GC-APCI) calcd. for $C_{14}H_{12}F_2OS$ [M+] *m/z* 266.0571, found 266.0570.

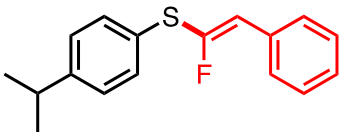

(1-Fluoro-2-phenylvinyl)(4-isopropylphenyl)sulfane (3.2ab). The general decarbonylation procedure was followed using 0.3 mmol of the corresponding thioester. Purification by flash chromatography on silica gel (hexanes/EtOAc, 99:1) afforded **3.2ab** as a thick oil (72 mg, 88% yield). **^{1}H NMR** (500 MHz, $CDCl_3$) δ 7.56–7.49 (multiple peaks, 2H), 7.47–7.40 (multiple peaks, 2H), 7.38–7.32 (multiple peaks, 2H), 7.31–7.25 (m, 1H), 7.24–7.19 (multiple peaks, 2H), 6.26 (d, *J* = 32.3 Hz, 1H), 2.90 (hept, *J* = 6.9 Hz, 1H), 1.25 (d, *J* = 6.9 Hz, 6H). **^{13}C NMR** (176 MHz, $CDCl_3$) δ 153.79, 152.03, 148.90, 133.05 (d, *J* = 5.6 Hz), 130.55, 128.77 (d, *J* = 7.9 Hz), 128.58, 127.99 (d, *J* = 2.4 Hz), 127.49, 116.93 (d, *J* = 12.8 Hz), 33.80, 23.87. **^{19}F NMR** (471 MHz, $CDCl_3$)

δ –86.81 (d, *J* = 32.3 Hz, 1F). **HRMS** (EI) calcd. for $C_{17}H_{17}FS$ [M+] *m/z* 272.1035, found 272.1038.

Catalyst screening for thiol trifluoromethylation

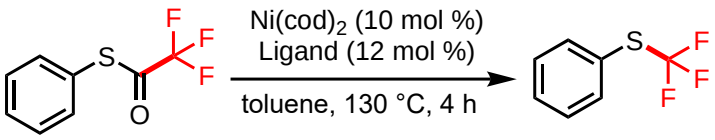

entry	[M]	ligand	% yield[b]
1	$Ni(cod)_2$	dppf	0
2	$Ni(cod)_2$	dpePhos	0
3	$Ni(cod)_2$	Xantphos	0
4	$Pd(dba)_2$	dppf	0
5	$Pd(dba)_2$	dpePhos	0
6	$Pd(dba)_2$	Xantphos	0
7	$Pd(dba)_2$	$P(Ad)Bn_2$	0
8	$Pd(dba)_2$	$P(Ad)_2Bn$	0

[a]24 mol% used, [b]Yields determined by ^{19}F NMR

General procedure for optimizing the catalytic decarbonylation of difluoromethyl thiophenol ester 1a. $Ni(cod)_2$ (4.1 mg, 0.015 mmol, 0.1 equiv) or $Pd(dba)_2$ (13.7 mg, 0.015 mmol, 0.1 equiv) and the appropriate phosphine ligand (0.036 mmol, 0.24 equiv for monodentate ligands; 0.018 mmol, 0.12 equiv for bidentate ligands) were dissolved in 0.3 mL of solvent. The solution was stirred at room temperature for 15 min at which point the catalyst solution was transferred to *S*-phenyl 2,2,2,-trifluoroethanethiolate (30.9 mg, 0.15 mmol, 1.0 equiv) in a tall 10 mL vial. The vial was sealed with a Teflon-lined screw cap, brought out of the glovebox, and stirred at 130 °C. After 4 h of heating, the reaction mixture was allowed to cool to room temperature. A stock solution of

4-fluorotoluene was prepared (0.5 M in toluene) and added to the cooled reaction mixture (0.3 mL, 0.15 mmol, 1 equiv). A sample of the crude reaction mixture with internal standard was removed for NMR analysis. Formation of $PhSCF_3$ could not be observed by ^{19}F NMR spectroscopy.

Stoichiometric decarbonylation of trifluoromethylthioesters

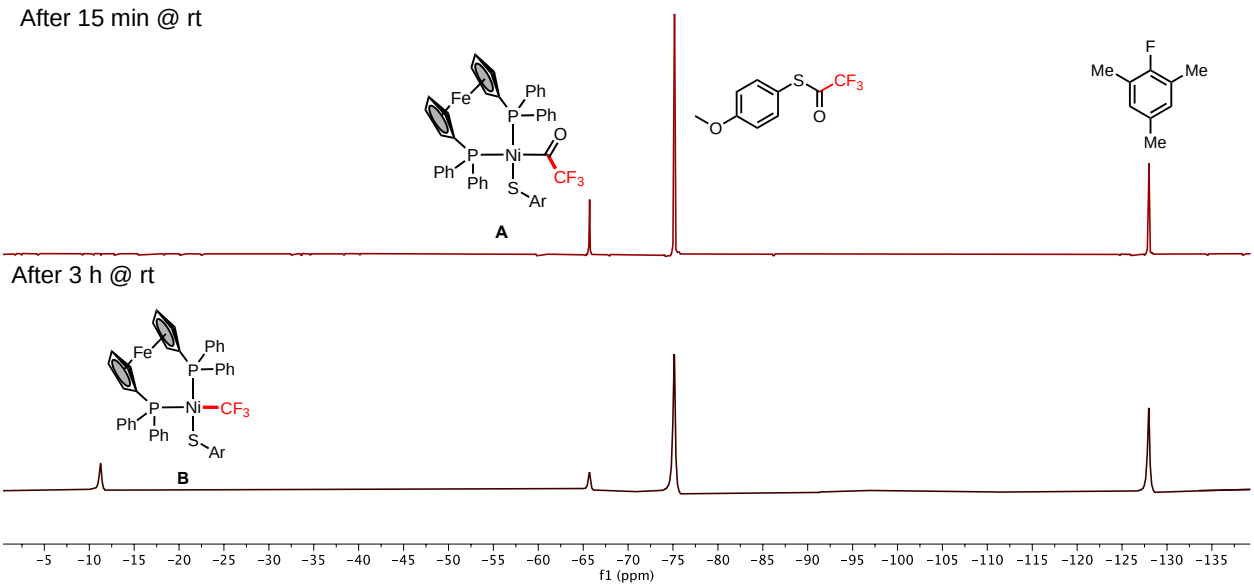

Figure 3.S5. ^{19}F NMR spectral data.

Stoichiometric decarbonylation of trifluoromethylthioesters. $Ni(cod)_2$ (20.6 mg, 0.075 mmol, 1.5 equiv) and dppf (30.3 mg, 0.075 mmol, 1.5 equiv) were dissolved in 0.5 mL of toluene. The solution was stirred at room temperature for 15 min, at which point it was transferred to a pre-weighed mixture of *S*-(4-methoxyphenyl) 2,2,2,-trifluoroethanethiolate (11.8 mg, 0.05 mmol, 1.0 equiv) and the internal standard 2-fluoromesitylene (0.05 mmol, 1.0 equiv). After mixing, the solution was transferred to a screw cap NMR tube and sealed with a Teflon-lined cap. The reaction mixture kept at room temperature and ^{19}F NMR spectrum was recorded (Figure 3.S5).

Heteroaromatic thiols and other failed substrates

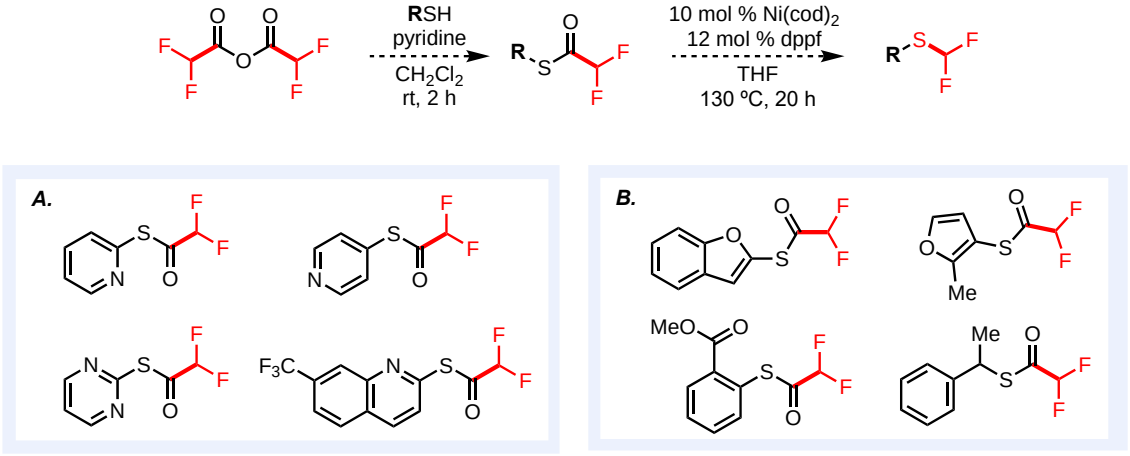

Figure 3.S6. (a) Attempts at synthesis of these heteroaromatic substrates resulted in *N*-acylation. (b) No decarbonylation observed after 20 h at 130 °C.

3.7 References

1) Ichiishi, N.; Malapit, C. A.; Wozniak, L.; Sanford, M. S., *Org. Lett*. **2018**, *20*, 44–47.
2) Purser, S.; Moore, P. R.; Swallow, S.; Gouverneur, V. Fluorine in medicinal chemistry. Chem. Soc. Rev. 2008, 37, 320–330.
3) Hagmann, W. K. The Many Roles for Fluorine in Medicinal Chemistry. J. Med. Chem. 2008, 51, 4359–4369.
4) Meanwell, N. A., *J. Med. Chem.* **2011**, *54*, 2529–2591.
5) Leroux, F.; Jeschke, P.; Schlosser, M. *Chem. Rev*. **2005**, *105*, 827–856.
6) Zafrani, Y.; Yeffet, D.; Sod-Moriah, G.; Berliner, A.; Amier, D.; Marciano, D.; Gershonov, E.; Saphier, S., *J. Med. Chem.* **2017**, *60*, 797–804.
7) Röschenthaler, G. V.; Kazakova, O Nenajdenko, V. Springer: Moscow, 2014.
8) Xiong, H.; Pannecoucke, X.; Besset, T. *Chem. Eur. J*. **2016**, 16734–16749.
9) Hine, J.; Porter, J. J. *J. Am. Chem. Soc.* **1957**, *79*, 5493¬–5496.
10) Langlois, B. R. *J. Fluorine Chem*. **1988**, *41*, 247–261.
11) Mehta, V. P.; Greaney, M. F. *Org. Lett.* **2013**, *15*, 5036–5039.
12) Zhang, W.; Wang, F.; Hu, J. *Org. Lett.* **2009**, *11*, 2109–2112.
13) Zafrani, Y.; Sod-Moriah, G.; Segall, Y. *Tetrahedron* **2009**, *65*, 5278–5283.
14) Fier, P. S.; Hartwig, J. F. *Angew. Chem. Int. Ed*. **2013**, *52*, 2092–2095.
15) Thomoson, C. S.; Dolbier Jr., W. R. *J. Org. Chem*. **2013**, *78*, 8904–8908.
16) Deng, X.-Y.; Lin, J.-H.; Zheng, J.; Xiao, J.-C. *Chem. Commun*. **2015**, *51*, 8805–8808.
17) Orsi, D. L.; Easley, B. J.; Lick, A. M.; Altman, R. A. *Org. Lett*. **2017**, *19*, 1570–1573.
18) Straathof, N. J. W.; Tegelbeckers, B. J. P.; Hessel, V; Wang, X.; Noël, T. *Chem. Sci*. **2014**, *5*, 4768–4773.
19) Bottecchia, C.; Wei, X.-J.; Kuijpers, K. P. L.; Hessel, V.; Noël, T.. *J. Org. Chem.* **2016**. *81*, 7301–7307.
20) Arimori, S.; Matsubara, O.; Takada, M.; Shiro, M.; Shibata, N. R. Soc. Open Sci. 2016, 3, 160102.
21) Ran, Y.; Lin, Q.-Y.; Xu, X.-H.; Qing, F.-L. J. Org. Chem. 2017, 82, 7373–7378. (c)
22) Yang, J.; Jiang, M.; Jin, Y.; Yang, H.; Fu, H. Org. Lett. 2017, 19, 2758–2761.
23) Wu, J.; Gu, Y.; Leng, X.; Shen, Q.. Angew. Chem. Int. Ed. 2015, 54, 7648–7652.
24) Zhu, D.; Gu, Y.; Lu, L.; Shen, Q.. J. Am. Chem. 2015, 137, 10547–10553.
25) Chen, S.; Zheng, M.; Liao, X.; Weng, Z., *J. Org. Chem*. **2016**, *81*, 7993–8000.
26) Beatty, J. W.; Douglas, J. J.; Cole, K. P.; Stephenson, C. R. J. *Nat. Commun.* **2015**, 6, 7919–7925.
27) Kyohide, M.; Etsuko, T.; Midori, A.; Kiyosi, K. *Chem. Lett*. **1981**, *10*, 1719–1720.
28) Chen, M.; Buchwald, S. L.. *Angew. Chem. Int. Ed*. **2013**, *52*, 11628–11631.
29) Ambler, B. R.; Zhu, L.; Altman, R. A. *J. Org. Chem.* **2015**, *80*, 8449–8457.
30) Ambler, B. R.; Santosh, P.; Altman, R. A. *Org. Lett.* **2015**, *17*, 2506–2509.
31) Sun, A. C.; McClain, E. J.; Beatty, J. W.; Stephenson, C. R. J. *Org. Lett*. **2018**, *20*, 3487–3490.
32) Tung, T. T.; Christensen, S. B.; Nielsen, J. *Chem. Eur. J*. 2017, 23, 18125–18128.
33) Yang, M.-H.; Orsi, D. L; Altman, R. A. *Angew. Chem. Int. Ed.* **2015**, *54*, 2361–2365.
34) Yang, M.-H.; Hunt, J. R.; Sharifi, N.; Altman, R. A., *Angew. Chem. Int. Ed.* **2016**, *55*, 9080–9083.
35) Ambler, B. R.; Yang, M.-H.; Altman, R. A. *Synlett*, **2016**, *27*, 2747–2755.
36) Maleckis, A.; Sanford, M. S. *Organometallics*, **2014**, *33*, 3831–3839.

37) Hirschbeck, V.; Gehrtz, P. H.; Fleischer, I., *Chem. Eur. J.* **2018**, *24*, 7092-7107.
38) Malapit, C. A.; Bour, J. R.; Brigham, C. E.; Sanford, M. S. Nature 2018, 563, 100¬104.
39) Liu, C.; Szostak, M. Chem. Commun. 2018, 54, 2130−2133.
40) Lee, S. C.; Liao, H. H.; Chatupheeraphat, A.; Rueping, M. Chem. Eur. J. 2018, 24, 3608−3612.
41) Ishitobi, K.; Isshiki, R; Asahara, K. K.; Lim, C.; Muto, K.; Yamaguchi, J. Chem. Lett. 2018, 47, 756−759.
42) Zheng, Z.-J.; Jiang, C.; Shao, P.-C.; Liu, W.-F.; Zhao, T.-T.; Xu, P.-F.; Wei, H. Chem. Commun. 2019, 55, 1907−1910.
43) Zhou, J.-Y.; Tao, S.-W.; Liu, R.-Q.; Zhu, Y.-M. J. Org. Chem. 2019, 84, 11891−11901.
44) Li, M.; Petersen, J. L.; Hoover, J. M. Org. Lett. 2017, 19, 638−641.
45) Cheng, Z.-F.; Tao, T.-T.; Feng, Y.-
46) S.; Tang, W.-K.; Xu, J.; Dai, J.-J.; Xu, H.-J J. Org. Chem. 2018, 83, 499−504.
47) Takise, R; Isshiki, R.; Muto, K.; Itami, K.; Yamaguchi, J. J. Am. Chem. Soc. 2017, 139, 3340−3343.
48) Mao, R.; Bera, S.; Cheseaux, A.; Hu, X. Chem. Sci. 2019, 10, 9555−9559.
49) Guo, L.; Rueping, M. Chem. - Eur. J. 2018, 24, 7794−7809.
50) Ferguson, D. M.; Bour, J. R.; Canty, A. J.; Kampf, J. W.; Sanford, M. S. *Organometallics* **2019**, *38*, 519−526.
51) Xu, L.; Vicic, D. A. J. Am. Chem. Soc. 2016, 138, 2536−2539.
52) Aikawa, K.; Serizawa, H.; Ishii, K.; Mikami, K. Org. Lett. 2016, 18, 3690−3693.
53) Mann, G.; Baranano, D.; Hartwig, J. F.; Rheingold, A. L.; Guzei, I. A. J. Am. Chem. Soc. 1998, 120 (36), 9205−9219.
54) Malapit, C. A.; Bour, J. R.; Laursen, S. R.; Sanford, M. S. J. Am. Chem. Soc. 2019, 141, 17322–17330.
55) Reina, A.; Krachko, T.; Onida, K.; Bouyssi, D.; Jeanneau, E.; Monteiro, N.; Amgoune, A. ACS Catal. 2020. 10, 3, 2189-2197.

Chapter 4 - Fluoroalkyl Cross-Coupling via Decarbonylative Transition Metal Catalysis

*Portions of this work have been published in:

Lalloo, N.; Malapit, C. A.; Taimoory, S. M; Brigham, C. E.; Sanford, M. S. Decarbonylative Fluoroalkylation at Palladium(II): From Fundamental Organometallic Studies to Catalysis. *J. Am. Chem. Soc.* **2021**, *143*, 18617–18625.

4.1 Background

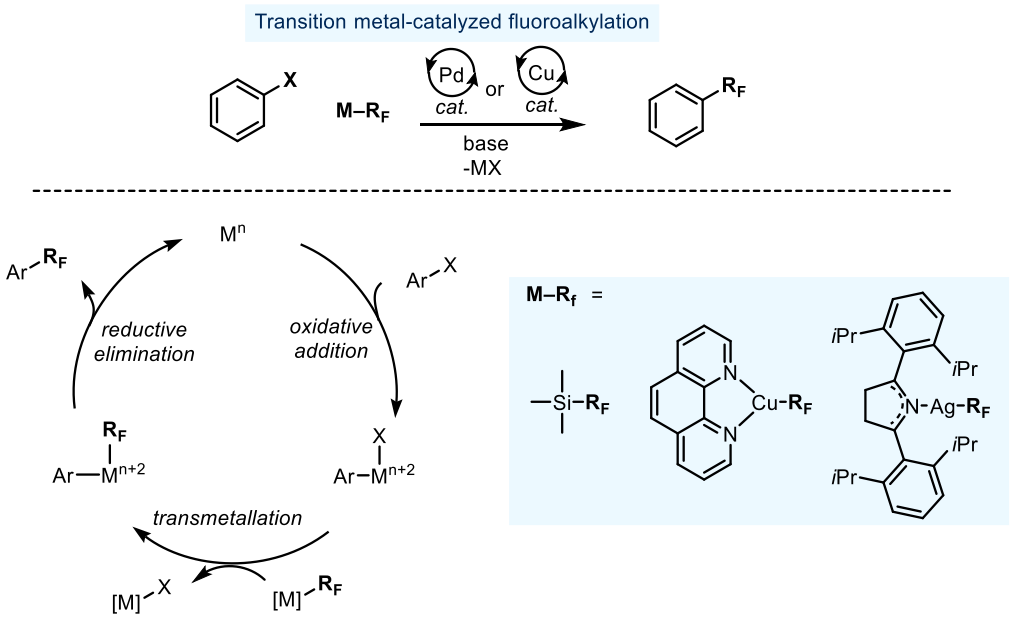

Figure 4-1. Traditional transition metal catalyzed fluoroalkylation methods.

Inspired by the work described in Chapter 3, we aimed to continue exploring the use of carboxylic acid-derived fluoroalkyl (R_F) electrophiles in decarbonylative catalysis. Fluoroalkyl substituents are commonly found in bioactive molecules, and their high demand has motivated significant research in catalytic methodologies for R_F installation. Generally, in transition metal

catalyzed fluoroalkylation reactions (most commonly with copper or palladium catalysts) organohalide electrophiles are coupled with organometallic fluoroalkyl reagents ([M]–R_F) such as fluoroalkyl silanes, fluoroalkyl cuprates, or fluooalkyl silver compounds (Figure 4-1). However, these are reactive organometallic reagents and are thus prone to decomposition under forcing reaction conditions. Furthermore, there is limited availability of these reagents for fluoroalkyl groups beyond CF_3, CF_2H, and CF_3CF_2. Fluoroalkyl carboxylic acids, on the other hand, are much more widely commercially available and can be derivatized for the purpose of "tuning" the electrophile. We propose that through an intermolecular decarbonylative approach, we can use fluoroalkyl carboxylic acid derived electrophiles for cross coupling with carbon nucleophiles (Figure 4-2).

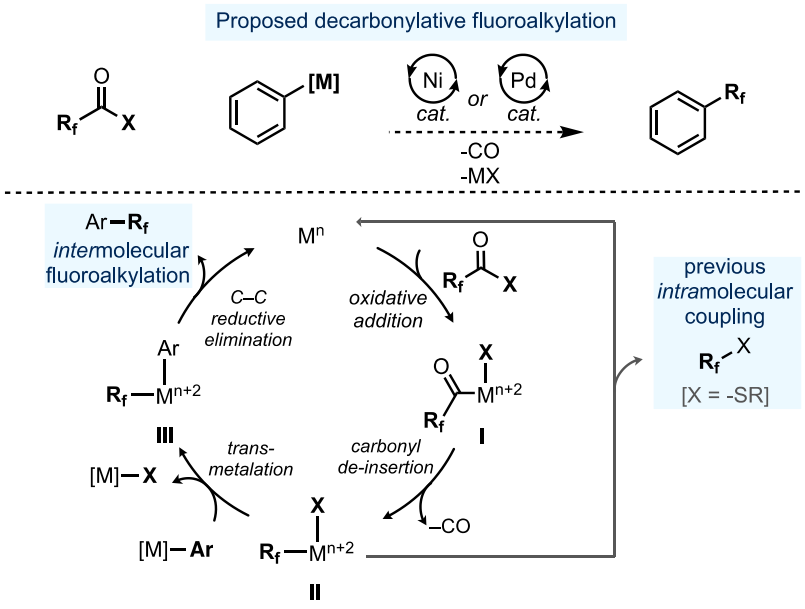

Figure 4-2. Proposed decarbonylative fluoroalkylation of arenes.

As described in Chapter 3, we have demonstrated that fluoroalkyl thioesters undergo Ni-catalyzed intramolecular decarbonylative S-R_F coupling. Analogous to the studies in Chapter 2, we hypothesized that with appropriate choice of fluoroalkyl acid derivative, $R_FC(O)X$, oxidative

addition followed by CO de-insertion would yield the stable, transmetalation-active fluoroalkyl-M^{II}-X intermediate **II** (Figure 4-2). To achieve this, the carboxylic acid substituent X should be chosen such that intramolecular X–R_F coupling from **II** is slow relative to transmetalation between **II** and [M]–Ar to form **III**. Subsequent Ar–R_F bond-forming reductive elimination would then yield the target intermolecular fluoroalkylation product.

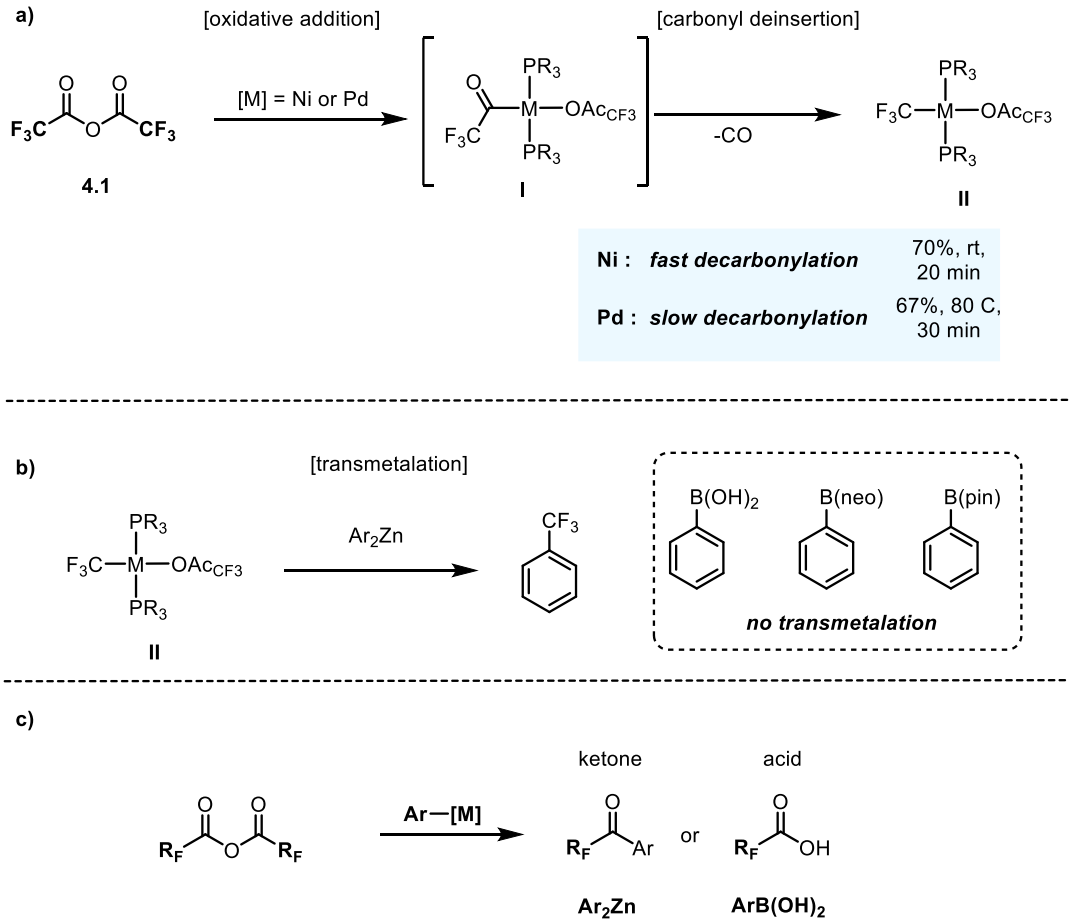

Figure 4-3. (a) Stoichiometric reactions of trifluoroacetic anhydride with palladium and nickel.[1,2] (b) Trifluoroacetate groups demonstrate poor transmetalation activity. (c) Incompatibility between electrophile and nucleophile have prevented successful catalytic decarbonylative cross coupling.

For the past decade, our group has been conducting organometallic studies of $R_FC(O)X$ oxidation addition and carbonyl de-insertion at both palladium and nickel. These studies began with graduate student Ansis Maleckis' work centered around the synthesis of palladium and nickel

complexes derived from trifluoromethyl acetic anhydride (Figure 4-3a). He showed that this highly electrophilic anhydride underwent facile oxidative addition at both Pd(0) and Ni(0) phosphine complexes to form **I** (Figure 4-3, a). The palladium showed a higher barrier for carbonyl de-insertion, requiring elevated temperatures to achieve conversion of the acyl intermediate **I** to the trifluoromethyl complex **II**. Nickel, on the other hand, underwent facile conversion from **I** to **II** within 20 min at room temperature.

Another major limiting factor to achieving catalysis in this system was the transmetalation step of the catalytic cycle. The trifluoroacetate ligand bound to the metal after oxidative addition poorly reactive for transmetalation. As such, transmetalation was only observed with highly nucleophilic diphenyl zinc, and not with aryl boron derivatives (Figure 4-3, b). Though Ph_2Zn was effective for stoichiometric transmetalation at isolable Pd-complexes, under catalytic conditions there was a fast background acylation reaction with the anhydride to form the trifluoromethyl ketone (Figure 4-3, c). Finally, once the target aryl-M^{II}-CF_3 complexes (**III**) were generated, reductive elimination to form aryl–CF_3 products was only feasible at Pd. Overall, these challenges precluded the development of a catalytic transformation the early studies.

After a brief hiatus, studies of decarbonylative fluoroalkylation reactions resumed in the Sanford lab several years ago. Dr. Christian Malapit and Naish Lalloo initiated stoichiometric investigations of the reaction of various Ni^0 and Pd^0 precursors with difluoromethyl acetic anhydride, a different anhydride than the one studied by Ansis. The difluoromethyl derivative was selected for several reasons. First, both the acid and anhydride are commercially available, facilitating the synthesis of derivatives. Second, we had recently discovered (see Chapter 3 of the current thesis) that difluoromethyl acyl species undergo carbonyl de-insertion at Ni(II). Finally, $C_{(sp2)}$-CF_2H bond-forming reductive elimination is known at both Ni(II) and Pd(II),[3-8] thus

minimizing challenges associated with that step of the catalytic cycle (which remains difficult for $R_F = CF_3$).

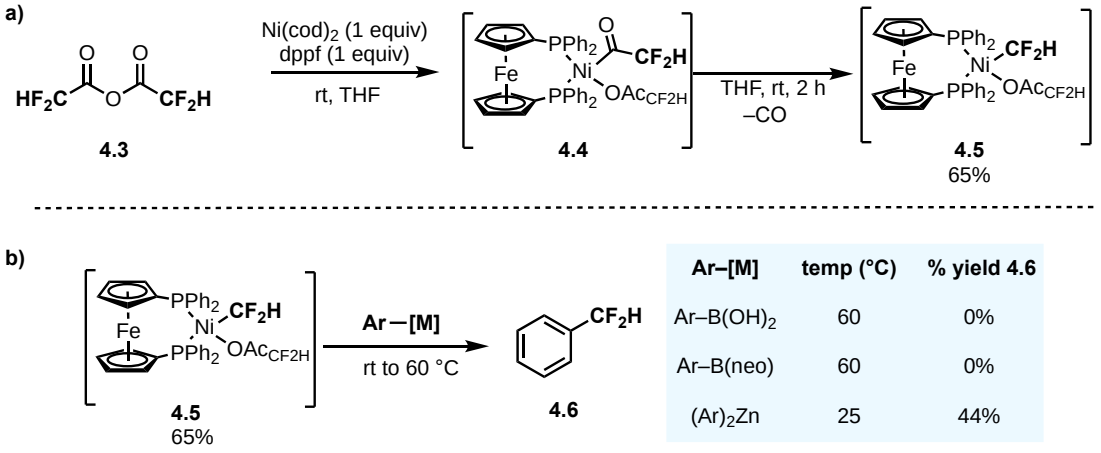

Figure 4-4. (a) Initial stoichiometric decarbonylation of difluoromethyl acetic anhydride at Ni0(dppf). (b) Diaryl zinc is the only nucleophile to transmetalate with Ni-acetate complex 4.5.

As shown in Figure 4-4, early work by Dr. Christian Malapit focused on the stoichiometric reaction of difluoromethyl acetic anhydride with $Ni^0(cod)_2$/dppf. He observed fast oxidative addition to form the Ni^{II}-acyl complex **4.4** at room temperature. Carbonyl de-insertion at **4.4** occurred fast at room temperature yielding **4.5** in 65% yield over 2 h (Figure 4-4, a). However, as shown in Figure 4-4, b, complex **4.5** showed low reactivity towards transmetalation. Similar to Ansis' earlier studies (Figure 4-3), only $ZnPh_2$ reacted with **4.5** to yield difluoromethyl benzene in 44% yield (via transmetalation followed by fast reductive elimination) at room temperature. As discussed earlier, Ph_2Zn undergoes uncatalyzed acylation with fluoroalkyl anhydrides, making this an incompatible pairing for catalysis.

More recently, Naish Lalloo discovered that difluoromethyl acetic anhydride undergoes stoichiometric oxidative addition at Pd(0) SPhos complexes (Figure 4-5). Carbonyl de-insertion proceeds at room temperature, yielding the isolable Pd-CF_2H product **4.8** in 91% yield over 10 h (Figure 4-5). Calculations carried out by Dr. S. Maryamdkht Taimoory found that attractive

interactions between the proton of the difluoromethyl group and an oxygen of the difluoroacetate ligand lowers the barrier for carbonyl deinsertion relative to the CF_3 analogues (which do not have a proton that can participate in an analogous interaction). Naish found that **4.8** underwent transmetalation with $ZnPh_2$ (similar to the results in Figure 4-3 and 4-4). However, he also observed 40% yield of the difluoromethyl arene with an aryl boronic acid as the transmetalating reagent. Unfortunately, subsequent studies revealed that boronic acids are also not compatible with the anhydride electrophile, as they promote its decomposition to difluoroacetic acid.

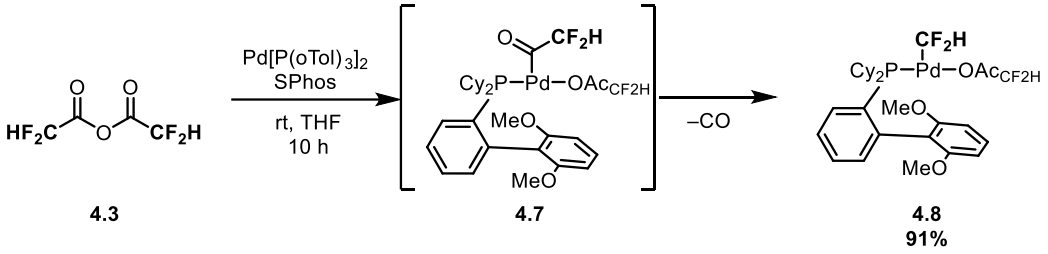

4.3 **4.7** **4.8** **91%**

Figure 4-5. Reported stoichiometric difluoroacetic anhydride decarbonylation with palladium.

These preliminary studies set the stage for my work in this area, which has focused on identifying a fluoroalkyl electrophile that: (1) is stable under the catalytic conditions, (2) is sufficiently reactive for oxidative addition at M^0, and (3) installs an X-type ligand that promotes transmetalation with aryl boronate esters or other weakly nucleophilic [M]-Ar derivatives. This chapter describes my examination of a series of electrophiles of general structure $R_FC(O)X$ in decarbonylative intermolecular coupling reactions catalyzed by both Ni and Pd. The effect of R_F, X, and the metal/ligand identity on outcomes in both stoichiometric and catalytic reactions is discussed. Ultimately, fluoroalkyl glutarimide derivatives were identified as $R_FC(O)X$ electrophiles with an optimal combination of properties for Pd-catalyzed decarbonylative coupling reactions.

4.2 Investigations with (fluoroalkyl)phenyl esters

4.2.1 (Difluoromethyl)acetic phenyl ester

Initial studies of difluoromethylation from difluoroacetic phenyl esters were carried out in collaboration with Dr. Christian Malapit. As shown in Figure 4-6, Christian attempted preliminary stoichiometric and catalytic trials with a nickel(0) ligated with the bidentate ligand diphenylphosphinoferrocene (dppf) . Stoichiometric reactions of the ester **4.9** with $Ni(cod)_2$/dppf showed that oxidative addition and carbonyl de-insertion occur at 60 °C to afford **II-a** in up to 20% yield (after 12 h) as determined by ^{19}F NMR spectroscopy based on a characteristic doublet at -95 ppm. Notably, the reactions were carried out at 60 ºC because oxidative addition was sluggish at room temperature. The putative Ni^{II}-acyl intermediate **1-a** was not detected by ^{19}F NMR spectroscopy, suggesting that CO de-insertion is relatively fast. The observed Ni^{II} product $(CF_2H)Ni^{II}(dppf)(OPh)$ was relatively unstable and started to decay between 12 and 24 h (Figure 4.6). However, $PhO–CF_2H$ coupling products were not detected, suggesting that the intramolecular reductive elimination is slow and decomposition proceeds via other pathways. This bodes well for a catalytic process where transmetalation must outcompete intramolecular $R_F–OPh$ coupling. Addition of *para*-methoxyphenyl boronic acid to the *in situ*-generated decarbonylated intermediate **II-a** resulted in rapid loss of **II-a** and concomitant growth of the difluoromethyl arene **4.11**, implicating the feasibility of transmetalation and reductive elimination.

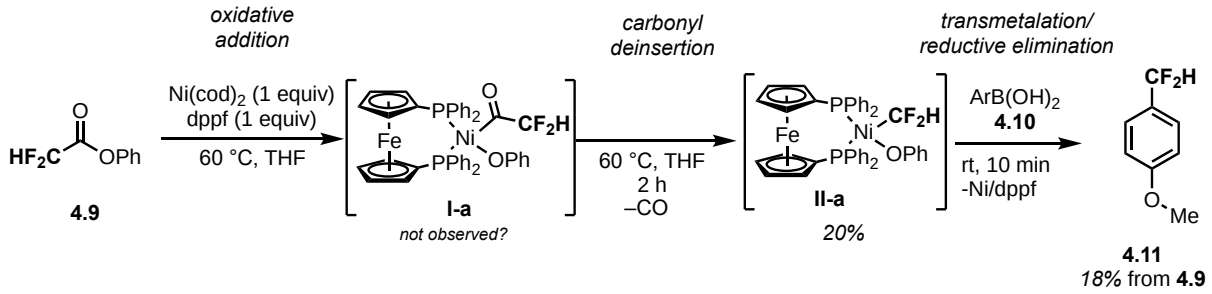

Figure 4-6. Stoichiometric reaction of **4.9** with $Ni^0((cod)_2$/dppf.

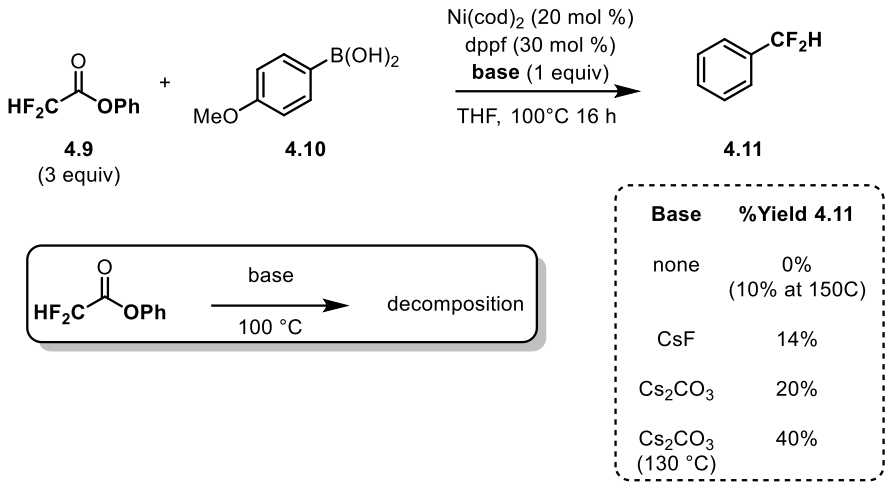

Figure 4-7. Attempts at difluoromethylation catalysis with nickel require base for transmetalation, though this also facilitates ester decomposition.

Based on these promising stoichiometric results, we attempted catalytic coupling reactions between **4.9** and *para*-methoxyphenylboronic acid (**4.10**) using 20 mol % $Ni(cod)_2$ and 30 mol % dppf as the catalyst. As shown in Figure 4-7, low (0-10%) yield of the desired difluoromethyl arene **4.11** was observed when the reaction was conducted at between 100-150 ºC in the absence of added base. Notably, the electrophile **4.9** was used in excess (3 equiv) to aid in the slow oxidative addition step, as well as to compensate for decomposition of **4.9** under catalytic conditions. Elevated temperatures were required to observe the product under base-free conditions (10% yield at 150 °C compared to 0% at 100 ºC). At 100-130 °C, the addition of base (CsF or Cs_2CO_3) was required to promote the coupling reaction, with the highest yield (40%) observed at 130 °C with 1 equiv of added Cs_2CO_3. However, the presence of base also promotes competing degradation of the electrophile, which precluded developing a high yielding catalytic transformation in this system.

Overall, the requirement for exogenous base in this system may be due to a slow transmetalation between the nickel phenolate intermediate and the boronic acid nucleophile under the catalytic conditions, although this reaction was relatively fast in the stoichiometric system

(Figure 4-6). Notably unlike our previous catalytic attempts with difluoromethyl thiophenol esters, we did not see any formation of the *intramolecular* C-O coupling ether product. Only one intramolecular decarbonylative C-O coupling has been reported, involving Ni^0/dcypt catalysis (dcypt = 3,4-bis(dicyclohexylphosphino)-thiophene) and picolinic acid-derived esters substrates.[9] When we tried using this ligand for phenol difluoromethylation with either nickel or palladium, no product **4.12** was observed, and the remaining mass balance was unreacted starting material (Figure 4-8).

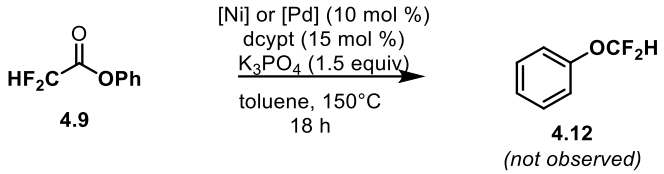

Figure 4-8. No intramolecular difluoromethylation is observed, even with dycypt as the ligand.

4.2.2 (Difluorophenyl)acetic phenyl esters

The phenyl ester of difluorobenzyl acetic acid (**4.13**, $R_F = CF_2Ph$) was next explored as this fluoroalkyl group proved competent for carbonyl de-insertion for thioether synthesis, and it is a relatively non-volatile fluoroalkyl acid to handle. Stoichiometric studies (Figure 4-9) revealed that oxidative addition of the difluorophenyl ester at Ni^0 was noticeably more challenging than with the difluoromethyl analogue. Attempts using the $Ni(cod)_2$/dppf system that was effective in Figure 4-6 yielded trace amounts of Ni-$C_{(acyl)}CF_2Ph$ signal (-98 ppm), and no apparent decarbonylated product with much of the mass balance remaining as unreacted starting material. This led us to move to more electron donating phosphine ligands, which should render the Ni^0 center more electron rich and thus more reactive towards oxidative addition. We found that P^nBu_3 was effective for promoting of oxidative addition and carbonyl de-insertion with the difluorobenzyl ester **4.13**, yielding 52% of $(PhF_2C)Ni(P^nBu_3)_2(OPh)$ (**II-b**) after 2 h at 60 ºC as determined by ^{19}F NMR

spectroscopy. This product was identified based on change in the chemical shift (-55.42 ppm) and multiplicity (t, J = 32.4 Hz) However, in this system, transmetalation proved challenging. The *in-situ* treatment of **II-b** with para-methoxyphenylboronic acid (**4.10**) resulted in decomposition of the fluoroalkyl nickel intermediate. The coupled product **4.14** was never detected by ^{19}F NMR spectroscopy.

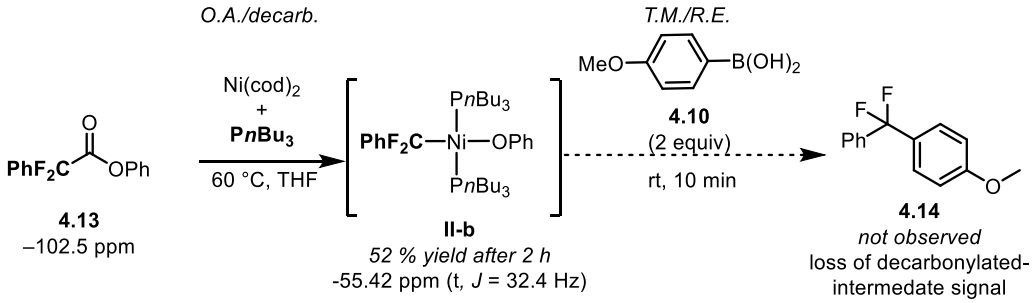

Figure 4-9. Stoichiometric reaction with difluorobenzylphenyl ester **4.13** with $Ni^0/PnBu_3$.

Catalysis was also examined for the decarbonylative coupling of difluorobenzyl phenyl ester **4-13** with phenyl boronic acid or phenyltrimethylsilane, and the results are summarized in Table 4-1. All attempts with palladium-based catalysts resulted in unreacted starting material due to challenging oxidative addition. Using Ni-based catalysts no product was observed with phenylboronic acid as the nucleophile, independent of the phosphine ligand was used (entries 1-6). This is consistent with the stoichiometric studies described above (Figure 4-9): with dppf oxidative addition was slow, while with P^nBu_3 transmetalation proved problematic. However, interestingly, upon moving to (trimethylsilyl)benzene as the nucleophile, the target product was formed in 3-9% yield with the P^nBu_3-ligated Ni catalyst (entries 8-10). The highest yields were observed with CsF as the base. However, additional attempts at optimization failed to deliver a full turnover of the catalyst.

Ultimately these studies suggest that phenyl esters would not be the electrophile of choice due to the observed modest transmetalation ability, and instability under basic conditions at high temperatures. As such, we next moved on to fluoroalkyl acid fluoride electrophiles.

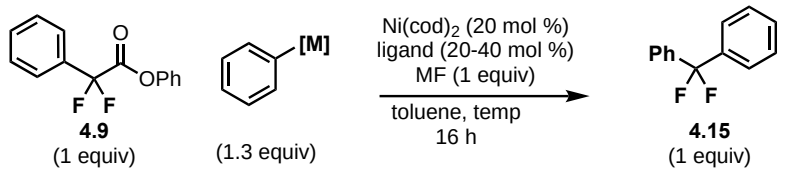

Entry	[M]	Ligand	Base	Temp (°C)	% Yield 4.15
1	-$B(OH)_2$	dppf	none	150	0
2	-$B(OH)_2$	dcypt	none	150	0
3	-$B(OH)_2$	Xantphos	none	150	0
4	-$B(OH)_2$	PPh_2Me	none	150	0
5	-$B(OH)_2$	PAd_2Bn	none	150	0
6	-$B(OH)_2$	P*n*Bu_3	none	150	0
7	-TMS	P*n*Bu_3	none	120	3
8	-TMS	P*n*Bu_3	KF	120	4
9	-TMS	P*n*Bu_3	CsF	120	9

Table 4-1. Exploring phenyl ester **4.9** as electrophile for catalytic decarbonylative difluorobenzylation

4.2 Investigations with (fluoroalkyl)acid fluorides

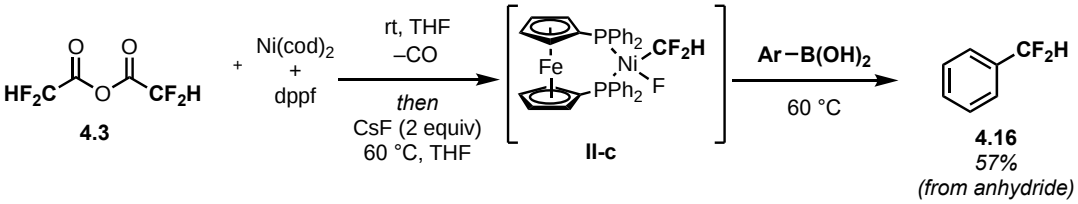

Figure 4-10. Addition of fluoride salt facilitates transmetalation from nickel-anhydrides.

Stoichiometric studies (conducted by Dr. Christian Malapit) suggested that acid fluorides might be ideal electrophiles for accelerating the key transmetalation step. Specifically, he showed that, following the reaction of anhydride **4.3** with $Ni(cod)_2$/dppf to form the

$Ni^{II}(CF_2H)$(trifluoroacetate) intermediate, the trifluoroacetate ligand could be replaced with fluoride using CsF (Figure 4-10). The resulting Ni–F complex **II-c** then underwent clean and high yielding transmetalation with phenyl boronic acid and subsequent reductive elimination to afford **4.16** in 57% yield (Figure 4-10). This is consistent with the studies in Chapter 2, showing that M-F intermediates are highly "transmetalation active".

Based on these preliminary results, we next moved to catalytic investigations. Initial experiments showed low yields/turnovers with nickel/dppf-based catalysts analogous. As such, Christian and Naish returned to Pd catalysts. They identified optimized conditions for intermolecular difluoromethylation by synthesizing stock solutions of difluoroacetic acid fluoride (DFAF). As mentioned earlier in this chapter, Naish found that Pd-CF_2H complexes could be synthesized at milder temperatures than Pd-CF_3 via decarbonylation due to hydrogen bond interactions that facilitate carbonyl de-insertion. With this same Pd/SPhos system, Naish was able to achieve catalytic difluoromethylation of electron deficient neopentyl boronate esters (Figure 4-11).

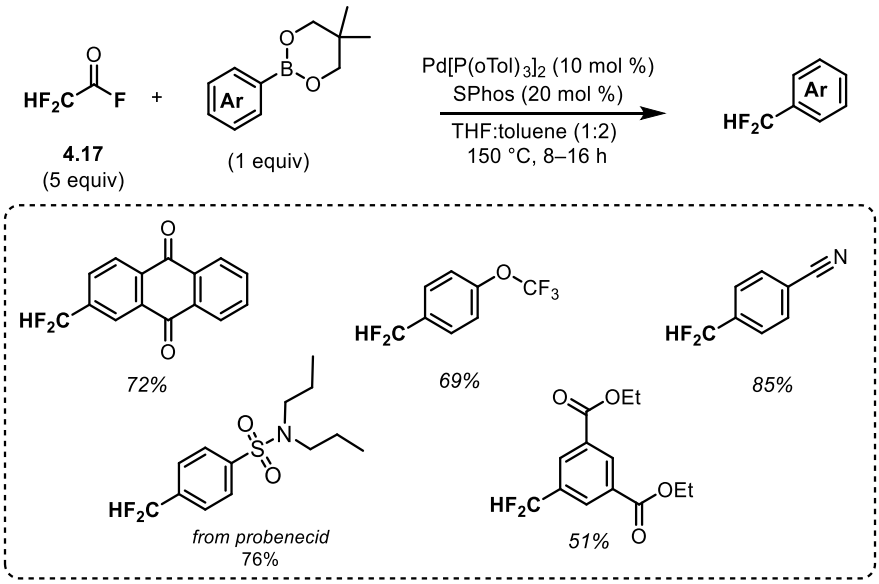

Figure 4-11. Palladium-catalyzed decarbonylative difluoromethylation of boronate esters.

With this precedent in hand, I evaluated the feasibility of an analogous catalytic transformation with difluorobenzyl acetyl fluoride **4.20**. The first challenge, however, was the synthesis of this acid fluoride. Attempts to synthesize **4.20** from the carboxylic acid **4.18** via conversion to the acid chloride (**4.19**) with oxalyl chloride, and then halide exchange with fluoride salts yielded no product (Figure 4-12). We next evaluated the use of Schoenebeck's trimethylammonium salt reagent, ($TMASCF_3$), for converting difluorophenyl acetic acid to the corresponding acid fluoride.[10] The reaction proceeded in quantitative yield when carried out under dry conditions in the glovebox. However, due to the volatility of the acid fluoride product, it could not be isolated from the reaction mixture. Thus, instead, we conducted this deoxyfluorination in toluene and prepared a 0.56 M stock solution after filtration through dry celite.

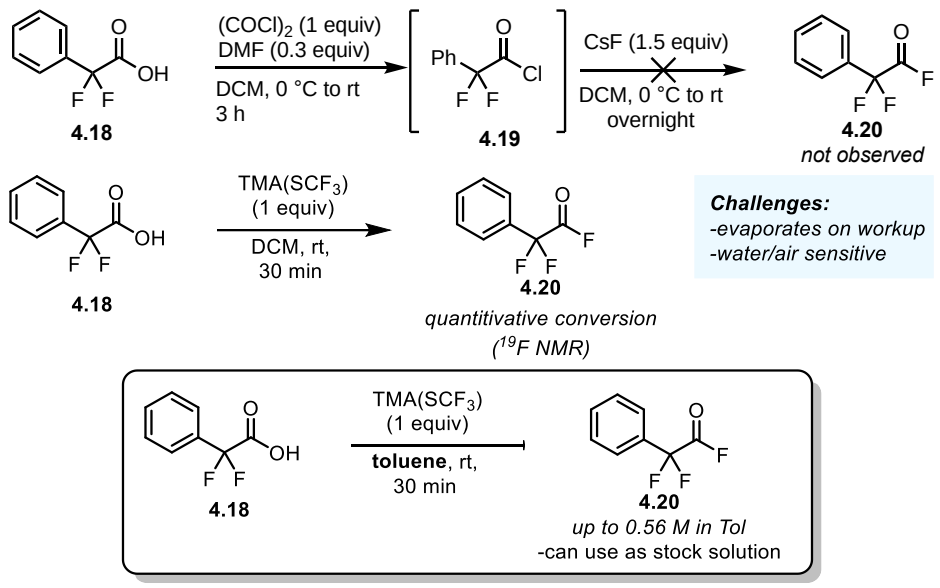

Figure 4-12. Generation of **4.20**.

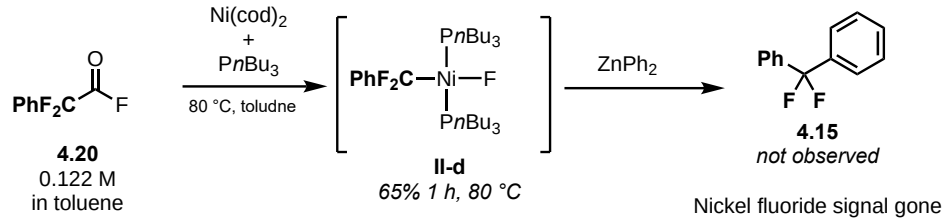

Figure 4-13. Reaction of **4.20** with $Ni^0/PnBu_3$.

Stoichiometric reactions between **4.20** and Ni/P^nBu_3 showed similar reactivity to the phenyl ester. Upon heating at 80 ºC for 1 h, we observed high yields of decarbonylated intermediate **II-d** (65% yield by ^{19}F NMR spectroscopy; Ni-CF_2Ph = -53 ppm, Ni-F = -360 ppm; Figure 4.13). However, upon the addition nucleophilic transmetalating reagents such as $ZnPh_2$, there was a loss of signal for intermediate **II-d**, and no arylated product was observed

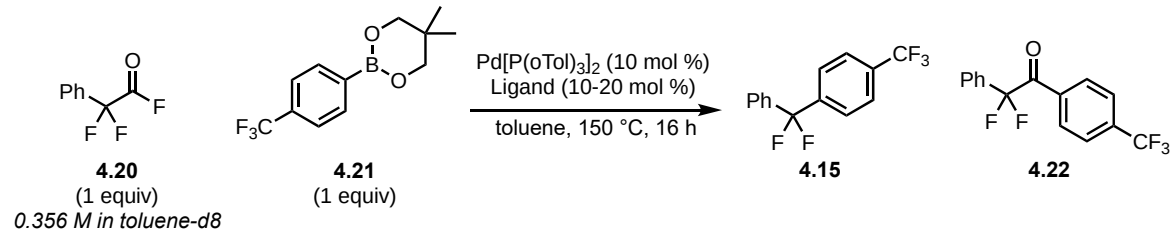

Entry	Ligand	%4.15	%4.22	remaining %4.20
1	SPhos	8	0	40
2	CataCXium A	1	0	60

Table 4-2. Pd-catalyzed coupling of **4.20** with **4.21**.

Attempts at catalysis to couple **4.20** with boronic acids and boronate esters using a nickel catalyst were unsuccessful. We thus shifted our efforts toward the palladium-catalyzed coupling of **4.20** with *para*-trifluoromethylboronate ester **4.21** (Table 4.2). inspired by our Naish's results in Figure 4.11. Catalytic attempts with palladium/SPhos (Naish's catalyst system) gave low (8%) yield of the desired product **4.15**. However, preparation of the acid fluoride solution was difficult to reliably reproduce at consistent concentrations. This issue led us to pursue a more easily isolable, less volatile electrophile for this coupling.

4.3 Investigations with (fluoroalkyl)gluatarimide

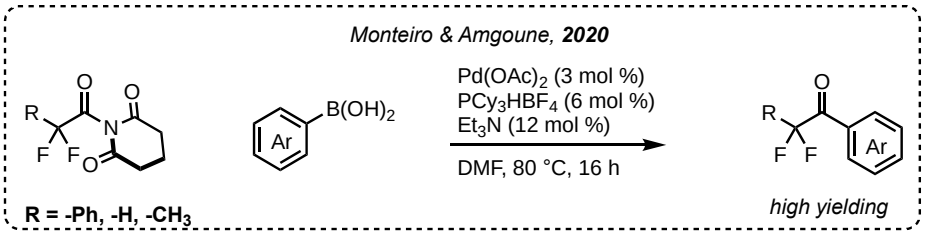

Figure 4-14. Palladium-catalyzed difluorobenzylacylation of boronic acids.

Glutarimide derivatives have been demonstrated to be good electrophiles in various Ni- and Pd-catalyzed coupling reactions.[11-14] The glutarimides generally are oriented in a "twisted" fashion where the two carbonyls of the glutarimide are out of plane from the carbonyl group. This disrupts the conjugation of the pi system, weakening that acyl-N bond and allowing for easier oxidative addition. While aryl-substituted glutarimides have been most commonly employed in catalysis, in 2020 Monteiro and Amgoune reported a non-decarbonylative Pd/PCy_3-catalyzed coupling of difluorobenzyl glutarimide **4.23** with boronic acids to form difluorobenzyl ketones (Figure 4-14).[14] We hypothesized that tuning the ligands in this system might enable a decarbonylative transformation to access difluorobenzylated arene products.

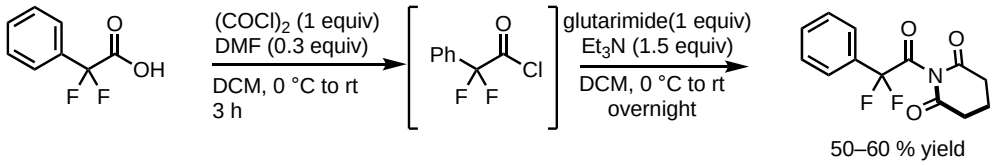

Figure 4-15. Synthesis of **4.23**.

Glutarimide electrophiles were synthesized following procedures reported by Amgoune (Figure 4-15).[14] Some re-optimization was necessary for the purification of the starting material, and this was accomplished in collaboration with Naish Lalloo. Naish found that after column

chromatography, a recrystallization from Et_2O layered with heptanes afforded the amides as white crystals. It was important to remove any remaining glutarimide, as that impurity recrystallized with the products. We noted that the fluoroalkyl glutarimides are also prone to decomposition on silica. Only the difluoropropionic acid-derived glutarimide did not require recrystallization as it is a clear oil.

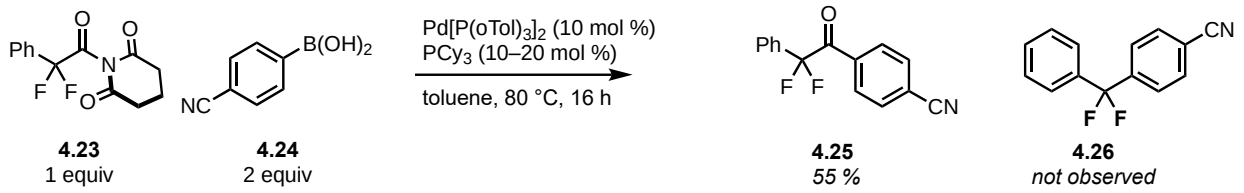

4.23 1 equiv | **4.24** 2 equiv | **4.25** *55 %* | **4.26** *not observed*

Figure 4-16. Carbonyl-retaining difluorobenzylation between **4.23** and **4.24** with Pd^0/PCy_3.

We began by repeating the conditions for acylation reported by Amgoune using glutarimide **4.23** and *para*-cyanophenylboronic acid (**4.24**). With $Pd[P(oTol)_3]_2$ as the Pd(0) precatalyst, the ketone product **4.25** was formed in 55% yield, with no decarbonylated product **4.26** (Figure 4-16). However, switching from the boronic acid to the corresponding neopentyl boronate ester under otherwise identical conditions led to a change in selectivity (Figure 4-17, a). The fluoroalkylated arene was formed in 7% yield, while the ketone was formed in <1%. Further optimization by Naish Lalloo found that the bulky monodentate phosphine ligand CataXCium A (PAd_2Bu) was effective at promoting decarbonylation of this fluoroalkyl electrophile. Final optimization was carried out by first-year grad student Alex Bunnell. Optimized conditions for PhF_2C-coupling include raising the temperature to 100 °C, as well as using a Pd-precatalyst (Figure 4-17, b). The presence of $Pd[P(oTol)_3]_2$ seems to have negative effects on catalysis, as high loading of CataXCium A was needed. Stoichiometric reactions between $Pd[P(oTol)_3]_2$ and fluoroalkyl glutarimides without additional ligand generated palladium black. Additional difluorobenzyl acetic acid derivatives were synthesized with other functional groups on the aryl backbone (Figure

4-18). The derivatives bearing electron withdrawing substituents afforded higher yields than those with electron donating groups, likely due to slower oxidative addition and carbonyl de-insertion in the latter systems.

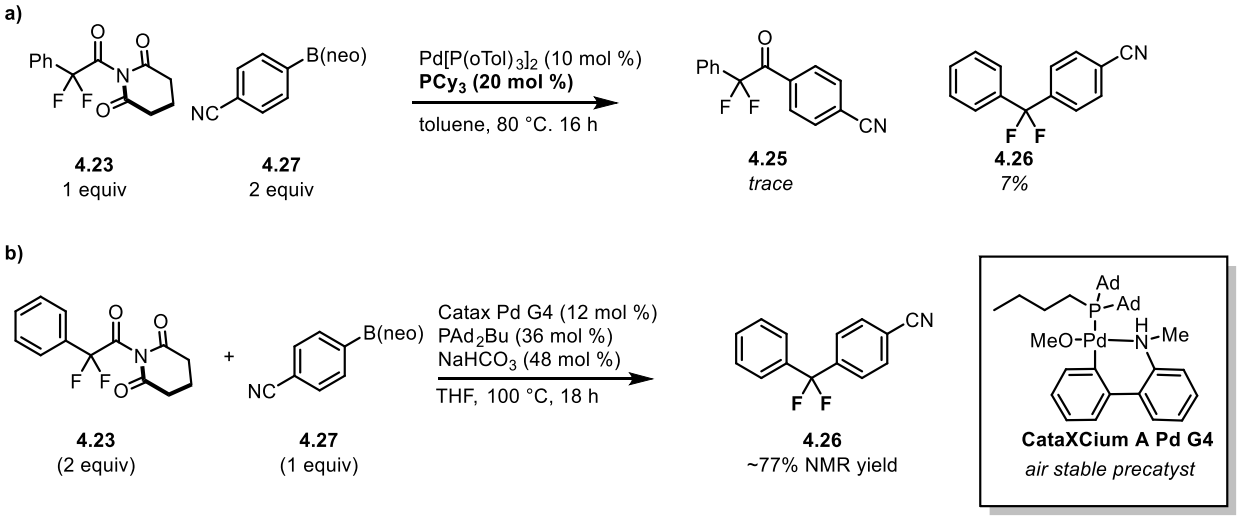

Figure 4-17. (a) Initial catalytic. (b) Final optimized conditions.

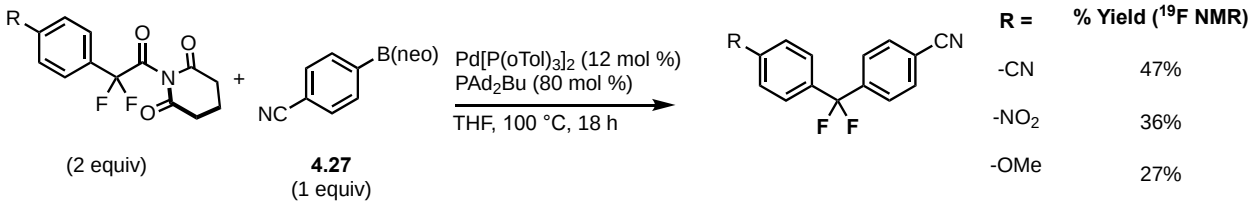

Figure 4-18. Catalytic attempts with other available electrophiles.

We also evaluated other fluoroalkyl glutarimide electrophiles. Amgoune and coworkers reported using that difluoromethyl (CF_2H) and difluoropropionic (CF_2Me) glutarimide were effective for their acyl coupling reaction. To investigate the analogous decarbonylative reactions, we started with a Pd^0/SPhos catalyst system analogous to that used by Naish for DFAF reactions. As shown in Figure 4-19, this catalyst afforded high selectivity (>95: 1) for the decarbonylated product, albeit in low yields (~10% by ^{19}F NMR) with boronate ester **4.27** as the nucleophilic

coupling partner. In contrast (Figure 4-19), boronic acid nucleophiles gave much higher yields, and were compatible with the glutarimide electrophile (unlike with DFAF). This suggests that glutarimide electrophiles may offer more flexibility than fluoride when it comes to its ability to transmetalate with boron nucleophiles at palladium.

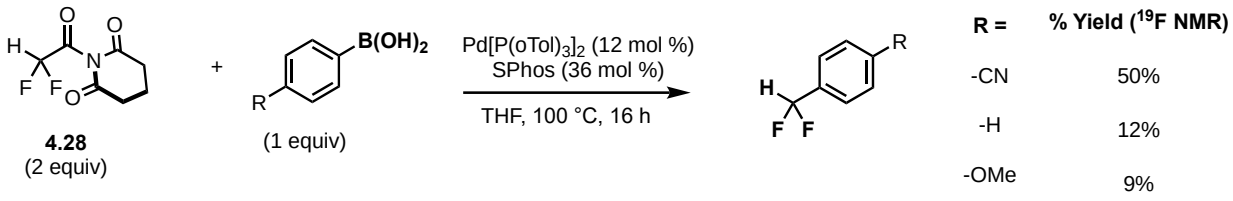

Figure 4-19. Difluoromethylation of boronic acids with varying *para*-functional groups.

Decarbonylative catalysis with difluoropropionic acid glutarimide **4.29** has thus far been unsuccessful, as there is rapid beta-hydride elimination after carbonyl deinsertion occurs (Figure 4-20). Lastly, trifluoromethylation was attempted using $Pd(dba)_2$ with CataXCium A as catalysts and neopentylboronate ester **4.27** as the coupling partner (Figure 4-21). No product was observed, and primarily starting material remained. Significant loss of starting material occurred with boronic acids resulting in a mixture of acid and ketone byproducts..

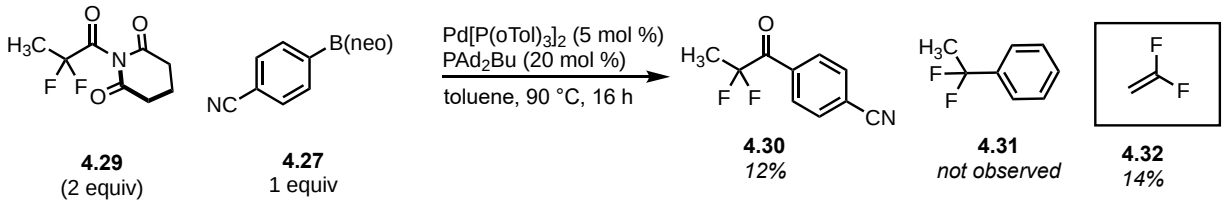

Figure 4-20. Catalytic attempt at decarbonylative fluoroalkylation with **4.29**.

Figure 4-21 Catalytic attempt at decarbonylative trifluoromethylation.

4.4 Conclusions

In summary, we have explored three types of fluoroalkyl electrophiles with the goal of developing a general decarbonylative fluoroalkylation. Phenyl ester electrophiles generally underwent slow oxidative addition, especially with palladium. Furthermore, all attempts at catalysis were low yielding due to slow transmetalation. Base-additives had minimal positive impact, as they also mediated decomposition of the electrophile.

Acid fluoride electrophiles were next explored. While a difluoromethyl arylation reaction was developed by Naish Lalloo, other fluoroalkyl acid fluoride electrophile afforded mixed results. The major challenge here is the synthesis and handling of the electrophiles. In contrast, using readily isolable glutarimide electrophiles, we have made significant progress in developing a decarbonylative fluoroalkylation method with a Pd/CataXCium A catalyst. Reaction optimization with the help of Naish Lalloo and Alex Bunnell revealed the need for CataXCium A for achieving difluorophenyl acetyl decarbonylation. Difluoromethyl electrophiles also work under these conditions with SPhos ligand as the optimal ligand and boronic acid as the optimal nucleophilic partner. Interestingly, this system is compatible with boron nucleophiles bearing electron-rich substituents, something that proved challenging for the DFAF system. Future outlook remains to explore the scope of this transformation and isolation of products, which is underway by Alex Bunnell. Further, isolation of key intermediates will be necessary to gain a better understanding of the reaction mechanism.

4.5 Experimental Procedures

Procedure for stoichiometric reaction of Ni(cod)$_2$/dppf with 4.9. Ni(cod)$_2$ (13.8 mg, 0.05 mmol, 1 equiv) and dppf (28 mg, 0.05 mmol, 1 equiv) were dissolved in 0.5 mL of THF. The solution was stirred at room temperature for 15 min, at which point it was transferred to a pre-weighed mixture of **4.9** (8.6 mg, 0.05 mmol, 1.0 equiv) and the internal standard 4-fluorotoluene (5.5 mg, 0.05 mmol, 1.0 equiv). The reaction was allowed to stir at 60 C for 2 h, at which point the solution was transferred to a screw cap NMR tube and sealed with a Teflon-lined cap. ^{19}F NMR was then recorded. ^{19}F NMR spectroscopic analysis showed trace amounts of a Ni-CF_2Ph signal (s, -98 ppm in THF).

Procedure for stoichiometric reaction of Ni(cod)$_2$/PnBu$_3$ with 4.9. Ni(cod)$_2$ (13.8 mg, 0.05 mmol, 1 equiv) and PnBu$_3$ (21 mg, 0.1 mmol, 2 equiv) were dissolved in 0.5 mL of THF. The solution was stirred at room temperature for 15 min, at which point it was transferred to a pre-weighed mixture of **4.9** (8.6 mg, 0.05 mmol, 1.0 equiv) and the internal standard 4-fluorotoluene (5.5 mg, 0.05 mmol, 1.0 equiv). The reaction was allowed to stir at 60 C for 2 h, at which point the solution was transferred to a screw cap NMR tube and sealed with a Teflon-lined cap. ^{19}F NMR was then recorded. ^{19}F NMR spectroscopic analysis showed high conversion to the decarbonylated complex at -98 ppm (t, J = 32.3 Hz) in THF). The NMR tube was then taken back into the glovebox, and boronic acid **4.10** was added, and the solution was allowed to stir at room temperature for 15 minutes. ^{19}F NMR spectroscopic analysis showed loss of signal at -98 ppm. **4.14** was not observed.

General procedure for catalytic fluoroalkylation Ni(cod)2 (5.5 mg, 0.02 mmol, 0.2 equiv) and the appropriate phosphine ligand (0.04 mmol, 0.4 equiv for monodentate ligands; 0.02 mmol, 0.02

equiv for bidentate ligands) were dissolved in 0.5 mL of solvent. The solution was stirred at room temperature for 15 min, after which the solution would be transferred into a preweighed, tall 10-mL vial loaded with **4.9** (24.8 mg, 0.1 mmol, 1.0 equiv) and nucleophile (0.13 mmol, 1.3 equiv). The vial was sealed with a Teflon-lined screw cap, brought out of the glovebox, and stirred at 120 °C or 150 °C. After 4 h of heating, the reaction mixture was allowed to cool to room temperature. A stock solution of 4-fluorotoluene was prepared (0.2 M in toluene) and added to the cooled reaction mixture (0.5 mL, 0.1 mmol, 1 equiv). A sample of the crude reaction mixture with internal standard was removed for NMR analysis. Yields of **4.15** reported were determined by 19F NMR spectroscopy (-87.6 ppm).

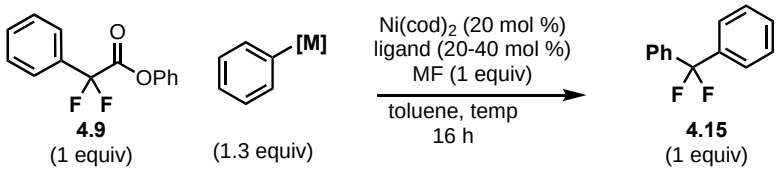

Entry	[M]	Ligand	Base	Temp (°C)	% Yield 4.15
1	-$B(OH)_2$	dppf	none	150	0
2	-$B(OH)_2$	dcypt	none	150	0
3	-$B(OH)_2$	Xantphos	none	150	0
4	-$B(OH)_2$	PPh_2Me	none	150	0
5	-$B(OH)_2$	PAd_2Bn	none	150	0
6	-$B(OH)_2$	P*n*Bu_3	none	150	0
7	-TMS	P*n*Bu_3	none	120	3
8	-TMS	P*n*Bu_3	KF	120	4
9	-TMS	P*n*Bu_3	CsF	120	9

Preparation of acid fluoride stock solution of 4.20. Acid fluoride **4.20** was prepared in a stock solution of toluene (up to 0.56 M) based on a modified literature procedure.[11] Carboxylic acid **4.18** (516 mg, 3.0 mmol, 1 equiv) and TMA(SCF_3) (525 mg, 3.0 mmol, 1 equiv) were weighed into a

20 mL vial in the glovebox. In some cases, color darkening and bubbling occurred when the reagents were left combined neat. 6 mL of toluene was added via syringe and the solution was stirred for 30 minutes at ambient temperature. The solution was filtered via syringe filtration. A sample of solution was taken and internal standard was added to determine concentrations. Acid fluoride was observed (s, 23.90 ppm, 1F; s, -98.05 ppm, 2F) with no remaining carboxylic acid.

Procedure for stoichiometric reaction of Ni(cod)$_2$/PnBu$_3$ with 4.20. Ni(cod)$_2$ (13.8 mg, 0.1 mmol, 1 equiv) and PnBu$_3$ (42 mg, 0.2 mmol, 2 equiv) were dissolved in 0.9 mL of THF along with internal standard 4-fluorotoluene (11 mg, 0.1 mmol, 1.0 equiv). The solution was stirred at room temperature for 15 min, at which point, acid fluoride **4.20** was added as a stock solution (0.56 M in toluene) (0.18 mL, 0.1 mmol, 1.0 equiv). The reaction was allowed to stir at 80 C for 2 h, at which point the solution was transferred to a screw cap NMR tube and sealed with a Teflon-lined cap. ^{19}F NMR was then recorded. ^{19}F NMR spectroscopic analysis showed high conversion to the decarbonylated complex (65% yield by ^{19}F NMR spectroscopy; Ni-CF_2Ph = -53 ppm, Ni-F = -360 ppm). The NMR tube was then taken back into the glovebox, and diphenyl zinc was added, and the solution was allowed to stir at room temperature for 15 minutes. ^{19}F NMR spectroscopic analysis showed loss of signal at -53 ppm. **4.15** was not observed.

General procdedure for catalytic coupling of 4.23 with boronic acids/boronate esters by palladium. Pd[P(oTol)$_3$]$_2$ (7.2 mg, 0.01 mmol was preweighed in the glovebox with ligand (0.01 mmol for bidentate ligands, 0.02 mmol for monodentate ligands) and dissolved in 0.3 mL toluene. The solution was allowed to stir at ambient temperature for 15 minutes. The Pd/ligand solution was then transferred to a tall 10 mL vial preweighed with **4.23** (xx mg, 0.1 mmol, 1.0 equiv) and

nucleophilic coupling reagent (0.2 mmol, 2.0 equiv). The vial was sealed with a Teflon-lined screw cap, brought out of the glovebox, and stirred at 80 °C. After 4 h of heating, the reaction mixture was allowed to cool to room temperature. A stock solution of 4-fluorotoluene was prepared (0.2 M in toluene) and added to the cooled reaction mixture (0.5 mL, 0.1 mmol, 1 equiv). A sample of the crude reaction mixture with internal standard was removed for NMR analysis. Yields of **4.26** reported were determined by 19F NMR spectroscopy (-87.6 ppm).

4.6 Referecnecs

1) Maleckis, A.; Sanford, M. S. *Organometallics*, **2014**, *33*, 2653–2660.
2) Maleckis, A.; Sanford, M. S. *Organometallics*, **2014**, *33*, 3831–3839.
3) Gu, Y.; Leng, X.; Shen, Q.. *Nat. Commun*. **2014**, *5*, 5405–5411.
4) Chang, D.; Gu, Y.; Shen, Q. *Chem. Eur. J*. **2015**, *21*, 6074−6078.
5) Aikawa, K.; Toya, W.; Nakamura, Y.; Mikami, K. *Org. Lett*. **2015**,*17*, 4996−4999.
6) Xu, L.; Vicic, D. A. *J. Am. Chem. Soc*. **2016**, *138*, 2536−2539.
7) Pan, F.; Boursalian, G. B.; Ritter, T. *Angew. Chem., Int. Ed*. **2018**, *57*, 16871−16876.
8) Motoashi, H.; Mikami, K.; *Org. Lett.* **2018**, *20*, 5340–5343.
9) Takise, R.; Isshiki, R.; Muto, K.; Itami, K.; Yamaguchi, J., *J. Am. Chem. Soc*. **2017**, *139*, 3340−3343.
10) Scattolin, T. Deckers, K.; Schoenebeck, F., *Organic Letters*, **2017,** *19*, 5740-5743.
11) Meng, G.; Szostak, M. *Org. Lett*. **2015**, *17*, 4364−4367.
12) Rahman, M. M; Liu, C.; Bisz, E.; Dziuk, B.; Lalancette, R.; Wang, Q.; Chen, H.; Szostak, R.; Szostak, M. *J. Org. Chem.* **2020**, *85*, 5475-5485.
13) Buchspies, J.; Szostak, M. *Catalysts*, **2019**, *9*, 53.
14) Reina, A.; Krachko, T.; Onida, K.; Bouyssi, D.; Jeanneau, E.; Monteiro, N.; Amgoune, A., *ACS Catalysis* **2020** *10*, 2189-2197.

Chapter 5 - Conclusion and Future Outlook

5.1 Introduction

At the outset of these investigations, we hoped to gain a better understanding of decarbonylative coupling reactions. The previous chapters outlined systematic investigations of decarbonylative coupling for a variety of acid electrophiles, ranging from aryl–C(O)X for $C_{(sp2)}$-$C_{(sp2)}$ and $C_{(sp2)}$-N cross-coupling, to fluoroalkyl (R_F) acid derivatives for intramolecular R_F-S coupling and intermolecular R_F-$C_{(sp2)}$ fluoroalkylations. In this chapter, I summarize key findings from these projects and discuss how these discoveries will impact further reaction development. Lastly, I address the current limitations and propose directions for future investigations.

5.2 Key findings and observations

5.2.1 *Nickel-fluoride activity for transmetallation*

Our investigations began with exploring the reactivity of aroyl fluorides with Ni(0) in the presence of monodentate phosphine ligands. At that point in time, there were few examples of decarbonylative coupling with acid halides, though there was precedent for their oxidative addition into group 10 metals. Acid fluorides were an interesting target as a potential starting point for decarbonylative fluorination via an intramolecular reaction pathway, analogous to our previous report of the decarbonylation of aroyl chlorides with palladium. By monitoring stoichiometric reactions of acid fluorides and $Ni(cod)_2/PR_3$ by ^{19}F and ^{31}P NMR, we identified key intermediates and observed effects of ligands on the rates of carbonyl de-insertion.

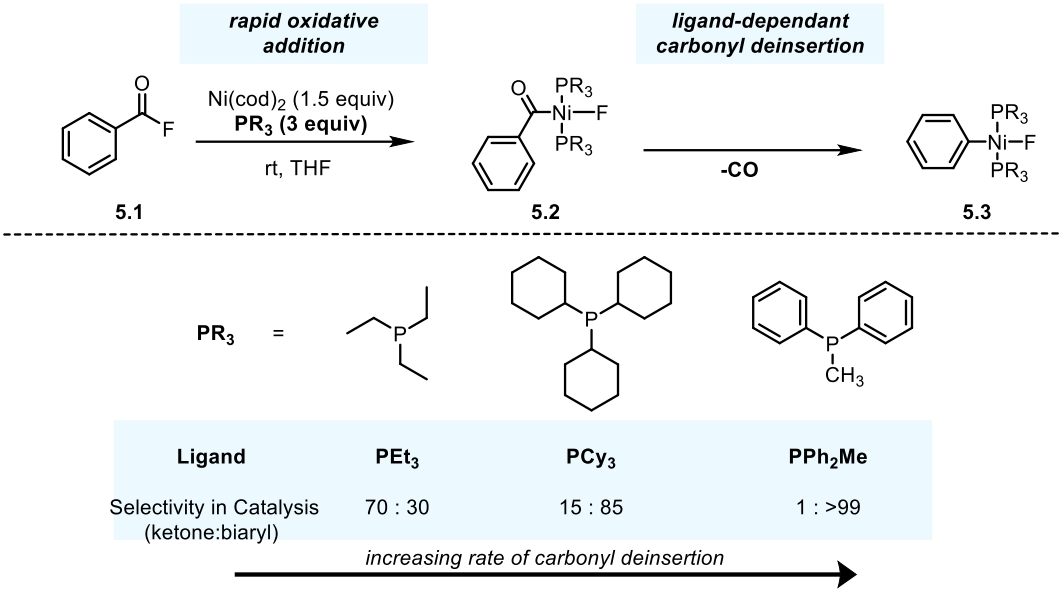

Figure 5-1. Relative rates of aryl carbonyl deinsertion on Ni(II) with monodentate phosphines.

In general, acid fluorides rapidly add into Ni(0) complexes bearing monodentate phosphine ligands at room temperature (Figure 5-1). For carbonyl deinsertion to occur, an open coordination site must be available for CO to migrate to. Increasing the electron donating ability of the phosphine ligand thus tends to slow carbonyl deinsertion, as electron-rich phosphine ligands are slower to dissociate, and the metal remains saturated. Increasing the steric bulk of the ligand can counteract this to an extent (for instance PCy_3 ligand Ni complexes undergo faster carbonyl de-insertion than the PEt_3 analogues). It is unclear if this increase in rate is due to a lower energy dissociation of the ligand or an influence of the ligand on the aryl carbonyl to induce carbonyl deinsertion or some combination of both. Electron-rich ligands also appear to stabilize these intermediates, as we were able to isolate acyl Ni PEt_3 (**5.2-PEt$_3$**) and the decarbonylated aryl-Ni-PCy_3 (**5.3-PCy$_3$**). Both intermediates were isolated with the phosphine ligands in a trans-configuration, signifying that the ligands must isomerize from the *cis*-configuration after oxidative addition.

We found that PPh_2Me was our "goldilocks" ligand, in terms of relative lability and steric bulk to induce carbonyl deinsertion on nickel. The Ni(0)/PPh_2Me system underwent oxidative addition and carbonyl deinsertion so rapidly that the oxidative addition product was too short-lived to be observed by NMR. While we were unable to isolate the observed Ni(Aryl)(F) product, we confirmed its identity via an alternative, non-decarbonylative synthetic pathway. Though carbonyl deinsertion occurs more rapidly with PPh_2Me than with PCy_3, we observed lower maximum yields of Ni(Aryl)(F) (up to 20% with PPh_2Me; ~65% with PCy_3), and over time the PPh_2Me ligated complex decomposed to unidentifiable metal species, suggesting that PPh_2Me may not have the same stabilizing effects as PCy_3, a feature that is likely beneficial for the carbonyl de-insertion step but likely less so for isolation.

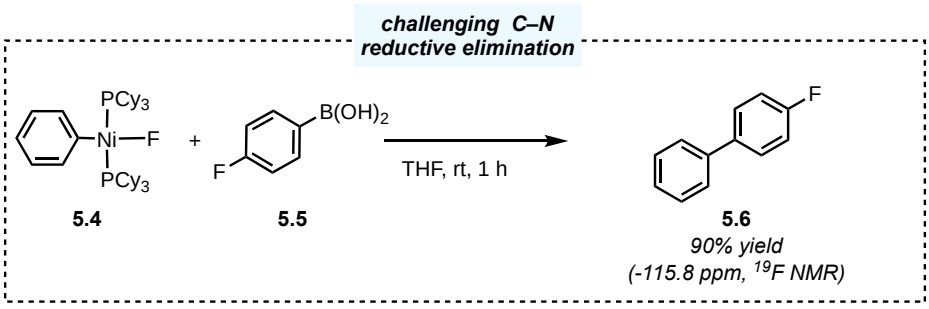

Figure 5-2. Stoichiometric biaryl synthesis with **5.4** and **5.5**.

When we first began this project, we envisioned that this decarbonylative pathway would be an efficient way to access aryl metal-fluoride complexes, from which we hoped to induce $C_{(sp2)}$-F reductive elimination to achieve aryl fluorination. However, $C_{(sp2)}$-F reductive elimination from Ni(II) is not known, and we were unable to observe aryl-fluorides when we heated these complexes or treated them with chemical oxidants. Not deterred, we hoped to utilize these nickel-fluorides as a possible intermediate for intermolecular functionalization of arenes. We observed that our isolated aryl-Ni-fluorides **5.4** readily reacted with aryl boronic acid **5.5** to give biaryl product **5.6** in quantitative yields at room temperature under base-free conditions (Figure 5-2). This

"transmetallation-activity" between nickel-fluorides and aryl boronic acids was significant, as it is generally well-accepted that Suzuki-Miyuara couplings require super-stoichiometric amounts of base to facilitate the activation of metal-halide intermediates before they undergo transmetallation. We synthesized analogous nickel-chloride and nickel-bromide complexes and showed that they did not exhibit the same reactivity and were inactive for transmetallation. After demonstrating that we can carry out each step stoichiometrically without the need for an exogeneous base, we developed a base-free nickel-catalyzed Suzuki-Miyuara coupling of acid fluorides with boronic acids. The scope for both aryl acid and aryl borane were broad, and importantly, base-sensitive boronic acids were tolerated under the reaction conditions.

5.2.2 *Aroyl Decarbonylation with N-Heterocyclic Carbenes for C-N Cross-Coupling*

After development of a base-free decarbonylative C-C coupling, we expanded our investigations to C-N bond formation. At this point, we had gained a sufficient understanding of aryl acid fluoride oxidative addition and carbonyl de-insertion at nickel. However, C-N reductive elimination products were not observed when subjecting **5.4** to (trimethylsilyl)-protected amines (Chapter 2, Figure 2-14b). We postulated that monoligated (tricyclohexyl)phosphine ligands were not sufficient for C-N bond formation, so we investigated other ligand classes that had greater precedent for this step, *N*-heterocyclic carbenes. Stoichiometric studies of the reaction between acid fluorides and Ni(0)-NHC precomplexes provided by the Montgomery lab were conducted, utilizing complexes bearing common NHC ligands such as IMes, SIPr, and IPr. These monoligated complexes rapidly underwent oxidative addition and carbonyl de-insertion under mild temperatures. Notably, we observed the acyl intermediates in all cases, so we concluded that the carbonyl deinsertion step was relatively slower than that with Ni/PPh_2Me.

All attempts at catalysis with these ligand systems failed to selectively yield the decarbonylated aryl amine product. Instead, background amidation between the acid fluoride and amine (silylated or unprotected) was observed. The only circumstance where we observed aryl amine with a Ni/NHC catalyst was when we carried out cross coupling with added PPh_2Me (Chapter 2, Figure 2-26). Here the decarbonylated product was formed in 7% yield. Stoichiometric reactions revealed the formation of a mixed NHC/PPh_2Me decarbonylated intermediate. ^{19}F NMR spectroscopic analysis showed signals diagnostic for (IPr)Ni(PPh_2Me)(Ph)F, which was the only Ni-F complex observed. It is still unclear exactly how this phosphine ligand is increasing the rate of decarbonylation. We preliminarily speculate that the addition of PPh_2Me may destabilize the acyl intermediate, thus inducing faster carbonyl deinsertion, while not saturating the complex by being overly coordinating to block the needed open coordination site. Bis(phosphine) nickel fluoride complexes were not observed, and we do not see C-N coupling from those previously isolated complexes, so we do not believe that these intermediates are involved in decarbonylative aryl amination.

5.2.3 *Fluoroalkyl acid derivatives for decarbonylative fluoroalkylation*

My focus for Chapter 3 and Chapter 4 was to transition our electrophile from aryl to (fluoro)alkyl carboxylic acids. Chapter 3 provided a proof-of-concept for using a broad array of fluoroalkyl acids for decarbonylative catalysis via an intramolecular C-S coupling involving nickel(0/II) catalysis. We generally observed facile carbonyl de-insertion in these systems, and the rate limiting step for this reaction was C-S reductive elimination from Ni(II). Large bidentate phosphine ligands were needed to facilitate this step (Chapter 3, Table 3-2). We note that there are fluoroalkyl groups for which the key bond forming step remains challenging: these include trifluoromethyl and pentafluoroethyl.

Achieving intermolecular decarbonylative cross coupling in Chapter 4 largely relied on blocking background decomposition of the starting material while maintaining a high enough level of reactivity for catalysis. This was achieved with careful selection of suitable acid derivatives and nucleophilic coupling partners. While acid fluorides show exceptional reactivity for transmetallation, the synthesis and handling of highly electrophilic fluoroalkyl acid fluorides remains problematic; indeed, to date we have only isolated fluoroalkyl acid fluorides as a stock solution in THF or toluene. Currently, work is underway to expand the fluoroalkyl scope of decarbonylative coupling by utilizing glutarimide-derived amide electrophiles, which are a more manageable electrophile type for synthesis with a variety of fluoroalkyl acids.

5.3 Future outlook

As outlined above, we have made significant progress in better understanding how to develop decarbonylative coupling methodologies, primarily with aryl and/or fluoroalkyl carboxylic acids. However, there are still limitations toward the development of more general conditions for decarbonylative coupling. While aryl acid derivatives have demonstrated to be excellent substrates for general C(sp2)–functionalization, reaction temperatures remain high due to catalyst inhibition by CO saturation to form nickel dicarbonyl. At this time, we have also been limited by difficult reductive eliminations from Ni(II), specifically C(sp2)–F bond formation for aryl fluoride synthesis from acid fluorides, as well as C-O reductive elimination for the conversion of esters to ethers. Perfluoroalkyl (RF = -CF3, -C2F5) reductive elimination from Ni(II) is also a significant limitation for fluoroalkyl thioether synthesis Further studies improving this reductive elimination steps, including systematic investigations identifying the required ligand structure, are needed.

Thioesters have provided a useful platform to test how well (fluoroalkyl)acyl nickel intermediates could undergo carbonyl deinsertion, as oxidative addition and reductive elimination are relatively facile, especially compared (fluoroalkyl)esters. The next significant step for these types of transformation would be to expand to alkyl carboxylic acids, which could also open the door to chiral decarbonylative couplings. A major challenge that remains is that systems that promote carbonyl deinsertion will also be prone to beta-hydride elimination. Our work with (fluoro)alkyl acids have provided a "bridge" from aryl carboxylic acids to alkyl acids. Systematic investigation of fluoroalkyl acids may allow us to study the reactivity of alkyl substrates by blocking C-H sites prone to beta-hydride elimination and allow for studies of the other catalytically relevant steps.